The characterization of the electric double layer capacitor (EDLC) and its application in micro grids using the hybrid energy storage system (HESS)

by

CHRISPIN TUMBA TSHIANI
57674728

submitted in accordance with the requirements for
the degree of

MASTER OF ENGINEERING: ENGINEEERING: ELECTRICAL (90121)
FIELD OF SPECIALIZATION: ENERGY SYSTEMS, POWER SYSTEMS, MICROGRIDS AND ELECTRONICS

at the

Department of Electrical Engineering
COLLEGE OF SCIENCE, ENGINEERING AND TECHNOLOGY (CSET)
UNIVERSITY OF SOUTH AFRICA (UNISA)

Supervisor: PROF. PATRICE UMENNE

August 2022

DECLARATION

I declare that "*The characterization of the Electric Double Layer Capacitor (EDLC) and its application in Micro grids using the hybrid energy storage system (HESS*)" is my own work and that all the sources that I have used or quoted have been indicated and acknowledged by means of complete references.

I further declare that I have submitted the thesis/dissertation to originality checking software and that it falls within the accepted requirements for originality.

I further declare that I have not previously submitted this work, or part of it, for examination at UNISA for another qualification or at any other higher education institution.

CT TSHIANI Date: 18 August 2022

COPYRIGHT CLASSIFICATION

© University of South Africa 2022

DEDICATION

I dedicate this thesis to my daughter, the love of my life Eliana Kitenge Tshiani, from whom all my motivation to achieve greatness comes from.

ACKNOWLEDGMENT

The completion of this research would not have been possible with the help, support, and encouragement of the following people

My mother, extended family and friends for their support and encouragement

I am very grateful to my supervisor Prof Umenne for all the guidance and mentorships.

I am also grateful to CBI electric for sponsoring my studies and allowing me to use their facilities.

Finally, I would like to thank the almighty God for the ability that HE has given me to be able to embark on this journey.

ABSTRACT

Electrical energy storage is very important. Energy storage devices such as batteries and capacitors can be used to store energy.

In this dissertation we investigate the use of a supercapacitor or electric double-layer capacitor (EDLC) to store energy.

The EDLC, also known as a supercapacitor, is a new type of electrical energy storage device used across many different fields in engineering. Firstly, two EDLC's of values 300 F and 400 F were characterized by connecting them in a laboratory experiment to produce their charge/discharge profiles under constant current. The EDLC's datasheet parameters including the capacitance and equivalent series resistance were then derived from the acquired charge/discharge profile. In addition to this, the experimental charge/discharge profiles were used to determine the parameters of the chosen EDLC's using the equivalent circuit model called the "two branch" or Faranda model.

The derived "two branch" equivalent circuit parameters were then used to design a Python/MATLAB/Simulink (PMS)-hybrid model of the EDLC's for simulation purposes. The PMS model used the derived parameters as inputs and produced simulated charge/discharge profiles for both the 300 F and 400 F EDLC's. By superimposition, the simulated and experimental charge/discharge profile were compared to evaluate the accuracy and validity of the proposed PMS model. This was done to enable future simulation in conjunction with a battery in a hybrid energy storage system (HESS) to show the potential of the EDLC in improving battery lifespan.

Following the above, a 65 F, 16.2 V EDLC supercapacitor was sourced due to its mid-range capacitance and voltage close to a 12 V DC supply. This was done to investigate whether the EDLC can help in reducing stress and prolong the battery lifespan in a hybrid energy storage system (HESS). A laboratory experiment was setup for the EDLC to produce its charge/discharge profile at a constant current of 5 and 10 A. As was done with the previous 300 F and 400 F, the 65F, 16.2 V Faranda or "two branch model"

mathematical parameters were extracted from the experimental charge/discharge profile in preparation for its modelling. In keeping with the laboratory experiment, the EDLC was connected with a 12 V lead-acid battery and a load to form a HESS, which was tested under difference load conditions. Experimental battery data such as voltage, current, state of charge (SOC) under HESS and battery energy storage system (BESS) without the EDLC were compared.

To simulate a HESS, the extracted parameters from the 65 F, 16.2 V EDLC were used as inputs to design the Python/MATLAB/Simulink (PMS) model of the EDLC. The PMS model of the EDLC was then used as a subcomponent in a HESS system modelled in MATLAB/Simulink. Using constant load conditions, the battery's voltage, current, power and state of charge (SOC) were analyzed for a BESS and HESS systems similar to what was done in the experimental setup. Experiment and simulation were then compared.

In conclusion, due to the high variation of battery parameters in the BESS setup for both experiment and simulation, and stability of the same battery values in the HESS setup, the EDLC in the HESS setup indeed reduces stress on the battery and prolongs battery lifespan.

The unique contribution of this work lies in the modelling of the EDLC using python programming language before integrating the python algorithm to MATLAB and Simulink to form the Python/MATLAB/Simulink (PMS) – hybrid model of the EDLC.

KEY TERMS

Battery Energy Storage System (BESS), Characterization, Electric Double-Layer Capacitor (EDLC), Hybrid Energy Storage System (HESS), Microgrid, Prolonging battery lifespan, Python/MATLAB/Simulink (PMS) – Hybrid Model, Supercapacitor.

LIST OF PUBLICATIONS

PUBLISHED

1. C.T. Tshiani, P. Umenne," The Characterization of the Electric Double-Layer Capacitor (EDLC) Using Python/MATLAB/Simulink (PMS)-Hybrid Model, Energies, vol. 15, issue no. 14, Article number 5193, Available online: https://doi.org/10.3390/en15145193

SUBMITTED

2. C. T. Tshiani, P. Umenne ," An investigation into the impact of the Electric Double Layer Capacitor (EDLC) in reducing battery stress and improving battery lifespan in a hybrid Energy Storage System (HESS) system", to add full citation when published.

TABLE OF CONTENTS

LIST OF TABLES

LIST OF FIGURES

LIST OF ABBREVIATIONS

Abbreviations	Terms
ε_o	Permittivity (or dielectric constant) of free space
ε_r	Permittivity of the insulating material
ΔU_3	The voltage drop at the beginning of the discharge process
ΔU	Change in voltage
Ar	Area
AC	Alternating Current
BESS	Battery energy storage system
C	Capacitance
CBI	Circuit Breaker Industries
CU	Charge used
D	Diameter
DC	Direct Current
E	Energy
EDLC	Electric Double Layer Capacitor
EIS	Electrochemical Impedance Spectroscopy
EMS	Energy Management System
EPR	Equivalent Parallel Resistance
ESR	Equivalent Series Resistance
FF	Fill Factor

HESS	Hybrid Energy Storage System
HGHP	High Gain High Power
I	Current
Isc	Short circuit current
MGCC	Micro grid Control Centre
MPPT	Maximum Power Point Tracker
NI	National Instrument
PC	Personal Computer
Pmax	Maximum power
PMS	Python/MATLAB/Simulink
PV	Photovoltaic
PWM	Pulse Width Modulation
Q	Charge in coulombs
RC	Resistor Capacitor
RDTC	Real Time Digital Simulator
SC	Supercapacitor
SCADA	Supervisory, Control and Data Acquisition
SOC	State of Charge
USA	United States of America
V	Voltage
Voc	Open circuit voltage
VCCS	Voltage Controlled Current Source

CHAPTER 1

INTRODUCTION

1.1 Introduction to the Electric Double-Layer Capacitor (EDLC)

This research is about the characterization of the electric double layer capacitor (EDLC) and its application in micro grids hybrid energy storage systems (HESS) to reduce battery stress caused by high power fluctuations from the load and thus help prolong battery lifespan [1].

The EDLC is a type of supercapacitor (SC) [2]. SC's are energy storage devices like conventional capacitors or lithium batteries [3]. A lot of modern devices have a need for energy storage [4]. Devices that one uses everyday like cell phones, cars, and watches to name but a few, have a need electric energy which is supplied from energy storage devices installed into it. Most widely used energy storage devices are conventional capacitors and batteries. Conventional capacitors have capacitance that can range from a few micro farads to thousands of micro farads. This is especially useful in applications that require fast charging/discharging, multiple charge/discharge cycles and high-power density [5]. Batteries on the other hand store energy in a chemical field and are useful in applications that require high energy density [6].

In the last few decades or so, a third option that is sort of a middle ground between the conventional capacitor and battery has been developed. This new energy storage device is called the supercapacitor. They are 3 types of SC. The EDLC, which is the subject of our investigation, the pseudo-SC, and the hybrid SC [1].

The SC was first proposed by Motorola in 1978 as a storage device which is an electrochemical device [7]. Its takes some of the good qualities of normal capacitors such as high-power density and fast charging/discharging qualities to become a sort of a middle ground energy storage device [8].

The research will aim to characterize the SC by looking at its composition, characteristics, how its stores energy and what makes it so different and many ways superior to the normal capacitor and lithium battery [9]. This characterization will be done by charging/discharging the EDLC at constant current in a laboratory experiment to obtain its charge/discharge profile. A known electric equivalent model of the SC and its mathematical model as a base for whom the parameters of the EDLC will be derived from the charge/discharge profile. The derived EDLC parameters will be used to model and simulate the SC in a Python/MATLAB/Simulink (PMS) environment. Simulation and experimental results will then be compared to determine the accuracy of the PMS model.

1.1.1 Literature Review on EDLC characterization

In this paper [10], the authors developed a new EDLC equivalent model called the “two branch model” or sometimes called the “Faranda model”. This model, although slighly different from other models, makes the derivation of equivalent circuit parameters (coefficients) much easier. Experimental tests were conducted on two brands of EDLC’s and parameters successfully extracted from them.

Another way of EDLC characterization which is a “three-port” model was proposed in article [11]. Here, the authors noted the deficiencies of the simple resistor capacitor (RC) equivalent circuit and went on to develop a new “three branch parallel model” with one of the branches incorporating a voltage dependend capacitor. Simulated and experimetal results were then compared to the datasheet values and the model proved correct.

The effect of heat on the characterization of the EDLC was studied in [12]. Here, the authors explored thermal modelling of the EDLC. A model was proposed and tested,with experimental and simulated results in agreement. Another research [13], described how to simulate a mathematical model for both the battery and EDLC in MATLAB/Simulink to be incorporated into a PV micro grid system. The same principal was applied in [14] to explore the effect of EDLC in energy storage systems. Simulated results and practical results were found to correlate.

In [15], a voltage current equation was used to propose an equivalent circuit for the EDLC. The authors further delivered an experimental method to derive the parameters of the EDLC. These were then used to simulate the model in MATLAB/Simulink. Simulated

values of the ESR and capacitance were compared with those in the datasheet and found to correlate.

Different methods on how to extract the parameters of the EDLC were investigated in [16]. The authors setup different laboratory experiments to obtain the charge/discharge profiles of the EDLC at constant current. Parameters of two 15 V, 52 F EDLC's were then derived experimentally and discussed.

The authors in [17] investigated the different types of supercapacitor models that have been proposed. They concluded that, while many models exist, each one has its own advantages and disadvantages depending on where the supercapacitor will be used. Similar research was conducted in the following referenced articles [18, 19].

The electrical characteristics, modelling, application, and future trends of SC was researched in [20]. The authors looked at the charge distribution on the electrodes surface, its high frequency behavior, electrical self-discharge and modelling and parameters. The application of SC in consumer electronics was also investigated.

Marin S. Halper and James C. Ellenbogen wrote a brief article comparing SCs and conventional capacitor [2]. They deduced that while the two-share similar capacitance, power, and energy equations, they differ in their composition. Conventional capacitors use a dielectric constant whereas SC use a thin separator immersed in an electrolyte. A quantitative modelling of the SC and equivalent circuits were also proposed.

In [21] the authors characterized packed electric double layer capacitors (EDLC's).

Similarly, Remi Kahwaji in his journal article titled "Supercapacitors: A short Literature Review" [22], did a summary of some of the research on SCs backgrounds, importance in the industry and comparisons with other energy storage devices. He deduced that the maximum SC voltage is determined and limited by the electrolyte decomposing at higher voltages whereas the capacitance is affected by the distance between the electrodes and

the surface area of the electrodes. He also delved into the difference ways of characterizing a SC.

John R. Miller and Patrice Simon in their article [7], looked at the history of SC, advantages and disadvantages compare to batteries plus the industry use of SC in hybrid cars.

In their journal paper titled “Characterization, Analysis and Modeling of an Ultra capacitor” [23], the authors analyzed two ways to characterize a SC namely the “constant current discharge and charge method” and the “constant power discharge and charge method”. For both methods simulations and experimental results proved to be accurate compared to the data provided in the datasheet of the SC under test

The journal article titled “Supercapacitors: Review of Materials and Fabrication Methods” [24], looked at the different types of SC and the materials used in them. For the EDLC, the use of carbon aerogels, activated carbon, carbon fibers and carbon nanotubes were examined. For the Pseudo capacitor metal oxides and conducting polymers. For the hybrid capacitors, carbon materials with conducting polymers or carbon materials with metal oxides. The feasibility of use of other materials such as nickel and cobalt were also discussed, and advantages and disadvantages noted.

In their journal article titled “A brief review on electrodes materials for supercapacitors” [25], authors zaharaddeen and Subramani examined the characteristics and storage principle of the SC. The use of different electrodes materials such as active carbon and metal oxide were investigated. They looked at the history of the SCs, types of SC and compared SC characteristics such as energy density and power density to other energy storage devices. It was concluded that SC are the energy storage devices of the future because of their stability and high-power density but a lot of work needs to be done to improve their energy density.

Similar research was done in the article titled “Supercapacitors: the near future of batteries “[26], whereas the authors in the journal article [27] went further and examined the charging and discharging cycle of the SC.

1.1.2 Theory of Electric Double Layer Capacitor

Conventional capacitors store energy in an electric field and consist of 2 electrodes separated by a dielectric material wrapped around an aluminum foil. SCs on the other hand also consist of 2 electrodes, but the electrodes are made of carbon materials or metal oxides and separated by a thin dielectric called a 'separator' that is immersed in an electrolyte. The difference between the two is clearly shown in Figure 1 below.

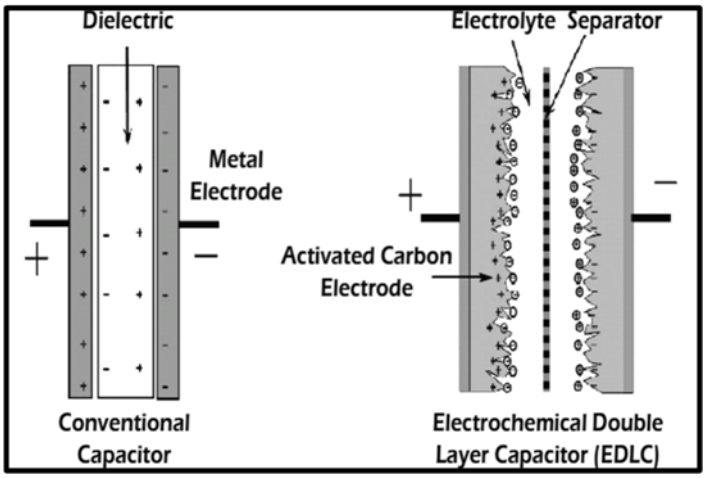

Figure 1 EDLC and conventional capacitors comparison [28]

The large surface area of the SC electrodes and thin separator, allow the SC to achieve capacitance much high than conventional capacitors [27]. SC are basically an improved version of conventional capacitors but are governed by the same equations.

Figure 2 below shows a microscopic view of the EDLS's porous carbon electrode

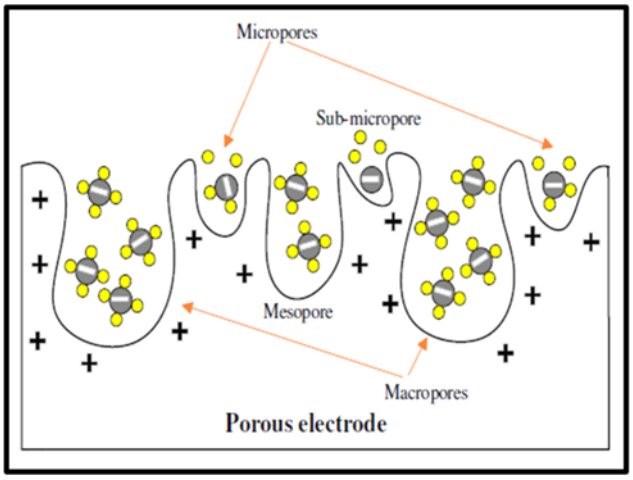

Figure 2 EDLC porous electrodes [29]

Clearly seen is the large surface area of the electrodes due to the uneven, porous electrodes. This is what enables the EDLC to achieve much greater capacitance than conventional capacitors.

As with conventional capacitor, when a voltage is applied across an EDLC, the charge that accumulates on each electrode is represented by:

$$Q = CV \tag{1}$$

where Q is the charge accumulated in coulombs, C the capacitance and V the applied voltage [2].

The relationship between capacitance, electrodes surface area and distance between the electrodes is denoted by the equation:

$$C = \varepsilon_o \varepsilon_r \frac{Ar}{D} \tag{2}$$

where D is distance between electrodes, Ar surface area of electrodes, ε_o the permittivity (or dielectric constant) of free space and ε_r the permittivity of the insulating material between the electrodes [2]. The above equations shows that capacitance is directly proportional to the surface area and inversely proportional to the distance between the electrodes. And as such, this equation illustrate why SC can achieve much higher capacitance then normal capacitors due to the increased surface area on the electrodes and the reduction of the distance between the electrodes.

The energy stored in a capacitor is represented by the equation below and it is a product of the capacitance and the voltage drop when a current is applied [2].

Energy stored in a capacitor:

$$E = \frac{1}{2}CV \tag{3}$$

Typically, the maximum operating voltage of one cell of SC is around 2.7 V, whereas conventional capacitors can go to 100V or even higher. This SC voltage limitation is due the breakdown potential of the electrolyte. In applications that require higher SC voltages, a bank of SCs connected in series is used.

Table 1 below shows comparison between different energy storage devices. It shows that SCs have relatively high-power density than lithium battery but lower energy density. Energy density refers to the amount of energy the device can store and power density the rate at which this stored energy is disbursed. While conventional capacitors and to some extent, SCs have higher power density then a battery, batteries have a much higher energy density than the formers. The figure also shows that conventional capacitors and SCs have very short charging/discharging times compared to batteries with a better charge/discharge efficiency too. Batteries also have very short “cycle number”, less than 1000, compared to times 10000 and more than 1 000 000 for SCs and conventional capacitors respectively.

Table 1 Comparison of energy storage devices [15, 18, 27, 30]

Parameters	**Lead-acid battery**	**Lithium-ion Battery**	**EDLC**
Specific energy density (Wh/kg)	10-100	150-200	1-10
Specific power density(W/kg)	<1000	<2000	<10000
Cycle life	1000	5000	>500000
Charge discharge efficiency	70-85%	99%	85-98%
Fast charge time	1-5 hour	0.5-3 hour	0.3-30sec
Discharge time	0.3-3 hour	0.3-3 hour	0.3-30sec
Calendar life(year)	5-15	10-20	20

1.1.3 Types of supercapacitors

There are 3 types of SCs distinguished by the process at which charge storage occurs, that is faradaic or non-faradaic, and the electrode's material composition.

Electric double layer capacitor (EDLC) supercapacitors

The first type is the EDLC which is the most popular and the subject of our research. The EDLC uses carbon materials on the electrodes. When a potential difference is applied across the electrodes, ion from electrolyte diffuse across the separator into the electrodes. The accumulation of ion charge on the surface area of the electrodes forms a double layer. EDLCs store charge electrostatically or in a non-faradaic way like conventional capacitors. This means transfer of charge between electrodes and electrolyte do not occur. And this makes the EDLC charge storage mechanism very reversible as there is no chemical breakdown resulting in a remarkably high charge/discharge cycle capability.

EDLC are the most widely used SC because of their use of carbon materials whose advantages include high surface area, availability, low cost and already know how manufacturing methods. These carbon materials can either be active carbon, graphene, carbon nanotubes or carbon aerogels. The carbon materials store electrons using the electrochemical double layer which is formed at the junction of the electrodes and the electrolyte.

Pseudo supercapacitors

Unlike EDLC, pseudo SCs use faradaic charge storage mechanism. This means that charge transfer between the electrodes and electrolyte do occur. Higher capacitance than ELDC are also achieved using these faradaic processes. Electrode's materials used for pseudo-SC include metal oxides and conducting polymers. Different types of metal oxides used can be nickel oxides, manganese oxide or iridium oxide. Metal oxides provide benefits such as high capacitance and low resistance which can make it easier to manufacturer high energy and high-power SCs.

Pseudo SCs are good for high energy density applications. Disadvantages include lower power density and less charge / recharge cycles.

Hybrid supercapacitors

Hybrid SC use the advantages and disadvantages of both the EDLC and Pseudo SC to sort of come up with a combination of the two that give a better performance. Use both the Faradaic processes which are associated with Pseudo SC and non-faradaic processes associated with EDLC to store energy. As a result, hybrid SC can achieve higher power and energy densities than EDLC without losing the cycle ability and price affordability that commonly occur with pseudo-SC. Three type of hybrid SC exist depending on their electrode's composition, namely composite, asymmetric and battery type.

1.1.4 EDLC parameters

The main parameters of the EDLC are the equivalent series resistance (ESR), capacitance (C) and equivalent parallel resistance (EPR). These parameters are further explained below:

ESR

The ESR is the equivalent resistance which is the total resistance of the SC that is due the materials. The materials include the electrodes, separator, and electrolyte to mention but a few. SC generally have incredibly low ESR, less than 1 milliohm, which contributes to their high-power density and energy efficiency. Factors like ageing and higher temperature can increase the ESR of the EDLC resulting in less power density and less efficiency.

Capacitance

As explained earlier the EDLC can achieve incredibly higher capacitance than conventional capacitors due to its composition and higher electrodes surface area. Capacitance can be described as the volume of charge that the device can store. EDLC can achieve capacitance values up to 10000 times that of electrolytic capacitors.

EPR

EPR is the resistance that determines the self-discharge ability of the EDLC. There for a higher EPR means the EDLC self-discharges less and a lower EPR means the EDLC self-discharges more. Typically, EDLCs and capacitors have EPR in the range of 1 kilo ohms and above. EPR is too affected by EDLC ageing and temperature

1.1.5 ESR, Capacitance and EPR measuring methods

Different EDLC ESR parameter acquisition methods have currently been researched. In his master's research thesis titled "Application of supercapacitor in electrical storage system" [28], the author from the University of Singapore investigated methods such as AC Electrochemical Impedance Spectroscopy (EIS), constant current pulse methods, Voltage recovering method and Instantaneous Voltage Drop Method. All proved to be reliable ESR parameter acquisition methods to various degrees. However, his research proved that the AC EIS to be the most reliable of them all.

In their journal article titled "Measurement Considerations on Some Parameters of Supercapacitors" [31], the authors identified and measured the main parameters of the SC. The ESR, capacitance, self-discharge resistance, maximum power, energy, and energy efficiency are some of the parameters that were either measured or calculated.

The impedance spectroscopy method was used to measure the ESR and volt-ampere method to measure the charge/discharge characteristics.

Below, each different technique will be described.

DC Measuring method

In this method measuring of its ESR and capacitance is done by obtaining its charge/ discharge prolife at constant DC current source. That is, the SC is first charge at constant current till it recharges it maximum voltage. Then thereafter discharged with a load at constant current.

In the DC method, the capacitance is calculated using the equation:

$$C = \frac{I\Delta t}{\Delta U} \tag{4}$$

where I is the constant current of discharge, $\Delta U = U_1 - U_2$, $U_1 = 80\% * U_{max}$, $U_1 = 40\% * U_{max}$, with U_{max} being the SC maximum voltage [12].

And the ESR is calculated using equation:

$$ESR = \frac{\Delta U_3}{I} \tag{5}$$

with I the constant discharge current and ΔU_3 the immediate voltage drop at the beginning of the discharge process [12]. Calculation of the ESR is better illustrated by the discharge Figure 3 below clearly showing the drop in voltage and current at the beginning of the discharge process.

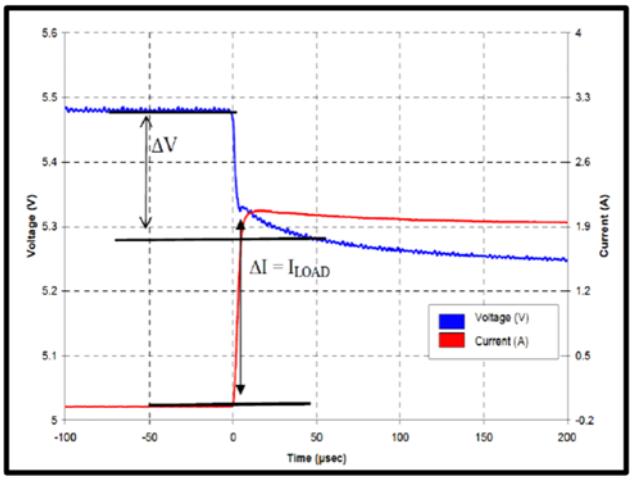

Figure 3 EDLC discharge profile [32]

AC Measuring method

In the AC measuring method, the electrochemical impedance spectroscopy (EIS) is used. This method consists of measuring the behavior and response of the SC to an injection of a signal of known amplitude and frequency. Using the EIS method requires specialized equipment, but the results are said to be very accurate.

EPR Measurement

To measure the equivalent parallel resistance (EPR), the SC is charged to a certain voltage and then left in its self-discharging state. The voltage across the capacitor will then decline according to the equation:

$$U = U_o e^{(-\frac{t}{RC})} \tag{6}$$

where U_0 and U are the voltages of the SC before and after discharging respectively, R the resistance, C the capacitance and t the discharge time [33].

EPR is then calculated using the formula [33]:

$$EPR = \frac{-(t_2 - t_1)}{\ln\left(\frac{U_2}{U_1}\right) * C} \tag{7}$$

1.1.6 Electric equivalent circuit models of EDLC

Basic RC Model

The EDLC can be represented by a very basic equivalent Resistance, Capacitance (RC)-circuit.

It consists of a series resistor which represents the equivalent series resistance (ESR), a capacitor (C) and the leakage current equivalent parallel resistor (EPR). This representation while commonly used and sufficient for most basic simulation, does not take into consideration the nonlinear behavior of the EDLC during charge/discharge cycles as shown in the Figure 4 below.

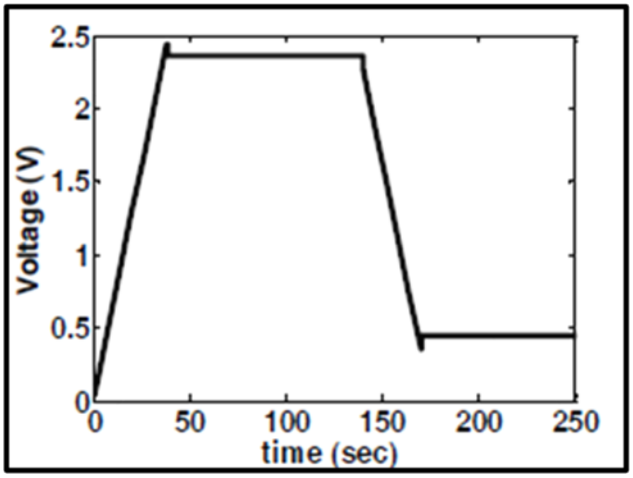

Figure 4 RC model charge/discharge profile [34]

Missing in the above figure is the distinct charge/discharge exponential curve that is the characteristics of capacitors.

Three branch model/ Zubieta model

The inadequacy of the basic RC model called for the development of other models to obtain more accurate simulations. One of those is the three-branch model often called the Zubieta model [11, 19], which consists of three parallel Resistance-Capacitance

branches with three-time constants to cater for the different time behavior of the EDLC during charge and discharging. It also contains a voltage dependent capacitor in the immediate branch whose value is dependent on the voltage.

Two branch model/ Faranda model

A model very similar to the Zubieta model and the model that we used as the EDLC's equivalent circuit model for this research, is the "two branch "or sometimes referred to as the "Faranda" model [10].

The "Two branch "model consists of the main branch that caters for the short term and medium-term behavior during the charge/discharge process. It consists of the resistor R0, main capacitor C0 in parallel with a voltage dependent capacitor C1. The second branch of the "Two branch" model caters for the long-term behavior of the EDLC. It has a resistor R2 and capacitor C2. The equivalent parallel resistor (EPR) which is responsible for the self-discharge behavior of the EDLC completes all the components of the "Two branch" model.

RC transmission model

The RC transmission line model as shown in Figure 5 is based on the porous electrodes' theory developed by de levie [35]. It attempts to capture the double layer capacitance and electrolyte resistance distributed throughout the SC. In this model both physical and electrochemical characteristics of the SC are simulated. Both long term and dynamic behaviors of the SC are considered so as its response to frequency from 10 MHz to 1 KHz.

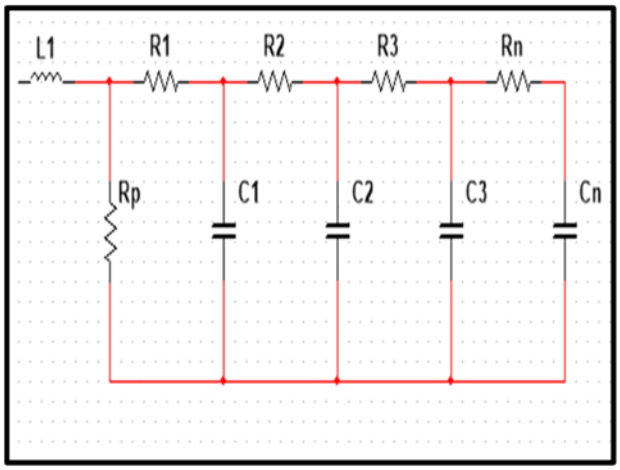

Figure 5 EDLC transmission model [36]

1.1.7 Various Application of EDLC in industry

The EDLC due to its capabilities has found many uses in numerous different industries.

Micro grids

Finally, the super capacitor as found its way in micro grids hybrid HESS for power stabilization Research has found that the SC because of it fast discharge and charging abilities provides the initial startup energy power to the grid and then allowing the batteries to pick up later when the power has stabilized. This has been shown to put less stress on the batteries and help prolong its lifespan. Different SC – batteries topologies have been researched and simulated to find the best setup to provide optimal performance.

Hybrid cars

In the Automobile industry for example, Hybrid cars use it for regenerating braking [32]. The EDLC has also proved useful in consumer electronic devices for power stabilization and energy storage.

Data storage

Data storage devices use the SC to power them when the main power is offline.

1.1.8 Future trends and development of EDLC

The EDLC is firmly entrenched as an energy storage device, and we have looked at its future trends and development.

One of the drawbacks so the EDLC its maximum voltage normally 2.7 V due to the electrolyte breaking down at higher voltages. To overcome these developments have focused on the use of different electrolyte solvents such as organic electrolytes which are stable at high voltages or ionic electrolytes.

Although the EDLC can achieve much higher capacitance than conventional capacitors, work is still going on to determine how the surface area of the electrodes can be increased even further to maximize the amount of charges that can be stored.

ELDC resistance also known as ESR is a very important parameter which affects a number of issues. EDLC typically have ESR in the milliohms region which is quite low. Because ESR affects things such as the power density of the EDLC, developments are being done to even lower the ESR even more even more to increase the power density.

1.2 Introduction to Micro grids hybrid energy storage systems (HESS)

One of the most important uses of the EDLC is in Micro grids. The abundance of renewable energy such as solar and wind energy, has led to the rapid development of Micro grids [37-39]. Some of the advantages of renewables compared to fossil fuels include abundance and environmental friendliness [40, 41]. It is estimated that as the renewable energy technology improves, the number of people and industries that depend on it in the future, will expand exponentially [42]. An example of a typical micro grid is shown below in Figure 6.

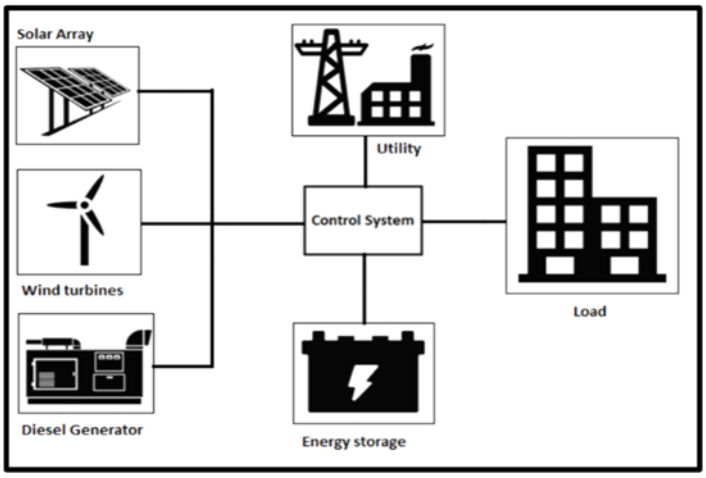

Figure 6 Micro grid [43]

Micro grids such as the one above, are small electricity supply systems that are either independent from [44] or connected to the main electricity grid. These renewable energies based micro grids can be used to supply electric power to communities replacing the traditional coal power stations. In European countries like Germany, a large proportion of the country's energy needs is supplied by renewable energy sources [45].

One of the challenges of electricity generated from renewable energy sources is where to store it [46, 47]. The need to store the generated energy arises from the inconsistent availability of the renewable energy source leading to stages where demand exceeds supply or supply exceeds demand. Factors like a rainy day or clouds can affect the amount of energy generated on a particular day by a solar based micro grid system which in turn leads to less energy available to the end users.

To compensate for this a battery energy storage system (BESS) [48] is built as part of the micro grid, to store excess electric energy when supply is high, and demand is low and to compensate for when supply is low and demand is high. One of the problems of BESS is the short lifespan of batteries that are used to store the energy generated. This is mainly due the stress put on the batteries because of high frequency fluctuation in power demand [49].

To help negate this and prolong the life of the battery, a hybrid energy storage system (HESS) consisting of SCs and batteries is used [50]. The research investigated the inner

workings and effectiveness of HESS systems through laboratory experiments and simulation. A HESS system will be built in the laboratory to experimentally obtain battery voltage, current, charge used and state of charge (SOC) under BESS and HESS topologies. The same will be repeated in a MATLAB/Simulink simulation environment that will in cooperate the PMS model created from the characterization of the EDLC. Experimental and simulated results will then be analyzed and compared.

1.2.1 What are Renewable Energy sources

Nonrenewable energy like fossil fuels are finite and would be eventually depleted. Renewable energy such as solar and wind energy are infinite and more environmentally friendly [51]. To harness the power of renewable for use in for example micro grid, instruments such as solar panels for solar energy and wind turbine for wind energy are utilized. Solar panels convert the sun's energy, also known as irradiance into electrical energy. Wind turbines convert the energy in the wind into mechanical energy which is then used to turn generator which produces electricity. Many governments have started to migrate to the use of renewable energy to provide a percentage of their electricity needs. Tax incentives and lower tariffs are offered to consumers and companies to encourage this process of moving to the use of renewable energy.

Apart from the obvious environmentally advantages provided by renewable energy, their use in micro grids to bring electricity remote areas, has been one of the key factors leading to their increased use.

Another renewable energy that has been around for a long time is hydro power. Many dams have been built to generate power from dams. This renewable energy source however requires the presence of large rivers and lakes in one's country. And for a country like South Africa which do not have large rivers this has produced to be a challenge and economically not viable. However large parts of the world, in countries like China and the United States of America (USA), big dams have been built across rivers and lakes produce large amounts of electricity to power large cities.

Other renewable energies such as geothermal energy and biomass energy have also been used to generate electricity in several countries.

1.2.2 Micro grid and HESS literature review

Micro grid literature review

In their journal article titled “A comprehensive study on micro grid technology” [52], the authors looked at the different Micro grid technology, including a study on energy storage systems, power loads and interconnection between different Micro grid systems. The article also discussed different techniques of Micro grid installed around the world and the pros and cons of each.

As mentioned earlier, micro grids, especially standalone types, are becoming exceedingly popular and easier ways to supply power to some of the most rural distant place in the world. In their article titled,” Design and modelling of a standalone DC-Micro grid for Off-grid Schools in rural areas of developing countries” [49], the authors proposed a DC Microgrid system to supply the electricity demand of a rural school located in Ethiopia. The simulation results and cost analysis showed that the proposed system would be an ideal option to electrify the rural school.

In his conference paper, ahmad M. Eid [53], also proposed and analyzed a DC microgrid consisting of a photovoltaic module controlled by MPPT, fuel cells, a battery storage system and AC and DC loads. A 12 pulse PWM inverter is used to convert the DC to AC and bidirectional DC/DC converters to charge and discharge the batteries. The system was simulated and found to able to supply the required performance requirements.

In their journal article titled,” Analysis, Modelling, and control of an AC microgrid system based on green energy” [54], the authors examined the controlled of the operation of the micro grid and main grid together with a changing load demand through a microgrid control center (MGCC). The article focused on proposing a proper and efficient MGCC control mechanism taking into account generated power and load demand. A model was simulated in MATLAB/Simulink and an efficient energy management way was developed for the MGCC.

As mentioned earlier, one of the major problems with microgrids especially the standalone types, is the short lifespan of batteries. In their article titled “Life cycle planning of battery energy storage system in off grid wind -solar-diesel microgrid” [55], the authors present a

life cycle planning methodology for energy storage systems in microgrid. A case study was done on a microgrid in Kythnos Island, Greece and an algorithm developed and presented to address the proposed model. Results and simulations showed the proposed model to be quite effective and reliable for off the microgrid grid energy storage systems.

The sizing of the batteries used in the microgrid storage systems has also been an interesting research topic. The authors in their article titled “Optimal sizing of a lithium battery energy storage system for grid-connected photovoltaic systems” [56], proposed a system focused on analyzing operating conditions such as nominal capacity, cycle depth, current state, state of charge levels of a lithium battery energy storage system. By looking at the average daily generated power and the average daily power demand, suitable battery sizing method was proposed that take into account the maximum power that needs to be stored and the cost of, therefore. It was further concluded that the proper utilization of the energy storage system is crucial to running an efficient microgrid.

One of the most crucial components of a micro grids are the DC-DC bidirectional converters. They control the charging of the energy storage systems when supply is high, and demand is low and control the discharging of the energy storage system when supply is low, and demand is high. This is crucial in maintaining the reliability of the microgrid. In his article titled “A simplified control strategy for Bidirectional DC-DC converter for DC microgrid application” [57], ahteshamul haque, proposes an automatic control mechanism that senses and compares voltages on each side of the converter. Software PSIM is used to simulate the circuit. Simulated results showed the proposed systems to be accurate, applicable, and cost effective when used in all modes of the bidirectional dc-dc converter.

Similarly, Daniel Zammit, Cyril Staines and alexander Micallef in their conference paper titled “Control of Buck and Boost Converters for Stand-Alone Microgrids” [58] presented a model to control a buck and boost converter in standalone microgrids using droop control method. The operation was simulated, results analyzed, and transfer functions derived from equivalent circuit.

Further research was done on the use of dc-dc converters in this referenced article [59]. The authors propose a novel high gain high power (HGHP) dc-dc converter for a DC

microgrid. Experimental tests are done to determine the suitable of the said system comparing performance parameters with existing state of the art converter topologies. Results showed the proposed system to be reliable and accurate across different load demands.

An EMS is a crucial component of any micro grid. It monitors the power generated, the load power demands and help maintain the reliability and stability of the whole system. Different EMS methods have been researched and utilized in various parts of the world. The authors in their article titled “Microgrids energy management systems: A critical review on methods, solutions, and Prospects” [60] presented different strategies and solutions for EMS.

In their conference paper titled “Modeling and control a DC-Microgrid Based on PV and HESS Hybrid Energy Storage System “[61], the authors presented a PV/Battery/SC based DC Micro-grid. Control of the HESS system, charging and discharging of both the battery and SC through bidirectional buck-boost converters, is discussed and investigated. The system was simulated on MATLAB/Simulink and the state of charge (SOC) of the battery, the currents, voltages, and powers curves were plotted. Results showed that the HESS systems reduce battery current stress, improve battery lifespan, and overall reduces cost of the system.

In “A SC/battery Hybrid Energy Storage System in the Micro grid” [62] conference paper, a battery/supercapacitor hybrid system was proposed by the authors. The system was simulated in a real time digital simulator (RTDS). A strategy to manage the power was proposed whereby the supercapacitor takes care of the power surplus/deficiency primarily and the battery acts in a supporting role to the supercapacitor by feeding energy to it. A sizing study was investigated to determine the optimum size of both the battery and supercapacitor to meet the correct power requirements. It was deduced from this study that; the supercapacitor protects the battery from high frequency power fluctuation and thus contributes to the stability and longevity of the Microgrid system.

In their article title “Dynamic power allocation of battery-supercapacitor hybrid energy storage for standalone PV microgrids application” [63], published in,” Sustainable Energy

Technology and Assessments", a hybrid energy storage system and a power management strategy are proposed by the authors. MATLAB/Simulink simulation models of the PV based micro grid are investigated. The authors take into consideration different solar irradiance profiles depending on various weather conditions and estimate load power consumptions are used to investigate the effectiveness of the HESS system. Simulations in the above-mentioned different conditions, and careful observation of the battery health, showed that the proposed system greatly reduces battery stress, improves battery lifespan, and thus contribute to the reduction of the overall cost of the system.

Other researchers have taken into consideration real life loads and proposed micro grid HESS systems based on them. In the article titled "Modelling of a hybrid energy storage system supplied by a photovoltaic source to feed a DC motor" [44], the authors model a PV, DC motor based micro grid hybrid system by simulating first the energy produced by the PV, then different phases of the currents, voltages and state pf charge of battery observed. It was noticed that the high currents necessary at the start of the DC motor, are supplied by the SC and not the battery, reduces electrical stress on the batteries and thus prolonging their lives.

HESS Modelling Literature Review

So far, a lot of the simulation of the hybrid energy storage systems and modelling of supercapacitors has been done in a purely MATLAB/Simulink environment. In [13-15] the authors modelled the EDLC in MATLAB/Simulink and simulated the HESS to determine the effect of the EDLC on the lifespan of the battery. In all these instances the MATLAB/Simulink EDLC model integrated well with the battery in the HESS and simulations showed it to reduce stress and thus help increase battery lifespan.

In this paper [64] the authors investigated a hybrid energy storage system (HESS) to cater for power fluctuations in a micro grid system. A control system based on a real time digital simulator was introduced together with a battery lifetime prediction model. Experimental and simulation results showed that the HESS had the lifespan of the battery increasing from 6.38 years to 9.21 years compared to a battery only system.

A new control system to reduce battery ageing in a supercapacitor and battery micro grid storage system was proposed by the authors in [65]. Simulations were done for a wind hybrid energy storage system and using the control system, a marked reduction was observed in the battery peak current and the ampere hour throughput which will lead to an extension of the battery lifespan.

Similar work was done by the authors in [66] in employing a power sharing method (PSM) in a li-ion battery and supercapacitor hybrid system. The hybrid PSM was tested in a 10 MW system in the UK and USA to determine the impact on the battery lifespan. Results showed that using the PSM and the hybrid storage system, the stress on the battery was significantly reduced.

1.2.3 Theory of Micro grids

Micro grids are becoming an immensely popular way to generate electricity in many countries due to their use of renewable energy sources. In their conference paper titled “Review of microgrid technology” [39], Hartono santoso and Rudy setlabudy looked at the composition and structure of microgrids. They found that microgrids can either be grid connected or standalone depending on the need and application. Grid connected micro grids as the name says, are connected to the main grid and are used to supplement the daily power usage. They are normally smaller in size and less complex than the stand-alone micro grids.

Standalone micro grids are used to supply power to remote areas and are not connected to the main grid. They serve the purpose of meeting the electricity needs of places that the main electricity needs would normally not reach.

The architecture of micro grids is usually composed of a renewable energy source such as wind turbines or Photovoltaic (PV) arrays to harness the sun’s irradiance. They also include maximum power point tracker (MPPT) to track the sun’s irradiance to maximum power output, an energy storage system, which can consist of batteries alone or a hybrid type consisting of batteries and SC, DC/DC converters to charge and discharge the storage systems and finally a load.

The control of micro grid is done through a power management system. The system is very prominent in grid connected Micro grid where it switches power to the load from the Micro grid to the main grid depending on availability and demand.

Advantages of Micro grid include, helping reduce the electricity cost to the user, because of the use of renewable energy, Micro grids tend to be more environmentally friendly and finally during peak load periods, Micro grid can help reduce power failure by supplying the extra energy needed. Some of the disadvantages of micro grid are the generated power needs to be stored in a storage system and this can prove to be quite a challenge. Difficulties in synchronizing with the main grid can also arise.

Micro grids can either be direct current (DC), alternating current (AC) or a hybrid type depending on the load requirements [39]. Most of the electrical infrastructure in the world

corresponds the AC power so as most equipment use AC power. Because of this, it is generally more convenient and practical to build an AC Micro grid. In an AC micro grid, the power generated by the renewables which is in the DC form is converted into AC by the use AC converters. DC Micro grid while rare and mostly needed for remote places, are easier to implement technically because the DC power from the renewable is directly fed to the load without the need or considerations of factors such as phase synchronization, reactive power, frequency, and AC converters. Hybrid Micro grid consist of both AC and DC sources and loads.

1.2.4 Micro grid Composition

Micro grids can be composed of different components depending on the renewable energy(s) used [67] and the type of load [68]. Some micro grids are grid connected, others standalone and the type of load can be either AC or DC or both. Here we shall look at the theory behind a simple PV array type micro grid as shown in Figure 7 below and its components.

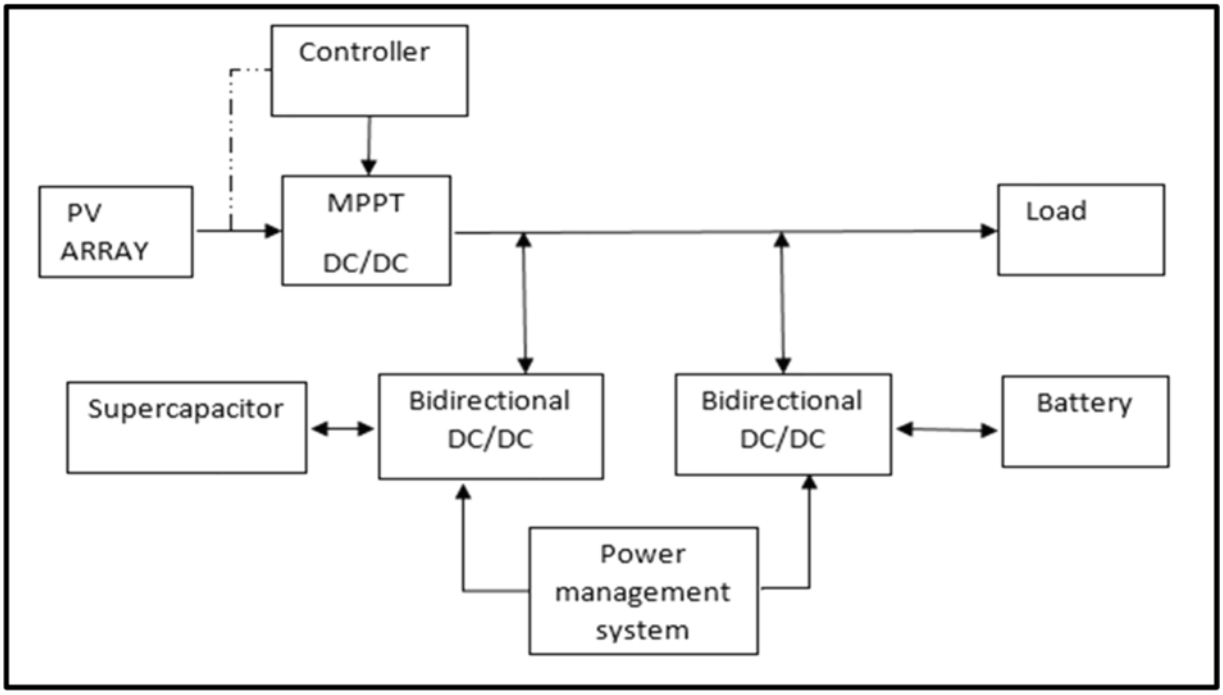

Figure 7 Micro Grid [46]

And Figure 8 below shows the different types of micro grids.

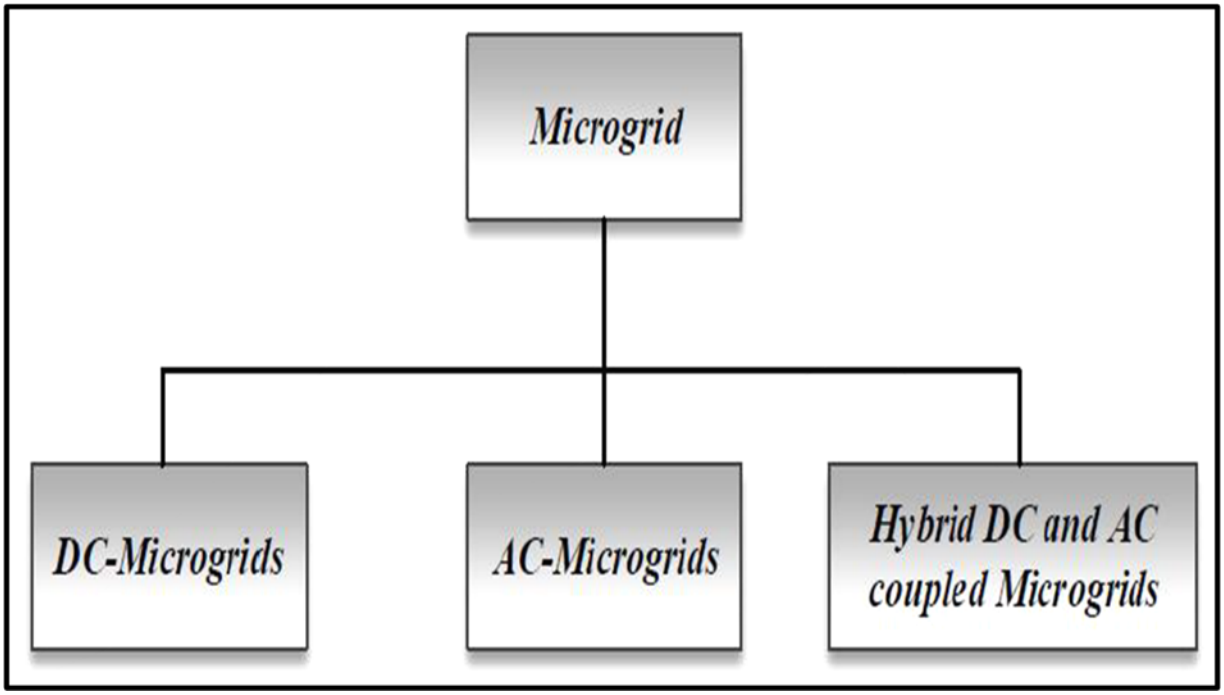

Figure 8 Types of Micro grids [69]

PV array

PV array also known as solar panels convert the energy from the sun into electricity. A PV panel is a collection of PV cells connected as shown in Figure 9 below. PV panels electrically connected together in series or parallel or both form a PV array. The electrical characteristics of a PV array such as the output current are dependent on the solar irradiance and the voltage output is affected by the temperature of the cells.

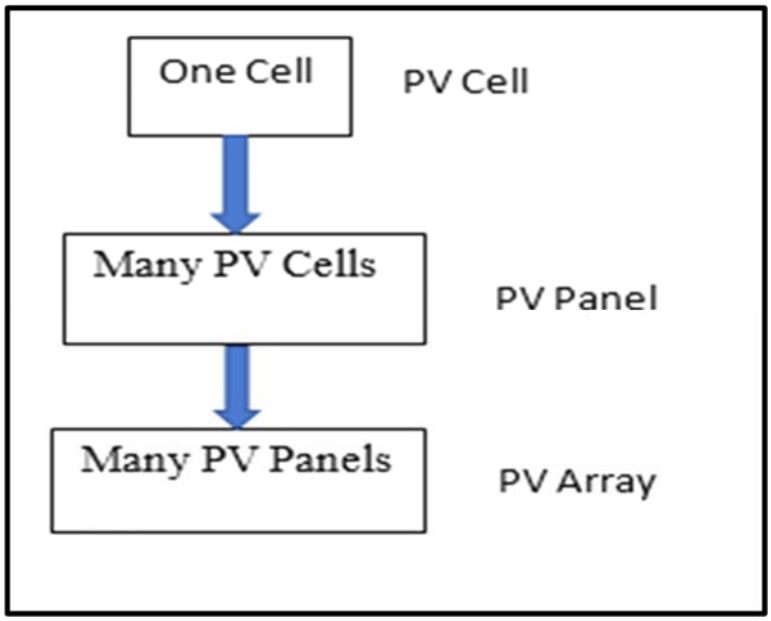

Figure 9 PV Array

Maximum Power Point Tracker (MPPT)

A lot of micro grids use a MPPT for optimization. Basically, an MPPT is like a dc-dc converter that tracks the power mismatches between the solar panels and the battery. Typical solar panels are rated 12V but output anything up to 18V. This is much higher than what is needed by a 12V battery to charge. The mismatch can cause a great loss of power in the system if not handled properly. What the MPPT does is converter the higher panel voltage to the lower battery voltage and at the same time increase the current output to utilize the full power capacity of the PV arrays. The most widely used MPPT technique is the perturb and observe (P&O) technique [70] where the output voltage and current of the PV arrays are tracked and processed.

Buck/Boost converter

Another important component of a micro grid are the bidirectional DC-DC converters. They are used to control the flow of power from source to battery and form battery to source. Figure 10 below shows a buck converter that lowers the output voltage.

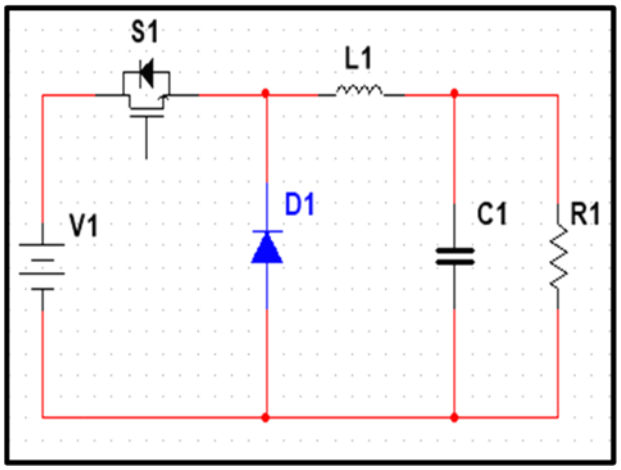

Figure 10 Buck Converter [58]

The DC- DC converter works in the buck mode when the battery is being charged. It lowers the higher output voltage from the PV array/MPPT to a sufficiently lower level to be able to charge the battery

Figure 11 below shows the boost mode which increases the output voltage.

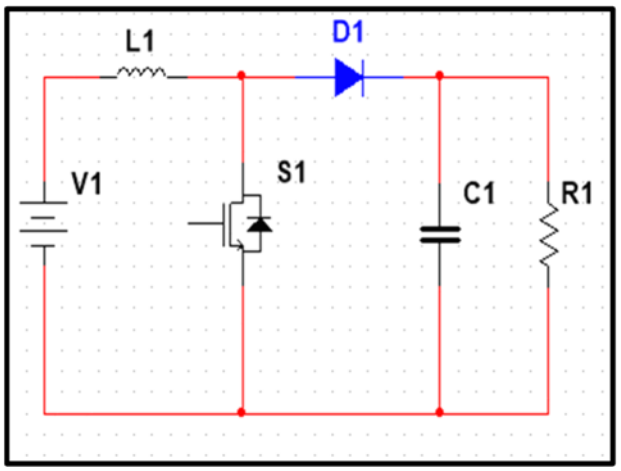

Figure 11 Boost Converter [58]

When the power from the PV array is not available or insufficient, the DC-DC converter works in a boost mode to supply the load the required high voltage. Control methods and voltage sensing circuitry is used in conjunction with the converters to make sure that the correct voltage is always supplied to the load and the battery.

Micro grid energy storage systems

One of the biggest challenges of micro grid is the storing of the energy it produces. Lead acid batteries are used in micro grids to store energy generated by renewables and usually only have a charge/discharge cycle of a few hundreds and thus need to be changed every other year. This adds to the general costs in the use of Micro grids. The battery lifespan is further reduced and affected by the high frequency power demands of the load.

Recent micro grids have employed a HESS which encompasses both a SC and a battery. In [71] different charging methods are used for the supercapacitor which is then combined with PV. The SC is used in HESS systems to help prolong battery life by minimizing the stress put on the batteries by power fluctuations.

Several factors can assist in determining the state and health of lead acid batteries. These include the SOC, temperature, internal resistance, and current limit.

A good way to measure the health of the battery system is by monitoring its SOC [72]. The SOC indicates the available capacity of the battery at any given time. This prevents us for example from over charging the battery which can result to adverse results. A SOC of 1 means the battery is fully charged. Similarly, an SOC of 0 indicates that the battery is fully discharged. Different models and algorisms can be used to estimate the SOC of a battery. The SOC can also be used to plot the ageing mechanism of the battery. Ageing of the battery normally result to an increase in internal resistance of the battery and less battery capacity. This will obviously affect the amount of energy the battery is able to release at any given time.

SOC estimation methods include:

- Direct measurement: This can be done by measuring the open circuit voltage, terminal voltage, or the impedance of the battery.

- Book-keeping estimation: here the coulomb counting method is utilized.

Energy management systems (EMS)

As mentioned earlier, micro grids can go from being standalone and only having one or two renewable energy sources, to grid connected that can similarly have one or two renewable energy sources. To carefully coordinate all these components, micro grids employ an EMS [73]. The EMS monitors the load requirement levels, the power generated from the renewables, the availability of power from the main grid and seamlessly switches from one to the other. The EMS assists in the use of the renewable in a micro grid in an efficient, reliable, stable, smart, and coordinated way [74].

Different EMS implementation methods exist [70] which use maximum power point tracking (MPPT) for efficient energy management. In [75] an energy management system is used in a PV/battery combination to control battery values.

1.3 PROBLEM STATEMENTS

1.3.1 Problem statement 1

Design a Python/MATLAB/Simulink (PMS) hybrid model of an EDLC using equivalent circuit model of a supercapacitor.

1.3.2 Problem statement 2

Use an EDLC together with batteries in a micro grid HESS to reduce battery stress and prolong battery lifespan.

1.3.3 Problem statement 3

Design a simple HESS system using battery, EDLC, DC supply and load.

1.4 Research objectives

The main aim of the research is to design a Python/MATLAB/Simulink hybrid model of an EDLC using the two-branch model of a supercapacitor.

Once we obtain the PMS-hybrid model of the EDLC, the PMS hybrid model will be placed in conjunction with a battery in a HESS system in order to show that the EDLC can be used to reduce the battery stress and improve its lifespan. The project will aim to design a simple HESS model.

1.5 Research Questions

1.5.1 Research question 1

Can we design a Python/MATLAB/Simulink hybrid model of a supercapacitor using the two model?

1.5.2 Research question 2

If an EDLC is combined with a battery in a HESS model, will it improve its lifespan?

1.5.3 Research question 3

Can one design a simple HESS model using a few electronic components such as DC supply, EDLC, Lead acid batteries and a load?

1.6 Research hypotheses

1.6.1 Research hypothesis 1

The charge/discharge profile of an EDLC can be used to derive its parameters.

1.6.2 Research hypothesis 2

The use of SC together with batteries in micro grid HESS systems help prolong battery lifespan.

1.7 Delimitation of the study

1.7.1 Delimitation of the study 1

The study will sorely focus on the characterization of the EDLC and its application in Micro grids HESS systems. It will briefly touch on other areas of EDLC applications such as usage in data storage devices, automobiles but will not go in depth and research.

1.7.2 Delimitation of the study 2

The research will focus on the advantages of HESS energy systems compared to the ESS (battery only) systems and the effect the use of a SC has only prolonging the life of lead acid batteries in standalone DC micro-grids.

- It will briefly touch on but will not depth into the operation of photovoltaic panels and MPPT
- It will not investigate the detail working of bidirectional buck/boost converters.

1.7.3 Delimitation of the study 2

The research will not look at the PV side of the micro grid, only the load demand perspective and do not build a full microgrid system

1.8 Benefit of the study.

The study will give us a better understanding of energy storage devices with particular emphasis on the EDLC.

By characterizing the EDLC, the study will give us an in-depth knowledge of the inner working of the EDLC.

The study will help us understand the use of renewable energy sources and there are utilized in micro grids.

The study will enable us to design a simulation model of the EDLC which can be used to replicate the character of any EDLC.

The study will give us an in-depth knowledge of micro grids systems with focus on how the EDLC plays an important part in the hybrid energy storage systems provide better power, current and voltage stability to the load and increase the lifespan of batteries.

By proposing and designing a simple HESS system for CBI electric, the study will help show how a micro grid using renewable resources can be useful in everyday life situations.

1.9 Methodology

1.9.1 EDLC characterization

The characterization of the EDLC was carried out experimentally and by simulation using the constant current method. Two EDLC of middle range values will be bought and using an experimental setup in the laboratory charge and discharged at constant current to obtain their charge/discharge profiles. The charge/discharge profiles will be used to derive the parameter values of a suitable known electrical equivalent circuit of the EDLC. An EDLC model will be created using a hybrid combination of Python/MATLAB/Simulink (PMS). Testing of the PMS model will be done by simulating it in MATLAB/Simulink using the derived equivalent circuit parameters to obtain simulated charge discharge profiles at constant current. Comparison of experimental charge discharge profiles and simulated charge/discharge profiles to determine accuracy of the proposed PMS model

1.9.2 Hybrid energy storage system (HESS) research methodology

To determine whether the EDLC has an effect in a HESS in reducing battery stress and thus prolonging battery lifespan, experimental extraction of parameters that would be used to build a simulated EDLC model. Then experimentally place the EDLC into the HESS with the battery is done in a laboratory. This will then be followed by setting up, in the laboratory, HESS containing the EDLC and a suitable lead acid battery, to experimentally collect battery data such as voltage, current, SOC, power in a BESS and HESS topology. This will be followed by the comparison of battery data obtained experimentally in BESS and HESS to show the effect the EDLC has on the system.

Following the laboratory experiments, the design of the simulated EDLC model potentially using Python/MATLAB/Simulink and testing of PMS model using EDLC parameters acquired will be carried out. Successful implementation of this, will lead to the encapsulation of the PMS model in a subsystem to be used in the HESS simulation. Battery data collected under BESS and HESS configurations, will be analysed to determine effect of EDLC in HESS.

1.10 Research budget

The total research cost is shown below in Table 2. This includes the cost of laboratory set up and for the simulations

Table 2 Research budget

Item/Activity	**Description**	**Cost (Rands)**
1	Supercapacitors	2000
2	Other Components	1000
3	Breadboards	1000
4	Functional signal generator	Free
5	Agilent digital Multimeter	Free
6	Accessories (Wires, side cutters etc.)	1000
7	Laptop	8000
8	Simulink software	Free
9	MATLAB/Octave	Free
10	Simscape Toolbox	1000
11	Tektronix 4 channel Oscilloscope	Free
12	Internet Research	2000
13	Labour 600 hours at R50/hr.	30000
14	Shunt	Free
15	Bench DC power	Free
16	Resistive load	Free
	Total	**46000**

1.11 Structure of the dissertation

Table 3 shows the times thesis proposal timeline encompassing everything from research on EDLCs, Micro grids, EDLC applications and HESS to name but a few.

Table 3 Proposal Plan

Task	Jan 2021	Feb 2021	March 2021	May 2021	June 2021	July 2021	Aug 2021	Sept 2021	Oct 2021	Nov 2021	Dec 2021
EDLC History research	→										
EDLC composition research		→									
EDLC ADV/DIS			→								
EDLC modelling research				→							
Simulation of models					→						
EDLC parameter acquisition methods						→					
Simulations							→				
EDLC application research								→			
Renewable energy research									→		
Micro grid research										→	
Simulation of HESS system										→	
Different HESS topologies										→	
Finalization of research proposal										→	→

Table 4 below shows the dissertation plan, including the experiments done on the EDLC, the modelling of the EDLC, the work done on the HESS and finally the compilation of the dissertation.

Table 4 Research methodology and thesis write up

Task	Jan 2022	Feb 2022	March 2022	May 2022	June 2022	July 2022	Aug 2022	Sept 2022	Oct 2022	Nov 2022	Dec 2022
EDLC MATLAB research	→										
EDLC experimental testing		→									
Analysis of experimental and simulated results			→								
EDLC parameter acquisition methods				→							
Formation of Simulated PMS EDLC model					→						
HESS Lab experiments					→						
Simulation of HESS using PMS EDLC Model						→					
Conference paper 1							→				
Conference paper 2								→			
Journal article									→		
CBI HESS system										→	
Thesis Writing and submission	→	→	→	→	→	→	→	→	→	→	→

CHAPTER 2

EXPERIMENTAL CHARACTERIZATION, MODELLING, AND PARAMETER EXTRACTION OF SOME SPECIFIC EDLC's

For this study, for the characterization of the EDLC, the "two branch" or Faranda equivalent circuit was chosen as our EDLC electrical representation. Two EDLC's of medium range size, namely the 300 F and 400 F shown in Figure 12 below were chosen for the purpose of extracting their parameters and modelling in Python/MATLAB/Simulink.

Figure 12 EDLC's

The voltage and ESR value of each EDLC is shown in Table 5 below. The values are obtained from its datasheet and will be compared to the value derived from our laboratory experiments.

Table 5 EDLC datasheet values

Capacitance	Max Voltage	ESR
400F	2.7 V	3.2mΩ
300F	2.7 V	6mΩ

2.1 Different EDLC equivalent circuit models and Mathematical equations of the "Two branch Model"

Figure 13 below shows the basic RC model of the EDLC consisting of the equivalent series resistance (ESR), leakage-current equivalent parallel resistance (EPR) and capacitance. As highlighted previously while this model is sufficient for basic EDLC simulations, it doesn't capture well the nonlinear part of the charge/discharge profile which are mainly exhibited in the medium to long time constants.

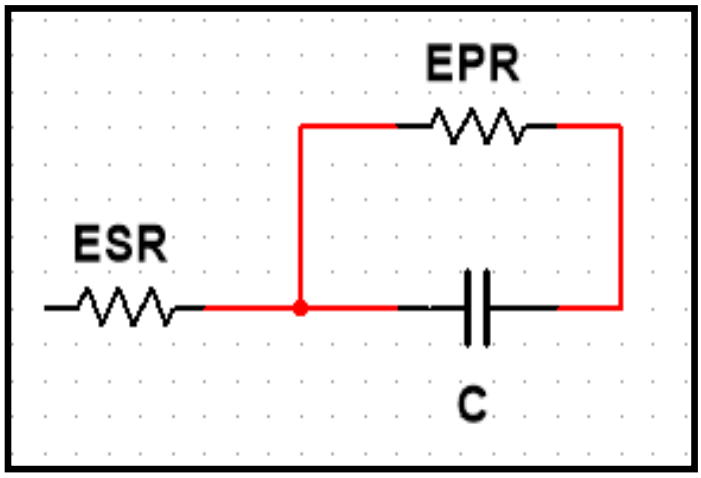

Figure 13 EDLC RC model [17]

A better equivalent circuit model for this application of representing the EDLC and extracting its charge/discharge profile, is the "two branch model "captured below in Figure 14.

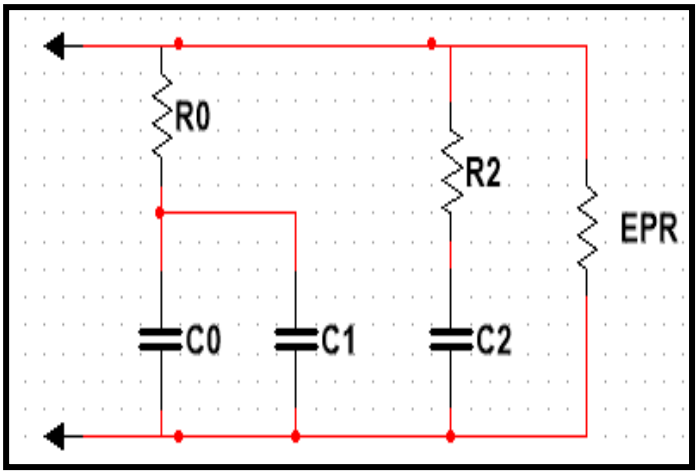

Figure 14 "Two branch" EDLC model [10]

This" two branch" model, which is the chosen model for our research, accurately depicts and shows both the non-linear and linear parts of the charge/discharge profiles under constant current. The "two branch" model gives more detail in the characterization of the supercapacitor.

Another model which can also be used is the "three branch model "shown below in Figure 15

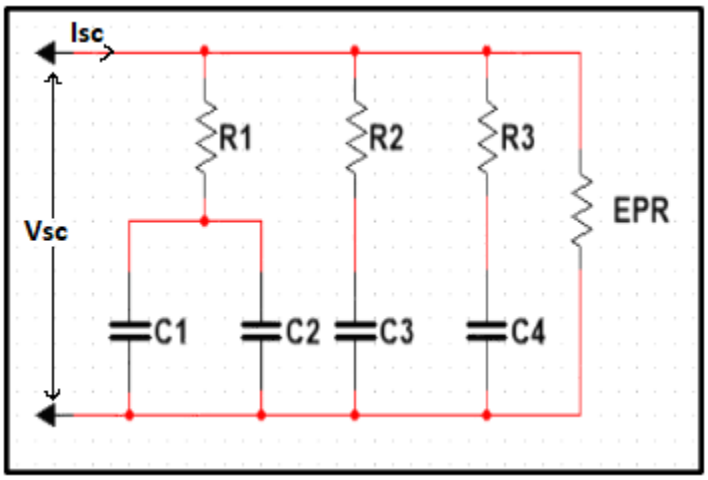

Figure 15 Three branch model [11]

The "three branch model" is an improvement on the "two branch model" and consists of 3 branches that cater for the short term, medium- and long-term behavior of the EDLC during charge/discharge.

The mathematical equations emerging from the two-branch electrical equivalent circuit of the EDLC described in [13] consists of equations (7-10) and represents all the branches of the “two branch” equivalent circuit model.

The voltage V_{sc} across the EDLC cell is represented by:

$$V_{SC} = N_S(V_1 + R_1 \left(\frac{I_{SC}}{N_P}\right)) \tag{7}$$

where N_s the number of SC cells in series, N_p the number of cells in parallel, I_{sc} the current of the Supercapacitor (SC) module and V_1 the voltage across the capacitors in the first branch of the equivalent circuit model [13].

The voltage and charge across the capacitor C_1 in the first branch are calculated using equations (8) and (9) respectively shown below.

$$V_1 = \frac{-C_0 + \sqrt{{C_0}^2 + 2C_v Q_1}}{C_v} \tag{8}$$

$$Q_1 = C_0 V_1 + \frac{1}{2} C_v {V_1}^2 \tag{9}$$

with Q_1 being the total charge accumulated across C_1, C_v the voltage dependent capacitance and C_0 the value of the capacitor in the first Resistance-Capacitance line [13].

Equally the voltage and charge of capacitor C_2 in the second branch are calculated using equations (10) and (11) respectively.

$$V_2 = \frac{1}{C_2} \int i_2 \ dt = \frac{1}{C_2} \int (V_1 - V_2)/R_2 \ dt \tag{10}$$

where C_2 and R_2 the values of the capacitor and resitance of the second branch equivalent circuit. V_2 , I_2 the voltage and current in the second branch [13].

$$Q_2 = V_2 C_2 \tag{11}$$

with Q_2 being the total charge, V_2 the voltage in the branch and C_2 the capacitance in the branch [15].

2.2 Methodology of the EDLC's

The characterization of the EDLC was conducted on two Eaton bussman EDLC's whose datasheet summary is shown in Table 7 below.

Table 6 EDLC's datasheet values

Capacitance	Max Voltage	ESR
400 F	2.7 V	3.2 mΩ
300 F	2.7 V	6 mΩ

2.2.1 Two branch model parameter extraction using circuit experiments

An experiment was setup in the laboratory to get the charge/discharge profiles of the EDLC's with charging performed at a constant current of 2 A till the EDLC's reached their maximum voltages of 2.7 V. Discharging was performed by removing the current and adding a load. By using the charging profile derived, parameters where extracted and used as an input to the "Two branch model" designed in the Python/MATLAB/Simulink (PMS) model. The mathematical equations used in the Python/MATLAB/Simulink PMS hybrid model are described as follows;

The first branch is made up of R_0 and C_1 [10] which cater for the short-term behavior of the EDLC during charging/discharging. To determine the value of the resistance R_0, the change in voltage right at the beginning of the charging profile is divided by the total constant current as shown in (6)

$$R_0 = \frac{\Delta V}{I_C} \tag{12}$$

with Δv being the change in voltage and I_c the charging current [10].

The capacitance C_1 consists of a capacitor C_o and a voltage dependent capacitor k_v. These are calculated by taking two points on the charge profile $\mathrm{P}_1(\mathrm{t}_1, \mathrm{v}_1)$ and $\mathrm{P}_2(\mathrm{t}_2, \mathrm{v}_2)$ as shown in Figure 16 and substituting the values in (13) and (14). Experiments done in [10] have shown that its good practice is to chose P_1 and P_2 at 1.2 V and 2.3 V respectively for a 2.7 V Supercapacitor.

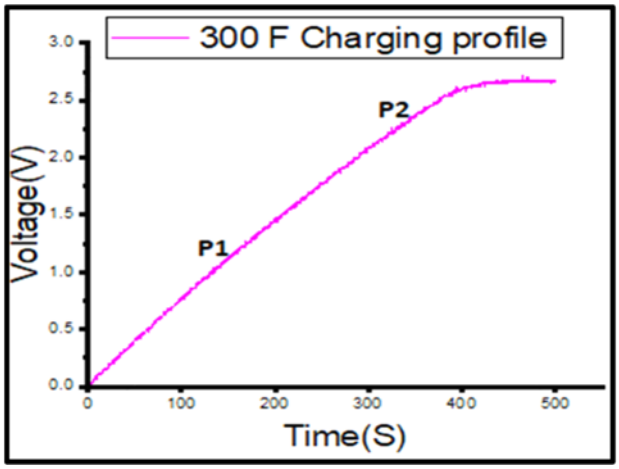

Figure 16 Charge profile points for parameter extraction

$$C_0 = \left(\frac{t_1}{V_1} - \frac{V_1.t_2 - t_1.V_2}{{V_2}^2 - V_1.V_2}\right).I_C \tag{13}$$

where V_1 is equals to 1.2 V and t_1 is the time at V_1 , V_2 is 2.3 V and t_2 is the time at V_2, and I_C is the charging current [10].

The value of k_v which is the voltage dependent capacitance is derived using equation (14)

$$k_v = 2.\left(\frac{V_1.t_2 - t_1.V_2}{V_1{V_2}^2 - {V_1}^2.V_2}\right).I_C \tag{14}$$

The second branch of the "two branch model" [10,15] is calculated using (15), consists of R_2 and C_2 ,catering for the long-term behaviour of the EDLC during the charging/discharging process [10].

$$\tau_2 = R_2 C_2 \tag{15}$$

A good value for time constant τ_2 is normally 240 s which is an estimated value based on the capacitance of the supercapacitor used in this case. C_2 is calculated using equation (16)[10].

$$Q_{tot} = I_C . T_C = C_2 . V_{2f} + \left(C_0 + \frac{k_v}{2} . V_{2f}\right) . V_{2f} \tag{16}$$

where Q_{tot} is the total EDLC accumulated charge, I_C the charging current, $\mathrm{V_{2f}}$ is measured at three times τ_2 and $\mathrm{T_C}$ is the time constant [10].

After calculating the value of C_2 , equation (15) is used to get the value of R_2.

2.2.2 Python/MATLAB/Simulink (PMS) hybrid model

Having acquired the parameter values of the supercapacitors for the two-branch equivalent model from the experimental laboratory wired circuit. An algorithm to model the EDLC was developed which was the python/MATLAB/Simulink (PMS) hybrid model using the same standard mathematical equations of a supercapacitor. The parameters from the experimental wired set up were used as inputs to the PMS model. The algorithm designed in the Python/MATLAB/Simulink (PMS) model was used to obtain a simulation model of the EDLC's. The PMS model was then simulated to acquire a charge profile for the supercapacitor. The key to the workings of the PMS model was in finding a solution for the differential mathematical equations that represent the supercapacitor using python programming. Comparison was made between the experimental data charge/discharge curves and PMS data charge/discharge curves of the supercapacitors to determine how accurate the model and its underlining algorithm really was.

2.2.3 Equivalent series resistance (ESR) and capacitance Calculation

The equivalent series resistance (ESR) and capacitance for the 300 F and 400 F EDLC's were calculated using the discharge profiles acquired both experimentally and by simulation and compared to datasheet values.

The ESR is measured at the beginning of the discharge profile using (17), with ΔV being the immediate drop in voltage observed on the discharge profile when a load is connected drawing a current ΔI [16].

$$ESR = \frac{\Delta V}{\Delta I} \tag{17}$$

The capacitance is determined using equations (18) and (19) using the linear part of the discharge profile.

$$C = \frac{\Delta Q}{\Delta V} \tag{18}$$

ΔQ the change in total charge and $\Delta V$the change in voltage [16]

The change ΔQ and ΔV are determined by taking two-time instants t_1 and t_2 in the linear part of the charge/discharge curve.

$$C = \frac{\int_{t_1}^{t_2} i\,(t)\,dt}{v_1 - v_2} \tag{19}$$

with V_1 the voltage at t_1,V_2 the voltage at t_2 and i the charge/discharge current [16].

2.3 Experimental setup

2.3.1 Parameters acquisition procedure and experimental setup

The experimental set up in the laboratory that is used to derive the EDLC's charge/discharge profile is shown in Figure 17. This charge/discharge profile is used to characterize the supercapacitors. The equipment used includes a Tektronix four channel digital storage oscilloscope with a bandwidth of 40 MHz and a sampling rate of 1 GS/s. A delta electronix 15 V 10 A adjustable DC current source to provide the constant current to charge the EDLC during the charging process. A 5.2 Ω, 20 W, variable resistor to act as a

load during the discharging process and a digital multimeter used to measure voltage across the EDLC and the current during the charge and discharge process.

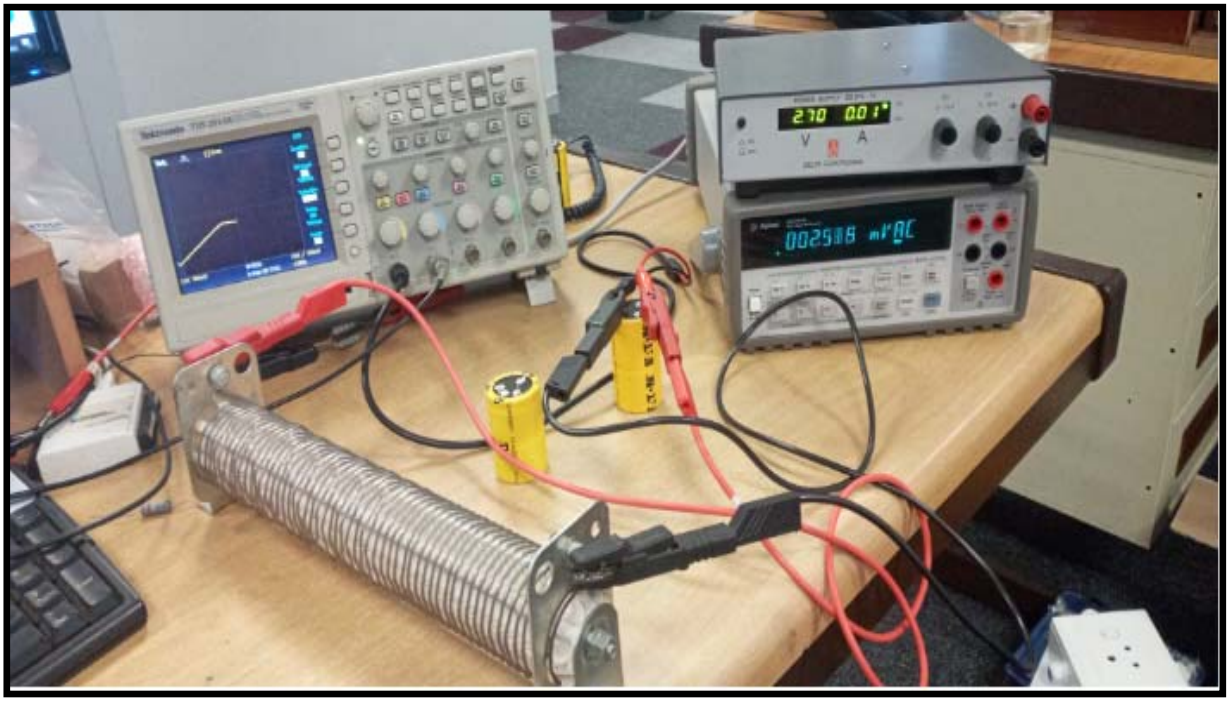

Figure 17 Laboratory experimental setup

During the charging process the current source was connected to the EDLC and the load disconnected. The EDLC was then charged at a constant current of 2 A till it reached its maximum voltage of 2.7 V. During the discharge process, the charged EDLC was disconnected from the current source and connected to the load, which was a variable potentiometer whose resistance was adjusted to 1.35 Ω to allow the EDLC to discharge at a current of 2 A.

2.4 Results

2.4.1 Experimental results

The experimental charge profile of both the 300 F and 400 F were acquired at 2 A constant current and shown in Figure 18. The 300 F ELDC clearly has a higher gradient curve and charges faster than the 400 F.

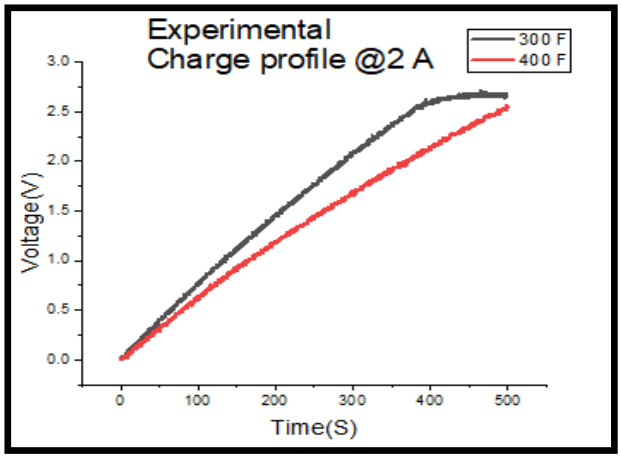

Figure 18 Experimental 300 F and 400 F charge profiles

The charge profile and data derived during the experiment were used to calculate the parameters/coefficients of the EDLC's two branch equivalent circuit. The results are shown in Table 7.

Table 7 EDLC parameters

Parameter	Eaton 300 F	Eaton 400 F
R_1[Ω]	0.01	0.01
C_0[F]	243.42	297.05
k_V[F/V]	50.4	70.46
R_2[Ω]	12.26	8.77
C_2[F]	19.57	27.36
EPR[Ω]	N/A	N/A

Similarly, the discharging of the EDLC was conducted at constant current of 2 A using 1.35 Ω load. The discharge profiles captured in Figure 19.

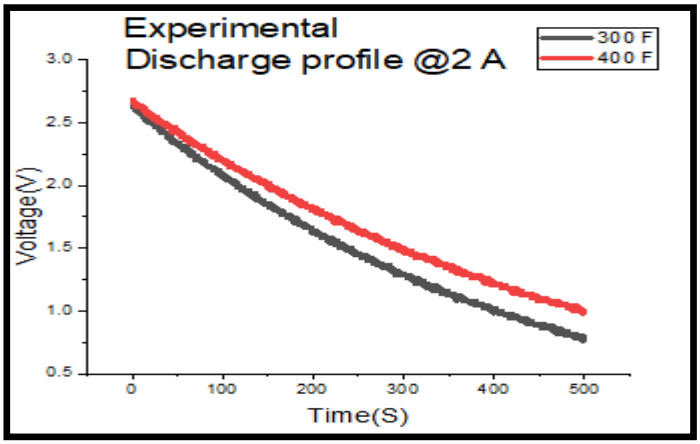

Figure 19 Experimental 300 F and 400 F discharge profile

As was expected, the 300 F EDLC discharges at a faster rate that is within a shorter time than the 400 F shown by the gradient being higher. The data from the discharge profile was used to calculate the ESR and capacitance for the respective EDLCs, the results of these are shown in Table 8

Table 8 Results 300 F and 400 F

	300 F	**400 F**
Load[Ω]	0.280	0.280
Current[A]	2	2
V_1[Volt]	2.752	2.744
V_1[Volt]	2.688	2.704
ΔV [Volt]	0.064	0.040
ESR [Ω]	0.0065	0.00408
Capacitance[F]	319 F	421 F

2.5 Conclusion.

The two port parameters of the supercapacitors where extracted. The charge/discharge profiles of a 300 and 400 F supercapacitors where given experimentally.

CHAPTER 3

DESIGN AND MODELLING OF THE EDLC'S USING THE PYTHON/MATLAB/SIMULINK (PMS)-HYBRID MODEL

This chapter deals with the design of the Python/MATLAB/Simulink (PMS)-hybrid model [76] which is used to characterize or model the 300 F and 400 F supercapacitors using the parameters extracted experimentally in the previous chapter as inputs to the PMS model. Figure 20 shows the layout of how the idea was implemented.

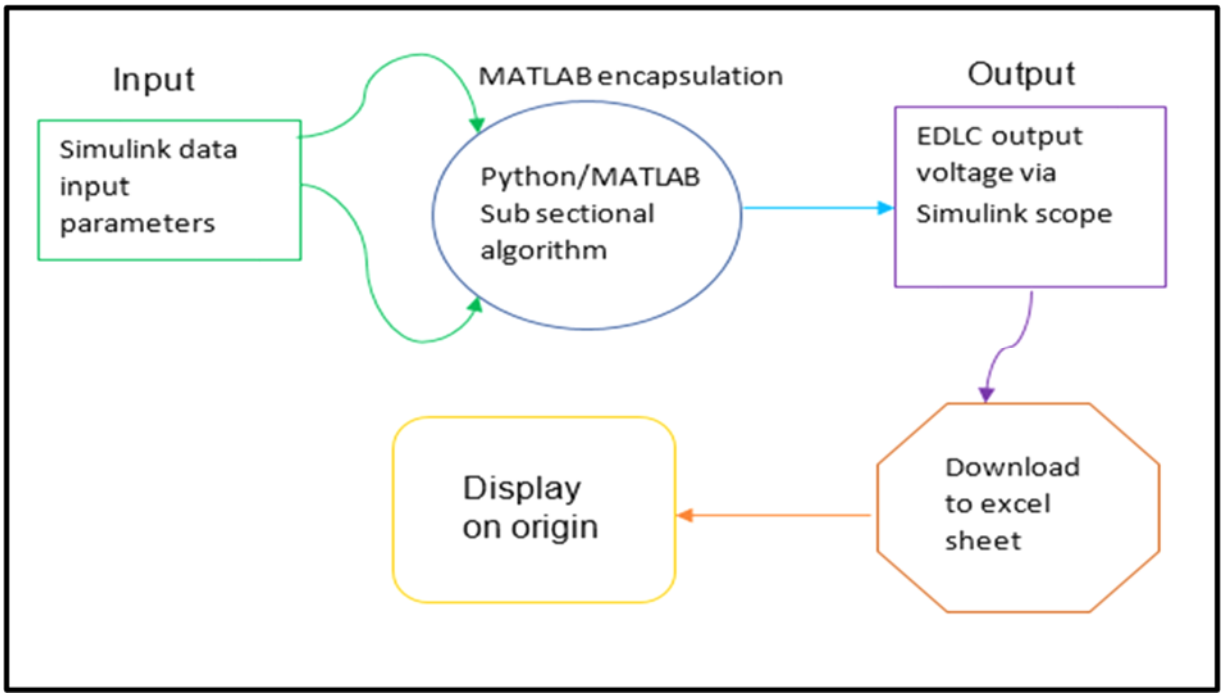

Figure 20 PMS model of a supercapacitor

The PMS model was envisioned as a different way from the widely used MATALB/Simulink method to model the EDLC. Analysis of previous models and the characteristics of the EDLC revealed the presence of 2 differential equations, as it will be discussed in more details later, which use the derived inputs to produce the exponential features of the charge/discharge profile of the EDLC. While this is easily and widely solved

in MATLAB/Simulink, the idea of solving the equations in a python code encapsulated in MATLAB by accessing the input parameters in Simulink and returning the final EDLC voltage Simulink, was both very appealing and provided many engineering problems to solve.

3.1 Model Description

A flowchart of the of the EDLC's mathematical model is shown in Figure 21. It consist of the derived parameters represented using the color green extracted from the experimental circuit. The input constant current is in violet and the output voltage is in red. The circle in orange represents the "feedback loop" and contains the variables Q_1 , Q_2 , V_1 and V_2 which are co dependent on each other. With Q_1 being the charge on capacitor C_1, Q_2 the charge on C_2. V_1 and V_2 being the voltages on the aforementioned capacitors respectively.

In the flowchart the input current is divided by the number of EDLC cells in parallel which in this case are set to one in code. The result of this is used as an input to the feedback loop. In the feedback loop, values of the codependent variables Q_1 , Q_2 , V_1 and V_2 , are calculated. This feedback loop is responsible for the exponential increase of the EDLC's voltage when constant current is applied.

The output of the feedback loop V_1 is then added and multiplied by the number of EDLC cells in series. In this case the number of EDLC cells in series is set to one, to provide an output which is the voltage across the EDLC.

This feedback loop and the division and multiplication of the EDLC cells is done using python code, subsequently the python code is encapsulated into MATLAB code in order to use the input and output functionality of Simulink to collate the data, thereby generating the PMS model. This procedure is summarized in the flow diagram shown in Figure 21 below.

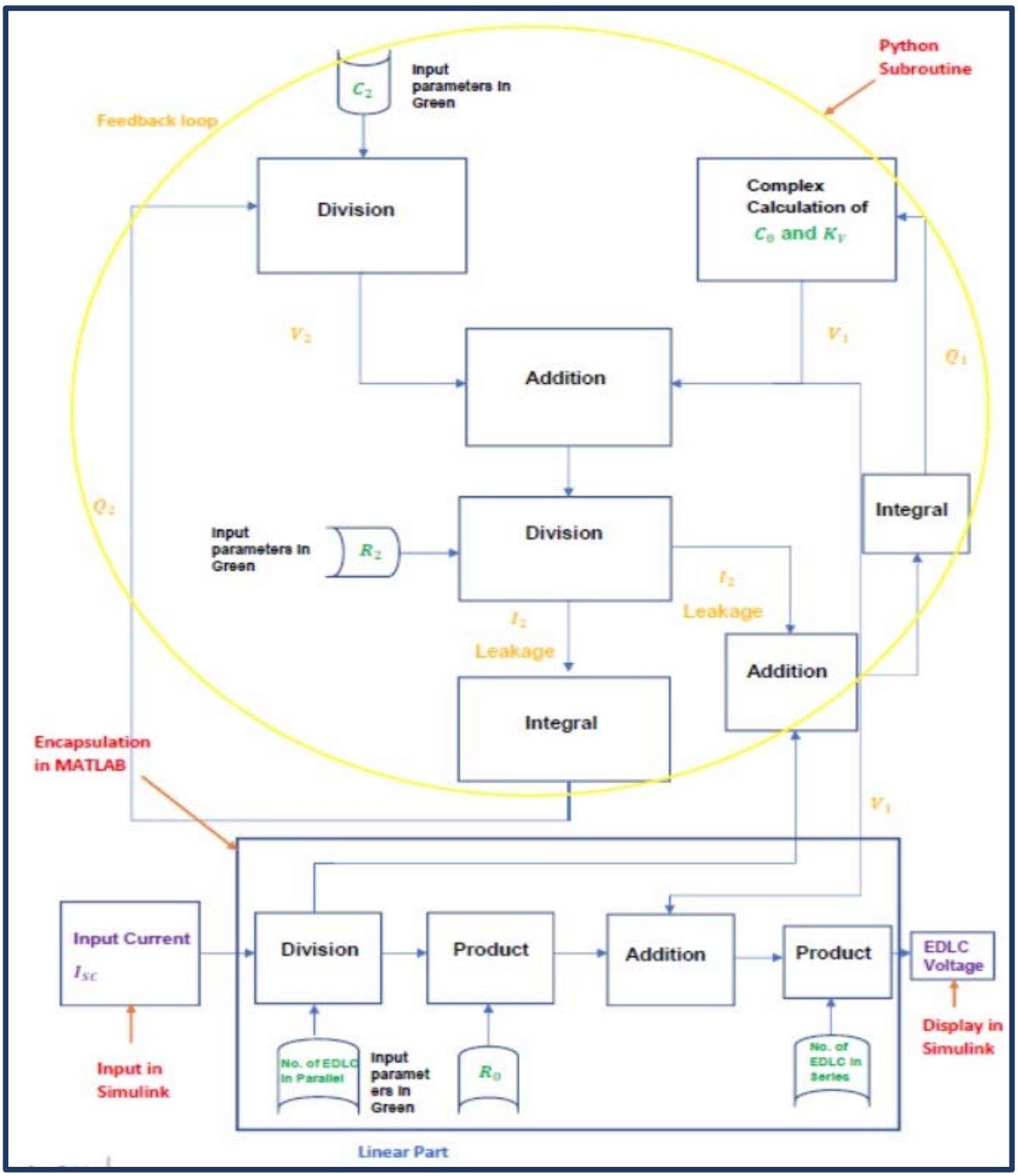

Figure 21 PMS EDLC flow chart/Algorithm

To get the values of the variables in the feedback loop the differential equations (20) and (21) [13, 15] were solved using code in python.

$$\frac{dQ_1}{dt} = \frac{I_{sc}}{N_p} - \frac{V_1 - V_2}{R_1} \quad (20)$$

$$\frac{dQ_2}{dt} = \frac{V_1 - V_2}{R_2} \quad (21)$$

These differential equations show the relationship between variables Q_1 , Q_2 , V_1 and V_2 and are what gives the EDLC its unique characteristics. The code in python takes in the parameters, that in this case are the two-branch model derived parameters. The differential equations are then solved using python programming. The values of Q_1 and Q_2 at any given point in time are return in a python list and used to calculate the value of V_1 and V_2.

A MATLAB code is used to import the python code into a MATLAB block function encapsulating the code and using the Simulink to display the input and output functionality

Figure 22 below shows the Python/MATLAB/Simulink (PMS) model consisting of the python/MATLAB function together with Simulink constant block for the values of the parameters and a scope and display to show the output voltage values.

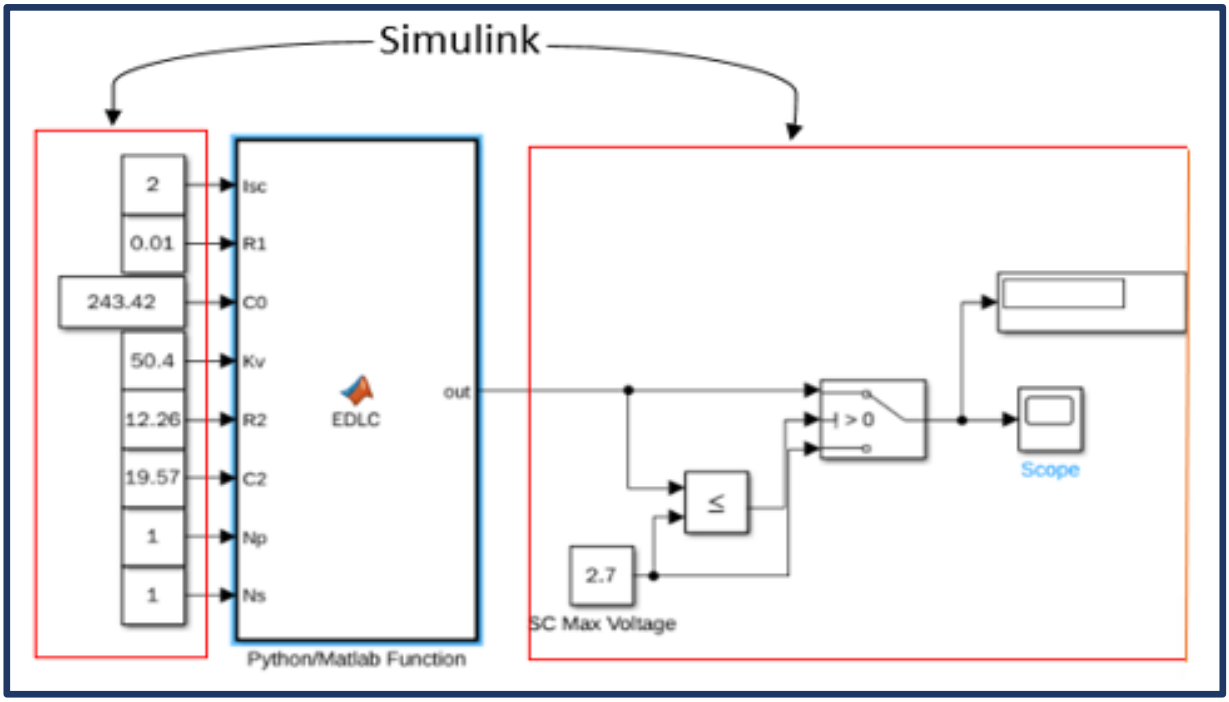

Figure 22 Python/MATLAB/Simulink (PMS) model

3.2 Simulation results

The simulated PMS charge/discharge profile for both the 300 F and 400 F is shown in Figure 23. The simulation was done at a constant current of 2 A. The 300 F charges faster, that is within a shorter time as can be seen by the higher gradient in charging and also discharges faster, that is within a shorter time as can be seen by the higher gradient in Figure 23.

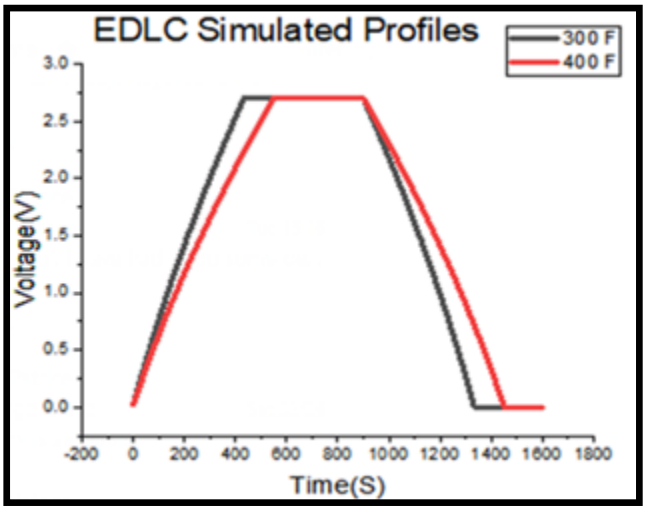

Figure 23 Simulated PMS charge/Discharge profile

3.3 Superimposition of Experimental Charge/discharge profiles on Simulated PMS Charge/discharge profiles

The results showed similarity between the experimental and simulated PMS charge profiles. Figure 24 shows the charge curve for the 300 F EDLC for the experimental circuit and for the simulated PMS model superimposed. This figure shows the two curves in a near perfect fit/match. This verifies the correct extraction of parameters from the live experimental wired set up to develop the PMS model.

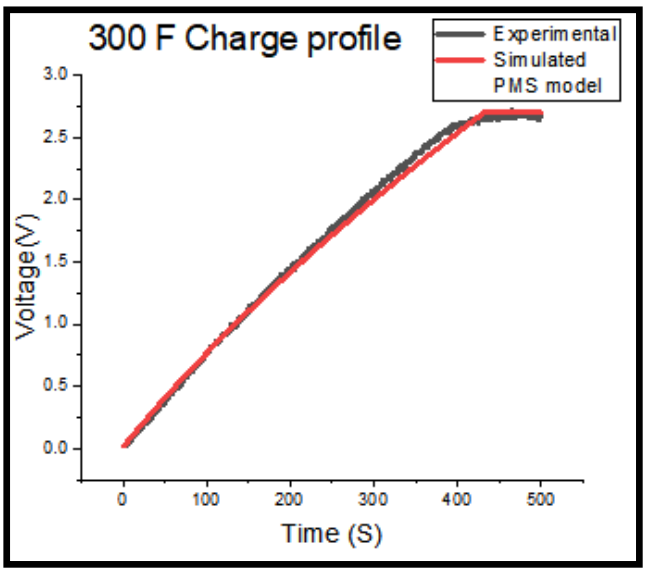

Figure 24 300 F EDLC superimposed experimental/PMS charge profile

Figure 25 shows the charge curve for the 400 F EDLC for the experimental circuit and for the simulated PMS model superimposed. This figure shows the two curves again show a nearly perfect fit/match. This again, verifies the correct extraction of parameters from the live experimental wired set up to develop the PMS model.

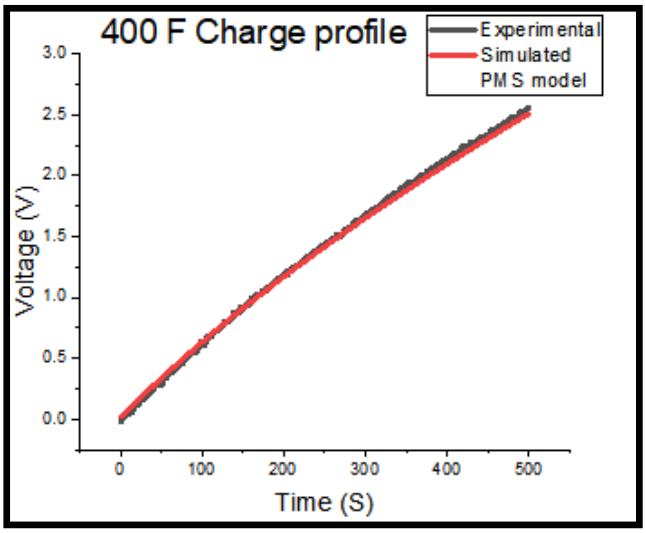

Figure 25 400 F EDLC superimposed experimental/PMS charge profile

Very noticeable is that the charge time for the two specific EDLC's namely the 300 F and 400 F EDLC's is quite large making the EDLC very useful to act as a buffer between the source voltage and battery in a microgrid system to improve battery life.

The two discharge profiles for the 300 F supercapacitor, that is for the experimental circuit and for the PMS model shown in Figure 26 are similar and show a nearly perfect match except for a slight deviation. This deviation arises as a result of the fact that the experimental discharge curve for the 300 F supercapacitor is a real-life representation of the supercapacitor while the PMS model is a simulation obtained from extracted parameters which summarizes the curve. The second reason for the deviation can be explained by the fact that the parameters are obtained from the charge profile not the discharge profile. The reason for this is because the parameters have to be entered once in the simulation EDLC model when it is used as a subcomponent in the HESS system in the future. Therefore, the parameters obtained from the charge profile will never be a perfect representation of the discharge profile.

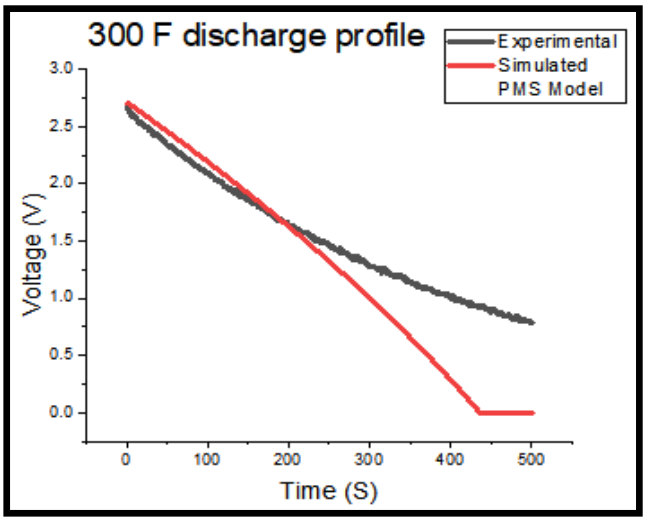

Figure 26 300 F combined experimental/PMS discharge profile

The same analysis applies to the two discharge profiles namely the experimental and simulated PMS model for the 400 F supercapacitor in Figure 27.

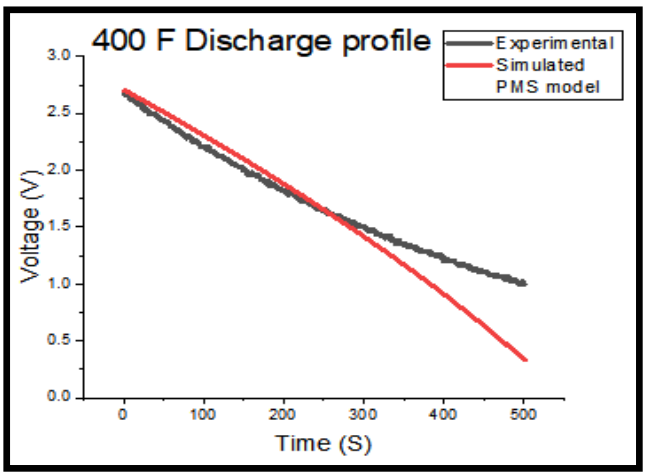

Figure 27 400 F combined experimental/PMS discharge profile

3.4 ESR and Capacitance results

The equivalent circuit parameters of the two-branch model obtained as per the procedure described in [10], for both the 300 F and 400 F Eaton busman EDLC's were found to be consistent with similar range datasheet EDLC values. The data showed that as the total capacitance of the EDLC increase so do the values of C_O , K_V and C_2. While the value of R_2 decreases.

The calculated ESR and capacitance of the 300 F and 400 F EDLCs showed a slight deviation from the values provided in the datasheet as shown in Table 9 below. This might be due to factors emanating from the laboratory set up such as contacts, reading meters, human error and variations in other factors that may differ from perfect clean room setups used to obtain datasheet values.

Table 9 ESR and Capacitance

	300 F		**400 F**	
	ESR (mΩ)	**Capacitance (Farads)**	**ESR**	**Capacitance (Farads)**
Datasheet	6 mΩ	300 F	3.2 mΩ	400 F
Experimental	6.5 mΩ	319 F	4.0 mΩ	421 F

The 5 % error in the ESR and Capacitance values in table 9 above is as a result of the fact that the experiment is not conducted in an ideal setting. So, the supercapacitors are charged /discharged through a load which is a potentiometer with coils. These coils might introduce a hysteresis in the EDLC, which when we calculate would lead to a 5 % error.

CHAPTER 4

EXPERIMENTAL EXTRACTION OF PARAMETERS FOR A SUPERCAPACITOR (EDLC), 65 F, 16.2 V AND LIVE EXPERIMENTAL IMPACT OF THIS EDLC ON BATTERY LIFESPAN IN A HESS

This chapter investigated the effect of the EDLC on the reduction of battery stress and thus prolonging battery lifespan in a hybrid energy storage system (HESS). An experimental setup was done in the laboratory where a 65 F, 16.2 V EDLC, an 8 Ah, 12 V lead acid battery were connected to a 5.2 Ω, 20 W, variable resistor load to form a HESS. The 65 F 16.2 V EDLC was chosen because it can handle the 12 V from the power supply source, while also being not too large of a storage device with regards to the capacitance in farads but large enough to show an effect on battery stress reduction

Lead acid battery datasheet parameters shown below in Table 10

Table 10 Lead acid battery datasheet parameters

Parameter	Value
Rating (Ah)	8
Voltage (V)	12
Total charge (Coulombs)	28800

It can be seen that the lead-acid battery is rated 8 ampere hours with a maximum voltage of 12 V. The lead acid battery also has at full capacity a total charge of 28800 coulombs.

EDLC datasheet values shown below in Table 11. The EDLC has a capacitance of 65 Farads and a maximum voltage of 16.2 V although, for the laboratory experiment the voltage will be limited to 12 V and pre-charged to 12 V to be compatible with the lead acid battery and power supply eliminating the use of DC/DC bidirectional converters.

Table 11 EDLC datasheet parameters

Parameter	Value
Capacitance (F)	65
Voltage (V)	16.2

4.1 Extraction of EDLC parameters

The first part of the laboratory experiment was to extract the 'two branch" equivalent circuit parameter values of the new 65 F 16.2 V EDLC as done previously in chapter 2 for the 300 F and 400 F EDLC's. This was crucial for the later use of these parameters to simulate Model the HESS EDLC and simulate the HESS in MATLAB/Simulink. The same process of charging/discharging the EDLC using constant current and obtaining its charge/discharge highlighted in chapter 2 was followed.

4.1.1 Results EDLC parameter extraction

The graph in Figure 28 below shows the EDLC's experimental charge profiles obtained at 5 and 10 A constant current, and super imposed on each other. It can be clearly seen that the 10 A graph has a much higher gradient than the 5 A graph resulting in it reaching the EDLC's maximum voltage of 16.2 V quicker. This is consistent and accurate reflection of charging the EDLC at a higher current.

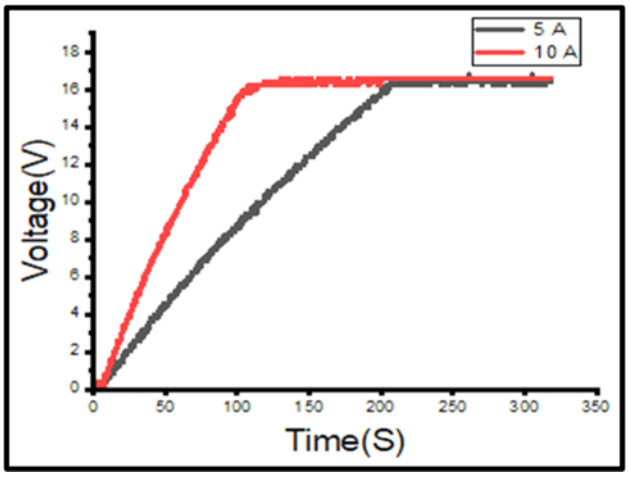

Figure 28 EDLC's Experimental charge profile at 5 A and 10 A

The experimental discharge profile of the EDLC is shown in Figure 29 below obtained at 5 and 10 A constant current. As expected, the EDLC discharges faster at a higher current, 10 A then at 5 A resulting in a higher gradient 10 A discharge profile.

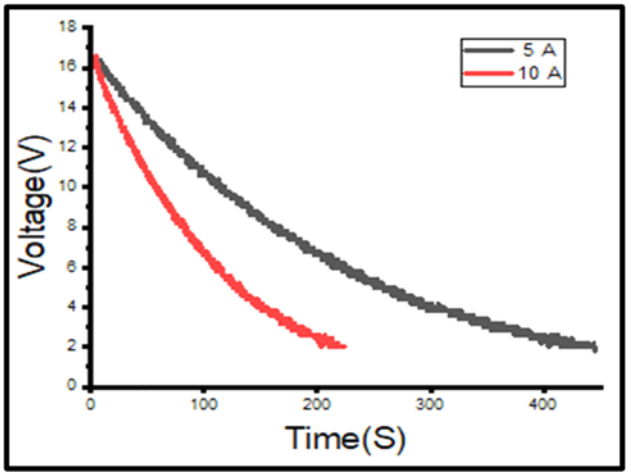

Figure 29 EDLC's Experimental discharge profile at 5 A and 10 A

The Table 12 below shows the equivalent circuit parameters of the HESS EDLC derived from the charge profile at 5 A constant current.

Table 12 EDLC derived parameters at 5 A

Parameter	**Value**
C0 (F)	51.2362
KV (F/V)	1.3541
C2 (F)	16.7331
R2 (Ω)	5.9762
R0 (Ω)	0.06

The values obtained at 5 A correlated for similar range EDLC with the values of C0, KV and C2 adding up to almost the total capacitance value as expected. The ESR value represented by R0 is also within acceptable limits.

The Table 13 below shows the EDLC's parameters derived from 10 A constant current

Table 13 EDLC derived parameters at 10 A

Parameter	Value
C0 (F)	56.3636
KV (F/V)	1.0101
C2 (F)	19.2031
R2 (Ω)	2.6037
R0 (Ω)	0.06

Slight differences can be observed in the equivalent circuit values of C0, KV, C2 and R2 for 5 and 10 A, but otherwise like the 5 A values, the 10 A parameters too, correlate to similar types in literature and are within acceptable ranges.

4.2 Design of the experimental HESS model

After deriving the HESS EDLC parameters, the second part of the laboratory experiment was to build a HESS. The experimental HESS components included the 65 F 16.2 V EDLC, a lead acid battery which are the main components of the HESS, a variable DC power supply to charge our battery and EDLC, a 5.2 Ω, 20 W, variable resistor load that can be setup to draw constant or variable current, a 20 A 200 mV shunt to measure the current drawn by the load and finally a 4 channel 20 MHZ Tektronix oscilloscope to capture the circuit voltage and current .A block diagram of the setup is shown in Figure 30 below

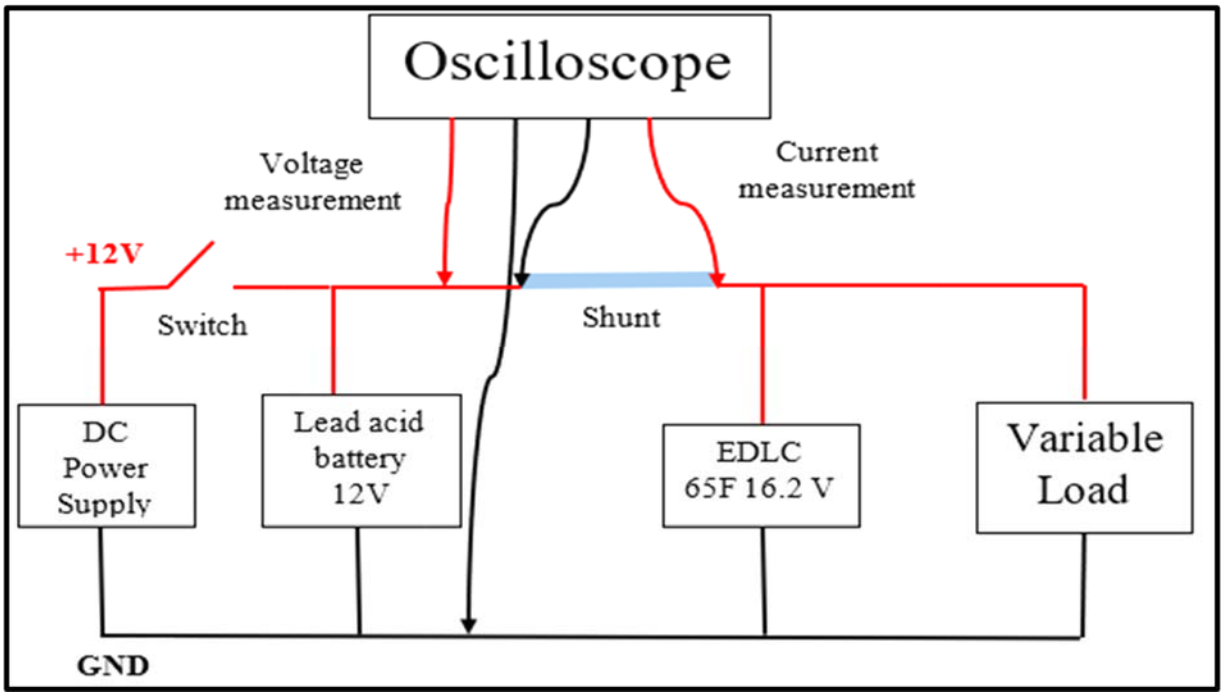

Figure 30 Experimental HESS block diagram

And Figure 31 Below shows the actual laboratory experiment with the EDLC, lead acid battery, shunt, oscilloscope, and variable load clearly seen. During the experiment, firstly both the battery and the EDLC are charged to 12 V through the power supply. As highlighted previously the charging of the 16.2 V EDLC was done at 12 V to avoid the addition of a DC-DC converter which was not designed. For the discharge process, the power supply is disconnected, and the load connected allowing the battery and EDLC to simultaneously discharge.

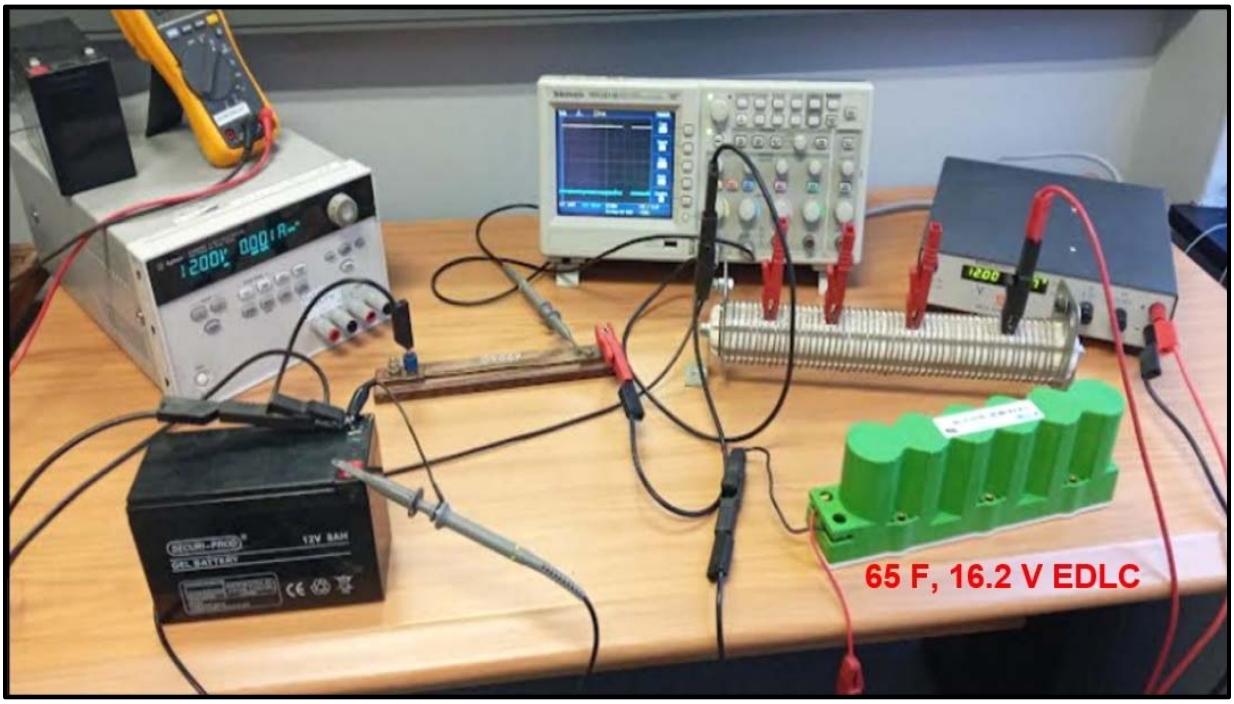

Figure 31 HESS laboratory setup

The experiment consisted of firstly connecting only the fully charged battery in the circuit in a battery energy storage system (BESS) configuration and collecting its voltage, current, power, charge use and state of charge (SOC) under constant load current. The equations (22-25) below of charge and SOC were used for our calculations.

Derived from [13, 61, 77], Total coulombs,

$$Total\ coulombs = 8\ Ah\ \times \frac{60\ min}{hr} \times \frac{60\ s}{min} \tag{22}$$

where Ah is the battery rating and I total coulombs is the maximum charge, the battery holds.

Derived from [13, 61, 77], charge used,

$$charge\ used = I\ \times\ \Delta t \tag{23}$$

where I is the total current and Δt is the time duration.

Derived from [13, 61, 77], battery charge remaining,

$$Battery\ charge\ remaining = total\ charge - charge\ used \tag{24}$$

Derived from [13, 61, 77], SOC,

$$SOC = \frac{total\ coulombs - \ coulombs\ used}{total\ coulombs} \times \ 100\% \tag{25}$$

where SOC is the state of charge of the battery

After doing the BESS experiement , the EDLC was added to the circuit by connecting it in parallel to the battery to turn it into a hybrid energy storage system (HESS). The voltage, current ,power , battery charge used and SOC were measured and derived similar to the BESS experiment. Comparison was then made between the battery data obtained under BESS and the battery data obtained under HESS to determine any similarity or difference.

Adding on to the above ,the laboratory experiement was repeated for both BESS and HESS under a variable load conditon , to provide a variable current with the voltage and current results recorded.

4.3 Results HESS laboratory experiment

4.3.1 Constant current results

The voltage results obtained experimentally for both the BESS and HESS are captured in Figure 32 below.

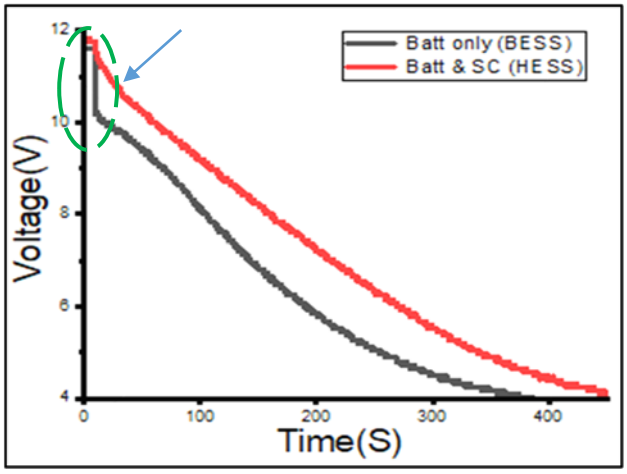

Figure 32 Experimental BESS and HESS voltage superimposed

The BESS graph shows an immediate deeper drop in voltage, highlighted in the green dashed circle, while the load is connected. This voltage drops although also noticed on the HESS, it's however less deep by 16.6 %. The decrease in voltage is also more gradual in the HESS than in a BESS configuration

The current results obtained experimentally for both the BESS and HESS are captured in Figure 33 below

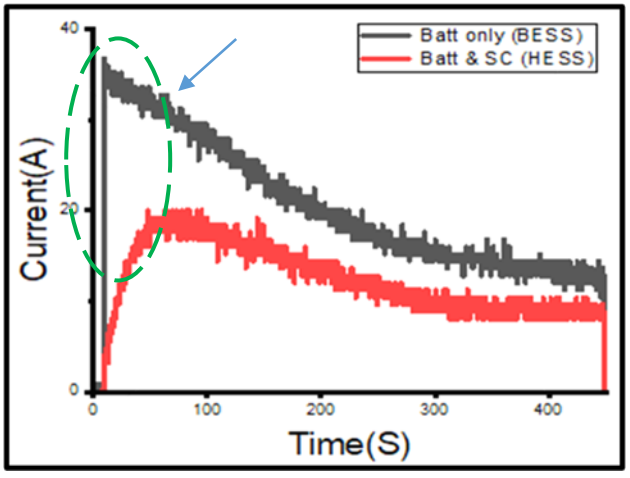

Figure 33 Experimental BESS and HESS currents superimposed

The green dashed circle shows that, the in rush current experienced by the battery in a BESS went as high as 37 A. And this increase in current was almost immediate. While in

a HESS the battery current drawn is almost 48.6 % lower, rises much slower with no sudden in rush current due to the presence of the EDLC.

The power results obtained experimentally for both the BESS and HESS are captured in Figure 34 below

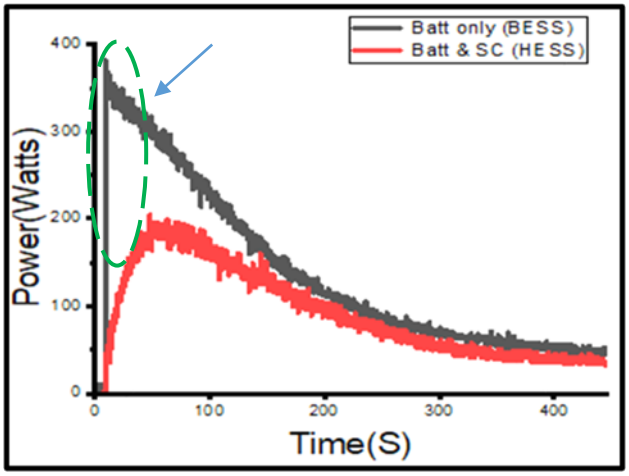

Figure 34 Experimental BESS and HESS power superimposed

It can be seen that the power drawn from the battery in the BESS is much high than a HESS and rises almost instantaneously

The charge used results obtained experimentally for both the BESS and HESS are captured in Figure 35 below

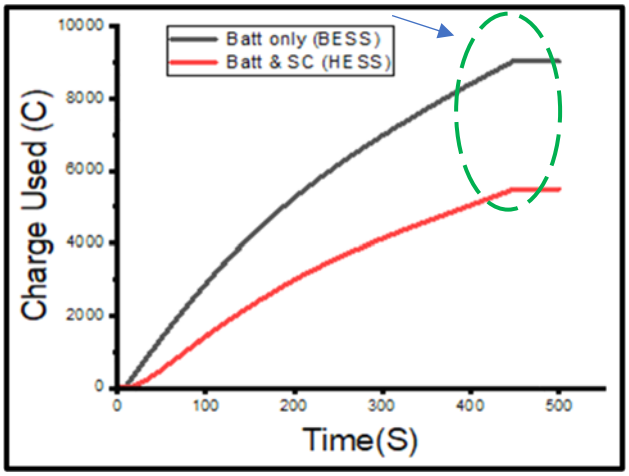

Figure 35 Experimental BESS and HESS charge used superimposed

In a HESS configuration, the amount of charge used from the battery during the discharge process is less than a BESS configuration as shown in the dashed green circle. The "charge used" curve in a BESS has a much steeper gradient than the HESS curve. Also, the HESS graph shows a reduced cumulative battery charge used at the end of the experiment (500 s) compared to the BESS.

The state of charge (SOC) results obtained experimentally for both the BESS and HESS are captured in Figure 36

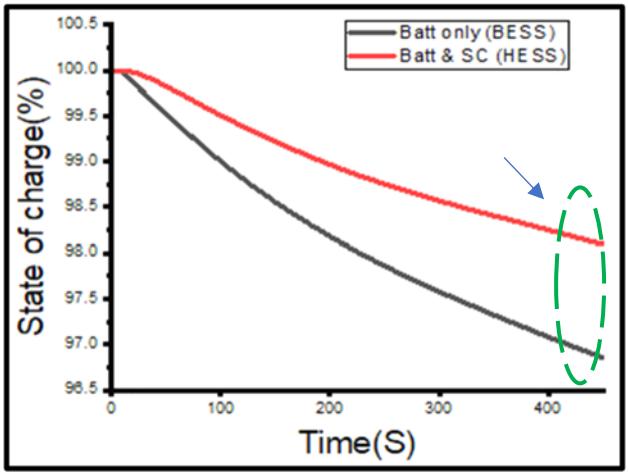

Figure 36 Experimental BESS and HESS SOC superimposed

The battery state of charge (SOC) as observed in a BESS decreased much faster with a steeper gradient than the HESS configuration. At the end of 500 s duration of the test, the final battery HESS SOC was higher (98.25 %) than the SOC of the battery in a BESS (96.75 %). This is a difference or an "improvement" of 1.50 % in the SOC.

4.3.2 Variable current results

Figure 37 below shows the voltage graphs of a BESS and HESS when a variable load was used. The load's resistance was varied every 10 seconds cycles by manually adjusting the connecting rods to raise the load resistance then lowering it to give a variable current cycle.

The 10 seconds is an approximate period of time taken that enables the voltage and current values to reach a steady state before a next transition is done.

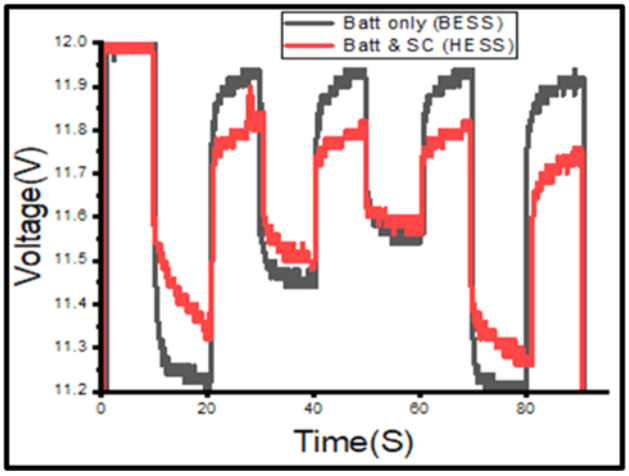

Figure 37 HESS and BESS experimental variable load voltage superimposed

Results showed that the battery voltage drop in a BESS was repeatedly deeper than in a HESS over the duration of the whole cycle signifying a higher usage of the battery and thus more stress exerted on it. The presence of the EDLC in the HESS negates some of the pressure or stress exerted on the battery by rapidly responding to the changing load requirements and supplying the needed power substituting for the battery.

Figure 38 below shows the current profile for the same variable load.

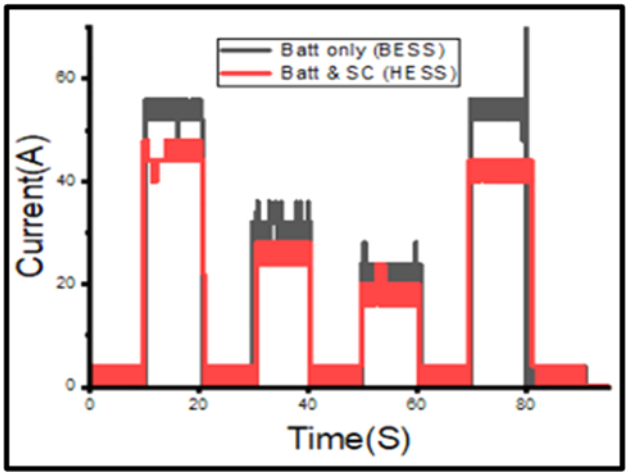

Figure 38 HESS and BESS experimental variable load currents superimposed

As with the voltage, the current drawn in a BESS including the initial in rush current, was higher than a HESS. This ultimately puts pressure on the battery which is reduced or negated in a HESS by the presence of the EDLC.

4.4 CONCLUSION

In this chapter an experimental HESS model was designed and tested. As a result, battery indicators such as battery voltage, current and SOC have been drawn in graphs with a constant load. The variation of battery voltage and current with respect to a changing load are also given. Battery voltage drops by 17%, battery current reduces by 48.6 % and the SOC increases by 1.5 % when the EDLC is added to the battery in a HESS configuration.

CHAPTER 5

THE EFFECT OF THE PYTHON/MATLAB/SIMULINK (PMS)-HYBRID MODEL OF A SUPERCAPACITOR ON BATTERY LIFESPAN IN A MATLAB/SIMULINK MODEL OF A HESS

5.1 Developing the simulation Python/MATLAB/Simulink (PMS)-hybrid model of the 65 F 16.2 V (EDLC) supercapacitor

This chapter deals with the simulation of the hybrid energy storage system (HESS) in a MATLAB/Simulink enviroment [78]. To simulate the HESS, an EDLC Python/Simulink/Model (PMS) which is an improvement to the one in chapter 3 , was created and is shown in the Figure 39 below

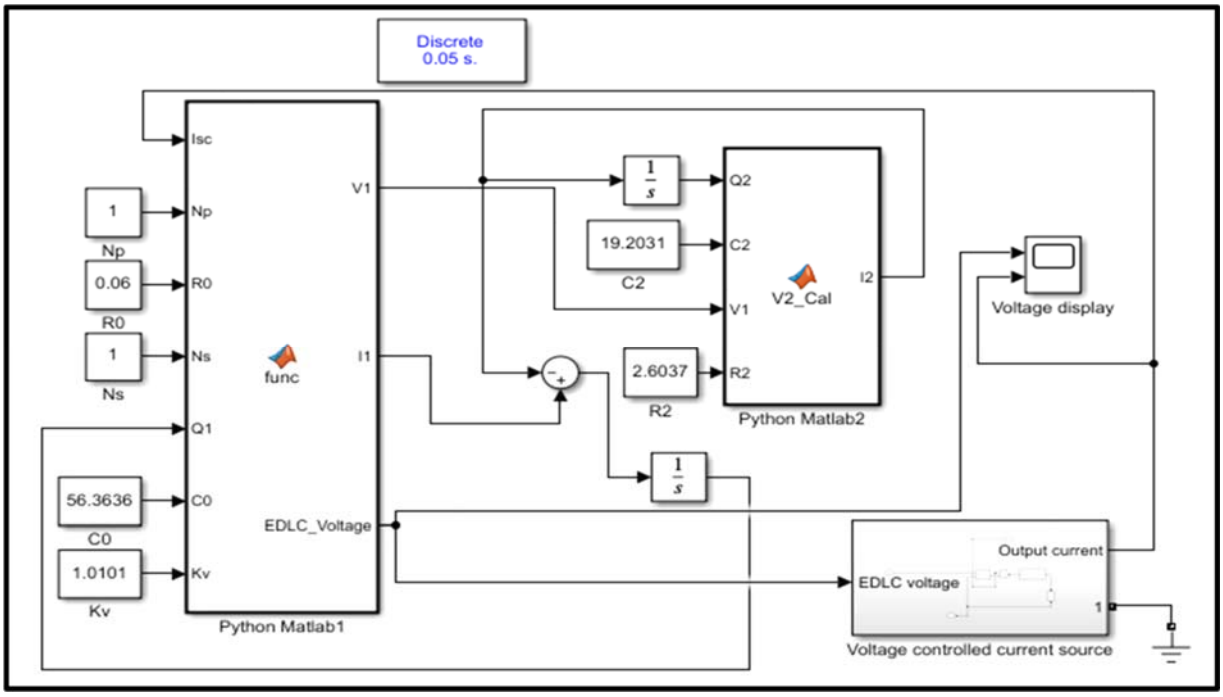

Figure 39 Python/MATLAB/Simulink (PMS) Model

The PMS model works by taking in the experimental derived parameters via Simulink, producing the distinct curve characteristics of the EDLC through a python code encapsulated in MATLAB. The results of which are return to Simulink where they can be displayed on a scope and downloaded to an excel files. Also of importance is the voltage controlled current source which helps supply input current to the model and converts the EDLC output voltage signal into an electrical signal compatible with the battery output. The simulated charge/discharge profile of the EDLC emanating from the PMS model were subsequently compared with the experimental charge/discharge profiles to evaluate the accuracy of the derived parameters and the proposed PMS model.

5.1.1 65 F EDLC simulation results

The simulated EDLC charge profile obtained using the PMS model is shown in Figure 40 for both 5 and 10 A superimposed. As in the experimental results, in the simulate charge profiles, the 10 A graph shows a much steeper gradient than the 5 A graph. Also, the 10 A graphs reaches the EDLC maximum voltage faster than the 5 A graphs

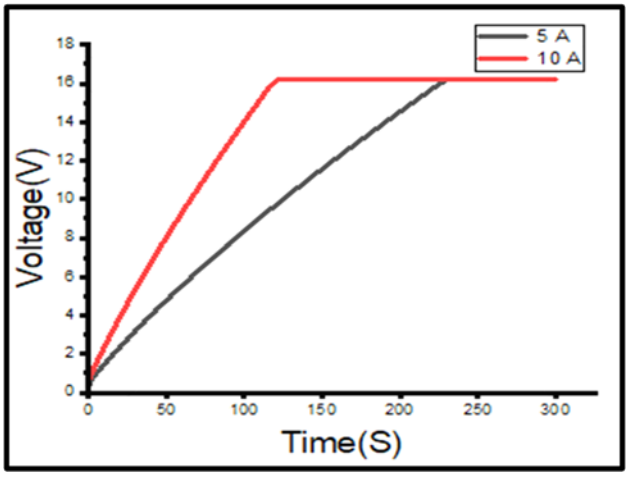

Figure 40 PMS EDLC simulated charge profile at 5 A and 10 A

The simulated discharge profile of the EDLC is shown in Figure 41 below. The simulated discharge profiles also show the EDLC discharging faster at 10 A than 5 A as expected.

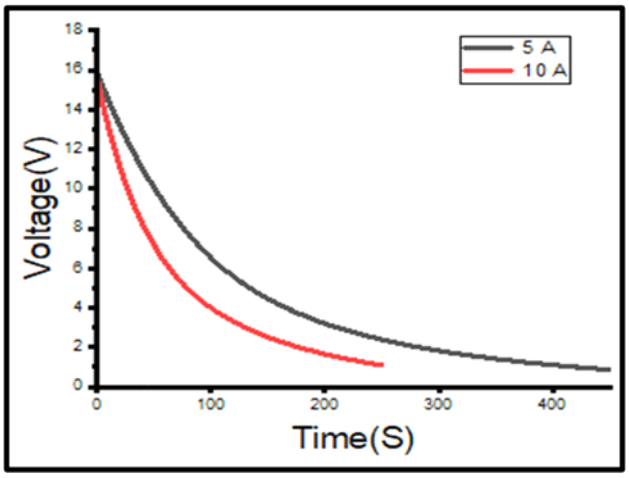

Figure 41 PMS EDLC simulated discharge profile at 5 A and 10 A

Figure 42 shows experimental charge/discharged profiles acquired in chapter 4 chapter and simulated charge profiles super imposed on each other to enable visual comparisons. In the charge profiles it can be seen that at both 5 and 10 A the experimental and simulated graphs mostly correlate. The slight differences can be explained by the presence of the voltage-controlled source in the simulated PMS model in Fig. 1 that converts a Simulink signal into an electrical signal.

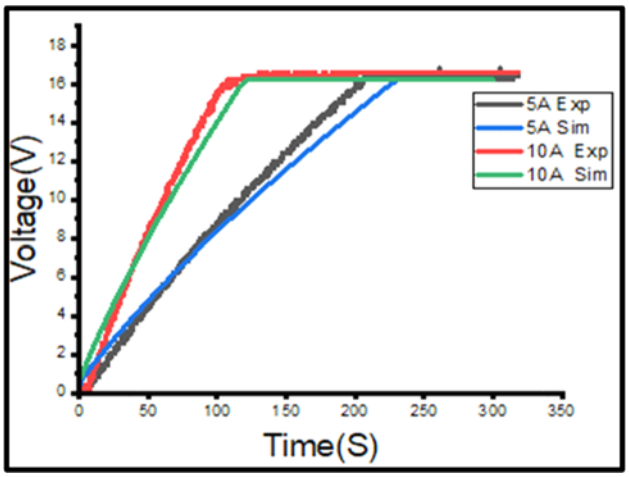

Figure 42 Experimental and simulated charge profiles superimposed at 5 A and 10 A

The FIGURE 43 shows experimental charge/discharge profiles from chapter 4 and simulated discharge profiles super imposed the discharge profiles show slightly more pronounced differences between the experimental and simulated graphs. Apart from the

voltage-controlled source contribution highlighted in the preceding paragraph, the other reason might be of the derived “two branch” model parameters being a summary, or an estimation obtained from the experimental charge profiles and inserted into the PMS model

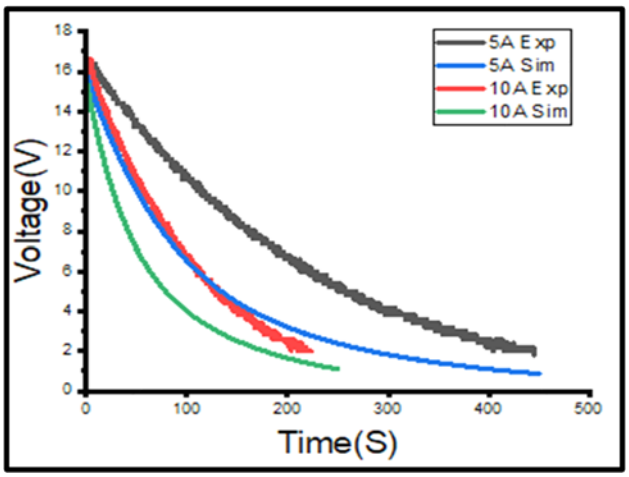

Figure 43 Experimental and simulated discharge profiles superimposed at 5 A and 10 A

5.2 HESS simulation Model

After modelling and testing the individual 65 F EDLC PMS model, it was then in cooperated in a subsystem, connect to an in-build MATLAB/Simulink lead acid battery a simulink resistive load and simulink scopes for data capturing for HESS simulation as shown in Figure 44 below

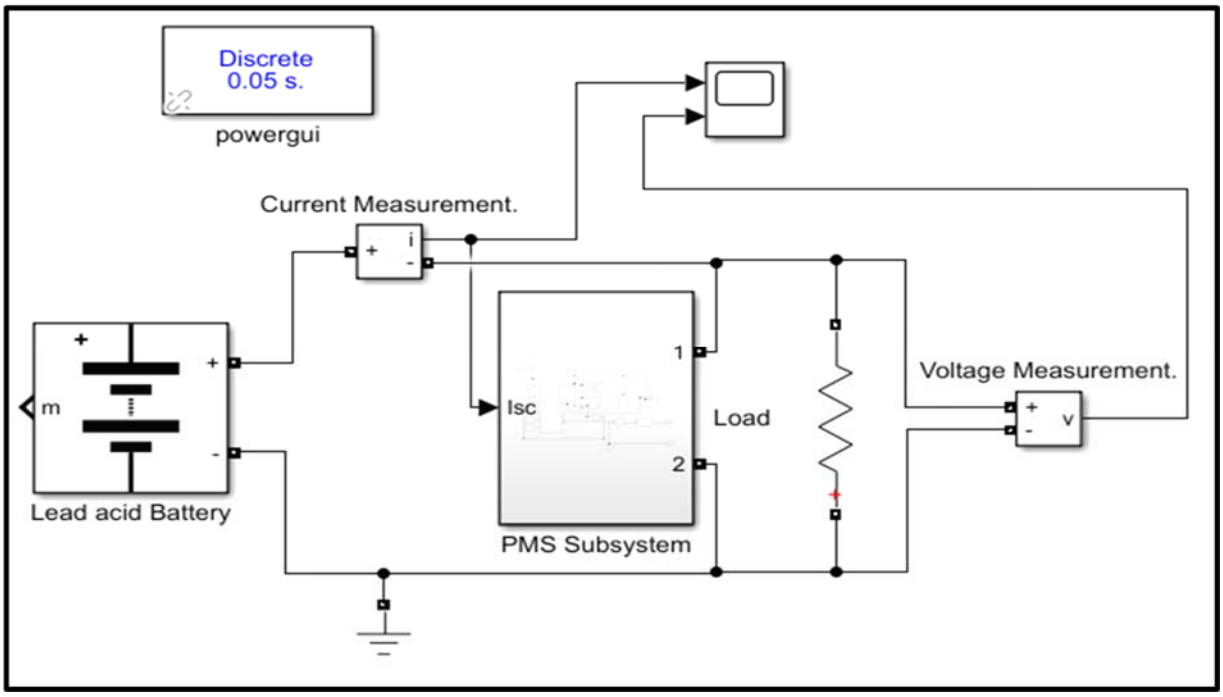

Figure 44 Simulated HESS

Similar to the lab experiment, the simulation was firstly done under a BESS setup with battery voltage, current and SOC captured. The same simulation with the same conditions was repeated under a HESS setup with the exact same data captured and recorded. Individual BESS and HESS simulation data were then compared. 5 and 10 A constant current was alternatives used for both BESS and HESS.

The resistor in Figure 44 above was used as a load for the HESS simulation. Its value was manually alternated in Simulink software between 2.4 Ω (to get simulation at 5 A constant current) and 1.2 Ω (to get a simulation at 10 A constant current).

5.2.1 HESS simulation results

The 5 A voltage Simulation results as shown in Figure 45 and proves that under BESS the battery voltage drops more significantly than under HESS and thus it can be said that less stress is exerted on the battery due to the presence of the EDLC in the HESS

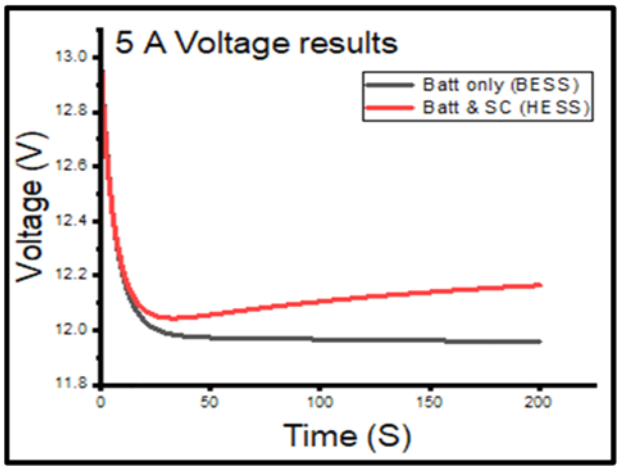

Figure 45 Simulated BESS and HESS battery voltage values discharged at 5 A

Similar to the 5 A voltage results, the 10 A voltage simulation voltage results as shown in Figure 46 below shows that the battery voltage under BESS drops lower than the battery voltage under HESS

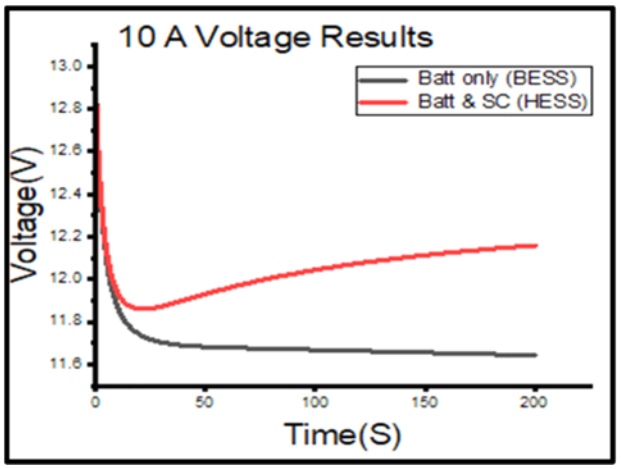

Figure 46 Simulated BESS and HESS voltage values discharged at 10 A

In Figure 47 it can be seen that under BESS, the battery currents for the 5 A topology remain constantly high and never drops hence more pressure is applied on the battery. But under HESS, the battery current gradually decreases and with time less and less battery current is used. This is due to the presence of the EDLC taking over the workload from the battery resulting in a relieve of stress on the battery.

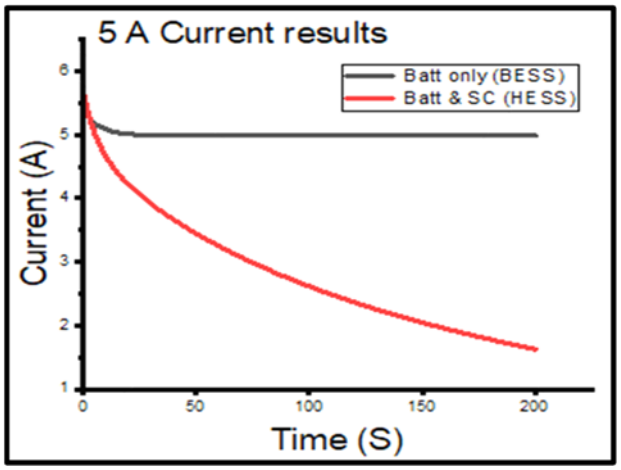

Figure 47 Simulated BESS and HESS battery current values discharged at 5 A

The 10 A HESS battery current topology shown in Figure 48 below closes resembles the 5 A topology a with a similar high use of battery current under BESS and a lower decreasing battery current usage under HESS

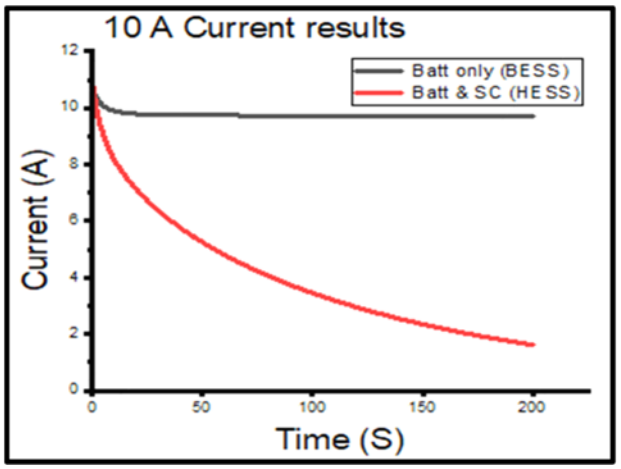

Figure 48 Simulated BESS and HESS battery current values discharged at 10 A

Simulation results also showed that the battery SOC decreases rapidly under BESS a shown in Figure 49 for 5 A topology, with a very steep gradient compared to a HESS where the battery SOC decreases gradually. Also, the final battery SOC in a BESS is much less than a HESS owing to the presence of the EDLC in a HESS.

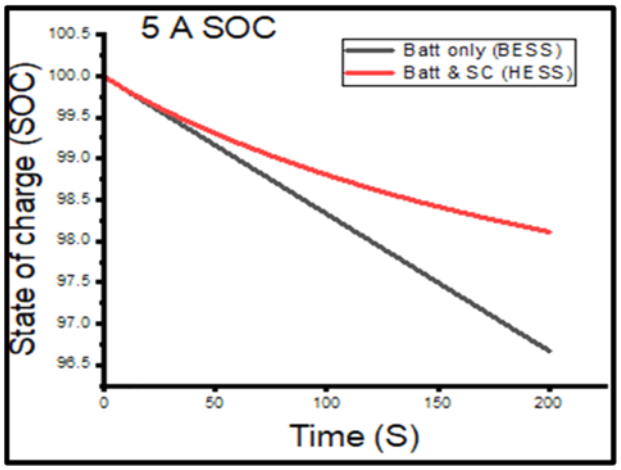

Figure 49 Simulated BESS and HESS SOC percentiles at 5 A

Almost the exact SOC graph is seen with the 10 A topology shown in Figure 50 below showing an improvement in the HESS due to the presence of the battery

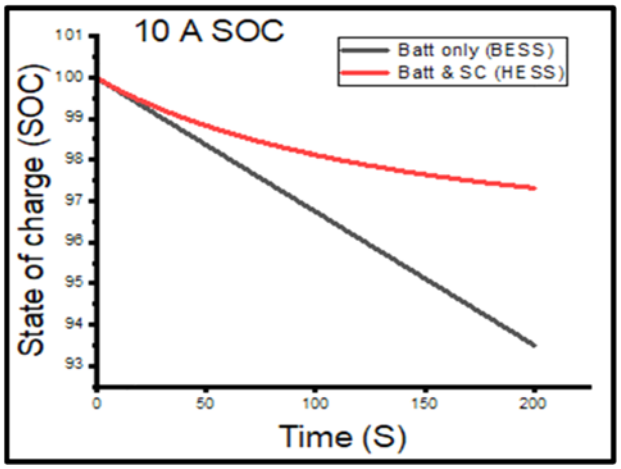

Figure 50 Simulated BESS and HESS SOC percentiles at 10 A

In all of the graghs and figures shown in chapter 4 and 5, it can be seen that the presence of the EDLC in a HESS both experiemtnal and by simulation ,has a positive effect on the health of the battery much so than an EDLC absent BESS. The effect on the battery indicators such as voltage, current and SOC are summarized in Table 14 below. Ageing process details are given in [65].

Table 14 Changes in Battery Stress indicators and lifespan [65, 78]

Stress factor	Reduction of stress factor	Reduction of aging
Battery Voltage values	Voltage drop reduced by 17 % with EDLC	Reduces the degradation of active material Lead dioxide (PbO_2)
Current discharge value	Initial current spike reduced by 48.6 % with EDLC	Reduces the formation of Lead Sulphate $(PbSO_4)$
Battery Power value	Initial spike in power demand reduced by 48.6 % with EDLC	Reduces the degradation of active material Lead dioxide (PbO_2)
Battery SOC percentile	1.50 % increase in SOC with an EDLC present within a duration of 5 mins.	Reduces the formation of Lead Sulphate $(PbSO_4)$
Battery Charge Utilization	Charge Used Dropped by 44% with the EDLC	Reduces the degradation of active material Lead dioxide (PbO_2)

Battery sulfation happens when crystals build up on the cells of the battery. While this process is normal and happens each time the battery is used, it can be exacerbated and sped up by rapid discharging, overcharging, and undercharging of the battery. In HESS because there is s reduction on the stress experience by the battery, it can be said that there is a reduction of battery sulfation leading to the prolonging of battery lifespan

Similarly, battery degradation or ageing is the changes that occur in a battery cell that might be either physical, chemical or both. Caused by factors such high voltage and current fluctuation. Again, as shown by both the experimental and simulation results, these can be said to be greatly reduced in a HESS than a BESS

CHAPTER 6

CONCLUSION and RECOMMENDATIONS

6.1 Conclusion

The electric double layer capacitors (EDLCs) and supercapacitors in general are the energy storage devices of the future due to their many advantages over existing energy storage devices (ESD's) and the potential scope of their future uses. In this research a 300 F EDLC and 400 F EDLC were characterized using the "two branch/Faranda" method. Experimental tests were done in the laboratory to derive electric equivalent circuit parameters from the charge/discharge profiles. These parameters were then introduced into a mathematical model of the supercapacitor which was designed in Python/MATLAB/Simulink (PMS) and then the model was simulated. The derived parameters were found to be consistent with similar range EDLC's in literature. Calculated ESR and capacitance values from experiments and simulations were found to be very close to datasheet values.

The simulated PMS and experimental charge/discharge profiles for both EDLC's were found to be almost identical in terms of the charge profiles and similar for the discharge profiles. However, a slight deviation occurred between the simulated PMS model and the experimental circuit for the discharge profile. This was due to the extracted parameters from the experimental circuit introduced to the PMS model having the effect of summarizing the curve. Also, the derived parameters were obtained from the charge profile not the discharge profile. This proves the accuracy of the mathematical Python/MATLAB/Simulink (PMS) model as a data representation of a supercapacitor.

Our research questions as mentioned in chapter 1 were:

1. Can a mathematical model be derived from an equivalent circuit of an EDLC?
2. Can a similar charge/discharge profile of an EDLC be obtained either by simulation in MATLAB/Simulink or laboratory experiments?

The above questions were answered by designing the PMS model with Python, MATLAB, and Simulink to form a hybrid model and by deriving the charge/discharge profiles of the

EDLC through simulation. Furthermore, the use of python to code the EDLC was a result of it being a flexible programming language and to make a unique contribution to knowledge.

In so far as the hybrid energy storage system (HESS) is concerned, a 65 F 16.2 V EDLC and a lead acid battery were used. “Two branch “electric equivalent circuit parameters of the 65 F EDLC were derived too from its charge/discharge profile in a laboratory experiment. These parameters were used to accurately model the 65 F EDLC in an improved Python/MATLAB/Simulink environment. The proposed EDLC PMS model was successfully incorporated in a MATLAB/Simulink subsystem together with a battery to form HESS for simulation purposes.

Experimental and simulation data showed that the battery in a BESS system experiences high level of voltage and current fluctuations that exert stress on the battery and therefore shorten its lifespan. To counter this an EDLC is connected in parallel with the battery to form a HESS. This Configuration with the EDLC after the battery before the load is primarily to study the load demand perspective from the load side. Experimental and simulation results showed that, in the HESS because of the EDLC’s high power density and rapid charge/discharge cycles, it absorbs a lot of the in-rush currents, voltage spikes and responds quicker to fluctuating power emanating from the load, thus protecting the battery. This in the long term “saves’ the battery and prolongs its lifespan reducing the overall cost associated with replacing batteries. The HESS experiments and simulations proves and gives a "one"/"1" result hypothesis, because what was envisaged in the hypothesis was shown in the results.

6.2 Recommendations and Contributions

The results from the research showed that the “Two branch” equivalent circuit model including its mathematical formulas, are an accurate representation of the EDLC and can be used to model an EDLC with relatively easy and obtain its parameters.

The research also showed that Python can be used in sub-sections of the algorithm to communicate with MATLAB to avoid issues of integration

The results from the study showed and recommends that the EDLC must be placed after the battery on the load side, when looking from the angle or perspective of the demands of the load with respect to current drawn from the battery on the load side.

Whether in hybrid cars or micro grid, it is preferable for the energy storage system to include both a battery and an EDLC to prolong battery lifespan and help reduce long term operational costs.

The contribution of this research is that when the EDLC is combined with a Lead-Acid battery in a HESS configuration the battery indicators such as the Battery voltage values reduce by 17%, the current value spike reduces by 48.6%, Battery power spike values reduce by 48.6%, the battery SOC percentile increase by 1.5% and the charge used drops by 44 % within a limited time.

6.3 Future work

This research sorely looked at the effect the EDLC has on reducing stress on the battery due to power fluctuations from the load side. Future work might include looking at the effect of an uneven supply emanating from a PV array, wind turbine or bench power supply that charges the battery and how the EDLC can acts as a buffer to protect the battery against surges and high voltages.

REFERENCES

[1] R. Carter , A. Cruden, P. Hall , "Optimizing for Efficiency or Battery Life in a Battery/Supercapacitor Electric Vehicle", IEEE Transactions on Vehicular Technology, 1 May 2012 , vol. 61, issue no. 4, pp. 1526-1533, Available Online : 10.1109/TVT.2012.2188551

[2] M. S. Halper and J. C. Elllenbogen, "Supercapacitors: A Brief Overview," The MITRE corporation , Book Chapter, March 2006, Available Online: https://www.mitre.org/sites/default/files/pdf/06_0667.pdf

[3] N. I. Jalal, R. I. Ibrahim and M. K. Oudah," A review on supercapacitors: types and components" , Journal of physics: conference series, August 2021, vol. 1973, issue no. 1, pp. 012015, Available Online: 10.1088/1742-6596/1973/1/012015

[4] E. Danlla, "History of the First Energy Storage Systems," in 3rd International Symposium on the History of Electrical Engineering and of Tertiary-Level Engineering Education, Iasi, Romania, 27-29 October 2010, Available Online: 10.13140/2.1.1564.7040

[5] C. Choi , A. David, D. Butts, R. Deblock. Q. Wei, J. Lau and B. Dunn, "Achieving high energy density and high power density with pseudocapacitive materials",Nature Reviews Materials, 2019, vol. 5, pp. 5-19, Available Online: 10.1038/s41578-019-0142-z

[6] R. Klaus Schmidt, "How Batteries Store and Release Energy: Explaining Basic Electrochemistry" ,journal of chemical education, 23 August 2018, vol. 95, issue no. 10, pp. 1801-1810, Available Online : https://doi.org/10.1021/acs.jchemed.8b00479

[7] J. R. Miller and P. Simon, "Fundamentals of Electrochemical Capacitor Design and Operation," The Electrochemical Society Interface, March 2008, vol. 17, issue no. 1, pp. 31-32, Available online: https://iopscience.iop.org/article/10.1149/2.F02081IF/pdf

[8] M. jayalakshmi and K. Balasubramanian, "Simple Capacitors to Supercapacitors- An Overview," International Journal of Electrochemical Science, November 2008, vol. 3, pp. 1196-121, Available online: http://www.electrochemsci.org/papers/vol3/3111196.pdf

[9] K. Vuorilehto and M. Nuutinen, "Supercapacitors- Basics and applications," SkeletonTech, 23 January 2014, Website, Available online: https://www.academia.edu/32049567/Supercapacitors_-basics_and_applications

[10] R. Faranda, M. Gallina and D. T. Son, "A new simplified model of Double-Layer Capacitors", International Conference on Clean Electrical Power, Capri, Italy, 21-23 May 2007, pp. 706-710, Available Online: https://doi.org/10.1109/ICCEP.2007.384288

[11] L. Zubieta and R. Bonert, "Characterization of Double-Layer Capacitors for Power Electronics Applications", IEEE transactions on Industry Applications, Jan/Feb 2000, vol. 36, Issue no. 1, pp. 199-205, Available Online: https://doi.org/10.1109/28.821816

[12] H. Gualous, H. Louahlia and R. Gallay, "Supercapacitor Characterization and Thermal Modelling With Reversible and Irreversible Heat Effect", IEEE transactions on Power Electronics, 21 April 2011, vol. 26, Issue no. 11, pp. 3402-3409, Available Online: https://doi.org/10.1109/TPEL.2011.2145422

[13] M. C. Argyrou, P. Christodoulides, C. C. Marouchos and S. A. Kalogirou, "Hybrid battery-supercapacitor mathematical modeling for PV application using Matlab/Simulink", 53rd International Universities Power Engineering Conference (UPEC) , Glasgow, UK, 4-7 September, 2018, pp. 1-6, Available Online: https://doi.org/10.1109/UPEC.2018.8541933

[14] K. Popoola, "Modelling and Simulation of Supercapacitor for Energy Storage Applications", ADBU-Journal of Engineering Technology (AJET), 18 June 2018, pp. 1-6, Available Online: https://core.ac.uk/display/386358319?source=4

[15] M. E. Sahin, F. Blaabjerg and A. Sangwongwanich, "Modelling of Supercapacitors Based on Simplified Equivalent Circuit", CPSS Transaction on Power Electronics and Applications, 8 April 2021, vol. 6, issue no. 1, pp. 31-39, Available Online: https://doi.org/10.24295/CPSSTPEA.2021.00003

[16] A. A. Gazwi and S.B. Tennakoon, "Modelling of Super Capacitor Modules and Parameter Extraction", 46th International Universities' Power Engineering Conference, Soest, Germany, 5-8 September 2011, pp. 1-6, Available Online: https://ieeexplore.ieee.org/document/6125630

[17] W. Kai, R. Baosen, L. Liwei, L. Yuhao, Z. Hongwei and S. Zongqiang, "A review of Modeling Research on Supercapacitor", Chinese Automation Congress (CAC) , Jinan, China, 20-22 October 2017, pp. 5998-6001, Availble Online: https://doi.org/10.1109/CAC.2017.8243857

[18] M. E. Sahin and F. Blaabjerg, "A Hybrid PV-Battery/Supercapacitor System and a Basic Active Power Control Proposal in MATLAB/Simulink", Electronics, 2020, vol. 9, issue no. 1, pp. 129, Availble Online: https://www.mdpi.com/2079-9292/9/1/129

[19] R. Negroiu, P. Svasta, A. Vasile, C. Ionescu and C. Marghescu, "Comparison between Zubieta Model of Supercapacitors and their Real Behavior", IEEE 22nd International Symposium for Design and Technology in Electronic Packaging (SIITME) , Oradea, Romania, 20-23 October 2016, pp. 196-199, Available Online: https://doi.org/10.1109/SIITME.2016.7777276

[20] A. Berrueta, A. Ursua, I. San Martin, A. Eftekhari and P. Sanchis, "Supercapacitors:Electrical Characteristics, Modelling, Applications, and Future Trends," IEEE Access, 26 April 2019, vol. 7, pp. 50869-50896, Available Online: 10.1109/ACCESS.2019.2908558

[21] T. Funaki, T. Hikihara, "Characterization and Modelling of the Voltage Dependency of Capacitance and Impedance Frequency Characteristics of Packed EDLC's", IEEE Transactions on Power Electronics, May 2008, vol. 23, Issue no. 3, pp. 1518-1525, Available online: https://doi.org/10.1109/TPEL.2008.921156

[22] R. Kahwaji, "Supercapacitors: A Short Literature Review," ResearchGate, 08 January 2019, Available Online: 10.13140/RG.2.2.14032.35846

[23] F. Yang, L. Lu, Y. Yang and H. Yongsheng, "Characterisation, Analysis and Modeling of an Ultracapacitor," World Electric Vehicle Journal, 2010, vol. 4, issue no. 2, pp. 358-369, Available online: https://doi.org/10.3390/wevj4020358

[24] M. Vangari and L. Jiang, "Supercapacitors: Review of Materials and Fabrication Methods," Journal of Energy Engineering, June 2013, vol. 139, issue no. 2, Available Online: https://doi.org/10.1061/(ASCE)EY.1943-7897.0000102

[25] S. I. Zaharaddeen, C. Subramani and S. S. Dash, "A Brief Review on Electrode Materials for Supercapacitor," International Journal of ELECTROCHEMICAL SCIENCE, 10 November 2016, vol. 11, pp. 10628-10643, Available Online: 10.20964/2016.12.50

[26] M. Gidwani, A. Bhagwani and N. Rohra, "Supercapacitors: the near Future of Batteries," International Journal of Engineering Inventions, October 2014, vol. 4, issue no. 5, pp. 22-27, Available online: https://www.semanticscholar.org/paper/Supercapacitors%3A-the-near-Future-of-Batteries-Gidwani-Bhagwani/f0c499805c4c834a652c8f1a8b2ae47b93fcd745

[27] P. G. Gautham, N. Shetty, S. Thakur, Rakshitha and K.B. Bommegowda, "Supercapacitor technology and its applications: A review," IOP Conference series: Materials Science and Engineering, 12-13 April 2019, vol. 561, issue no. 1, pp. 012105, Available Online: https://doi.org/10.1088/1757-899X/561/1/012105

[28] S. J. Artal, R. Bandres and G. Fernandez, "Ulises: Autonomous Mobile Robot Using UltraCapacitors-Storage Energy System," International Conference on Renewable Energies and Power Quality, Las Palmas de Gran Canaria, Spain, 16-15 April 2015, pp. 1105-1110, Available Online: https://doi.org/10.24084/repqj09.558

[29] A. Singh, N. A. Azeez and S. S. Williamson, "Dynamic modeling and characterization of ultracapacitors for electric transportation," IEEE 24th International Symposium on Industrial Electronics (ISIE), Buzios, Brazil, 03-05 June 2015, pp. 275-280, Available Online: https://doi.org/10.1109/ISIE.2015.7281481

[30] M. E. Sahin, "An investigation on supercapacitors applications with module designing and testing," Journal of Engineering Research, Issue. Online First Article, ISSN: 2307-1877, 2021, Available Online: https://doi.org/10.36909/jer.11481

[31] A. M. Puscas, M. Carp, P. Borza and I. Szekely, "Measurement Considerations on Some Parameters of Supercapacitors," Electrical and Mechanical Engineering, 2009, vol. 1, pp. 65-75, Available online: http://www.acta.sapientia.ro/acta-emeng/C1/emeng1-5.pdf

[32] N. A. Thong, "Application of Supercapacitor in Electrical Energy Storage Systems," Masters of Engineering thesis, National University of Singapore, Singapore, 2011, Available online: https://core.ac.uk/download/pdf/48643107.pdf

[33] V. Vanitha, S. Ashok, C. Anandanarayana, G. Balasubramanian and G. Gowrishankar, “Determination of equivalent circuit parameters of supercapacitor and its testing with three phase inverter”, International journal of electrical engineering, 2011, vol. 4, issue no. 5, pp. 567-584, Available online: http://www.irphouse.com/ijee/ijeev4n5_6.pdf

[34] L. Shi and M. L. Crow, "Comparison of ultracapacitor electric circuit models," IEEE Power and Energy Society General Meeting - Conversion and Delivery of Electrical Energy in the 21st Century, Pittsburg, PA, USA, 20-24 July 2008, pp. 1-6, Available Online: 10.1109/PES.2008.4596576

[35] R. De levie, "On porous electrodes in electrolyte solutions: I. Capacitance effects", Electrochimica Acta, October 1963, vol. 8, issue no. 10, pp. 751-780, Available online: https://doi.org/10.1016/0013-4686(63)80042-0

[36] I. N. Jiya, N. Gurusinghe and R. Gouws, "Electrical Circuit Modelling of Double Layer Capacitors for Power Electronics and Energy Storage Applications:A Review," Electronics, 2018, vol. 7, issue no. 11, pp. 268, Available Online: https://doi.org/10.3390/electronics7110268

[37] R. Shrivastwa, A. Hably, K. Melizi and S. Bacha, "Understanding Microgrids and Their Future Trends," IEEE International Conference on industrial Technology, Melbourne, Australia, 13-15 February 2019, pp. 1723-1728, Available online: 10.1109/ICIT.2019.8754952

[38] P. G. Patil, K. Venkateshwarlu and M. T. Patel, "Application of Super capacitor Energy Storage in Microgrid System," International Journal of Science, Engineering and technology Research (IJSETR) , March 2015, vol. 4, issue no. 3, pp. 589-594, Available Online: https://studylib.net/doc/18409610/application-of-super-capacitor-energy-storage-in-microgri...

[39] B. S. Hartono, Y. Budiyanto and R. Setiabudy, "Review of microgrid technology, "International Conference on QiR, Yogyakarta, Indonesia, 25-28 June 2013, pp. 127-132, Available Online:10.1109/QiR.2013.6632550

[40] U. Shahzad, "The Need for Renewable Energy Sources," International Journal of Information Technology and Electrical Engineering, August 2015, vol. 4, pp. 16-19, Available online:

https://www.researchgate.net/publication/316691176_The_Need_For_Renewable_Energy_Sources

[41] S. Abolhosseini, A. Heshmati and J. Altmann, "A Review of Renewable Energy Supply and Energy Efficiency Technology," IZA Discussion Paper No. 8145, April 2014, Available online: http://dx.doi.org/10.2139/ssrn.2432429

[42] G. Heal, "The Economics of Renewable Energy," NBER Working Paper No. w15081, June 2009, Available online: https://ssrn.com/abstract=1418939

[43] K. P. Vijayaragavan, "Feasibility of DC Microgrids for Rural Electrification," Master Level Thesis European Solar Engineering School No. 221, June 2017,Available online: https://www.diva-portal.org/smash/get/diva2:1135428/FULLTEXT01.pdf

[44] A. M. Camara, A. Djellad, P. O. Logerais, O. Riou and J. F. Durastanti, "Modelling of A Hybrid Energy Storage System Supplied by a Photovoltaic Source to feed a DC Motor," International Journal of Renewable and Sustainable Energy, January 2013, vol. 2, issue no. 6, pp. 222-228, Available online: 10.11648/j.ijrse.20130206.16

[45] M. J. Ross Jr., "Modelling and Control of a Microgrid using a Hybrid Energy Storage System with Supercapacitors," Masters thesis, Naval Postgraduate School, Monterey California, June 2018, Available online: https://upload.wikimedia.org/wikipedia/commons/9/95/MODELING_AND_CONTROL_OF_A_MICROGRID_USING_A_HYBRID_ENERGY_STORAGE_SYSTEM_WITH_SUPERCAPACITORS_%28IA_modelingandcontr1094559577%29.pdf

[46] W. Jing, C. H. Lai, W. S. Wong and M. D. Wong, "Dynamic Power Allocation of Battery-Supercapacitor Hybrid Energy Storage for Standalone PV Microgrid Application," Sustainable Energy Technology and Assessments, August 2017, vol. 22, pp. 55-64, Available Online: https://doi.org/10.1016/j.seta.2017.07.001

[47] R. Hemmati and H. Saboori, "Emergence of Hybrid energy storage systems in renewable energy and transport applications - A Review," Renewable and Sustainable Energy Review, November 2016, vol. 65, pp. 11-23, Available online: https://doi.org/10.1016/j.rser.2016.06.029

[48] X. Xiong and Y. Yang, "A Photovoltaic-Based DC Microgrid System: Analysis, Design and Experimental Results," Electronics, 2020, vol. 9, issue no. 6, pp. 941, Available Online: https://doi.org/10.3390/electronics9060941

[49] Y. B. Aemro, P. Moura and A.T. de Almeida, "Design and Modelling of a Standalone DC-Microgrid for Off-Grid Schools in Rural Areas of Developing Countries," Energies, 2 December 2020, vol. 13, issue no. 23, pp. 6379, Available Online: https://doi.org/10.3390/en13236379

[50] A. M. van Voorden, L. M. R. Elizondo, G. C. Paap, J. Verboomen and L. van der Sluis, "The Application of Super Capacitors to relieve Battery-storage systems in Autonomous Renewable Energy Systems", IEEE Lausanne Power Tech, Lausanne, Switzerland, 01-05 July 2007, pp. 479-484, Available Online: 10.1109/PCT.2007.4538364

[51] S. Hajiaghasi, A. Salemnia, M. Hamzeh," Hybrid energy storage system for microgrids applications: A review", Journal of Energy Storage", February 2019, vol. 21, pp. 543-570, Available Online: https://doi.org/10.1016/j.est.2018.12.017

[52] E. Hossain, E. Kabalci and R. Bayindir, "A comprehensive study on microgrid technology," International Journal of Renewable Energy Research, January 2014, vol. 4, issue no. 4, pp. 1094-1104, Available online: http://www.researchgate.net/publication/286382695_A_comprehensive_study_on_microgrid_technology

[53] A. Eid, "Stand-alone DC Micro-Grids: Analysis and Control," in The 2nd International Conference on Engineering and Applied Science (ICEAS'13), Tokyo, Japan, March 2013, Available online: https://www.researchgate.net/publication/235932777_Stand-alone_DC_micro-grids_analysis_and_control

[54] M. Elsied, A. Oukaour ,H. Gualous, Y. Slamani, R. Hassan and A. Amin, "Analysis,Modelling, and Control of an AC Microgrid System Based on Green Energy," International Conference on Renewable Energies and Power Quality, Cordoba, Spain, 8-10 April 2014, ISBN: 978-84-616-8196-9, Available online: 10.24084/repqj12.525

[55] Y. Zhang, J. Wang, A. Berizzi, and X. Cao, "Life Cycle Planning of Battery Energy Storage Systems in Off-grid Wind-Solar-Diesel Microgrid," IET Generation Transmission & Distribution, September 2018, vol. 12, issue no. 20, Available Online: https://doi.org/10.1049/iet-gtd.2018.5521

[56] J. Dulout, B. Jammes, C. Alonso, A. Anvari-Moghaddam, A. Luna and J. M. Guerrero, "Optimal sizing of a lithium battery energy storage system for grid-connected photovoltaic systems", IEEE Second International Conference on DC Microgrids (ICDCM), Nuremburg, Germany, 27-29 June 2017, pp. 582-587, Available online : 10.1109/ICDCM.2017.8001106

[57] A. Haque, "A simplified control strategy for Bi directional DC-DC converter for DC microgrid application," International Journal of Modern Trends in Engineering and Research, 2017, vol. 4, issue no. 10, Available Online: 10.21884/IJMTER.2017.4303.RSAEZ

[58] D. Zammit, C.S. Staines, M. Apap and A. Micallef, "Control of Buck and Boost Converters For Stand-Alone DC Microgrids," in Eighth International Symposium on Energy, Aberdeen, Scotland, 6-9 August 2018, Available online: https://www.researchgate.net/publication/328901677_Control_Of_Buck_and_Boost_Converters_For_Stand-Alone_DC_Microgrids

[59] B. S. Revathi, M. Prabhakar and F. Gonzalez-Longatt, "High gain-High power(HGHP) DC-DC converter for DC microgrid applications:Design and testing", International Transactions on Electrical Energy Systems, 22 November 2017, vol. 28 , issue no. 30, Available online: https://doi.org/10.1002/etep.2487

[60] F. M. Zia, E. Elbouchikhi and M. Benbouzid, "Microgrids energy management systems: A critical review on methods, solutions, and prospects," Applied Energy, 15 July 2018, vol. 222, pp. 1033-1055, Available online: https://doi.org/10.1016/j.apenergy.2018.04.103

[61] H. Oussama, A. Othmane, S. M. Amine, H. M. Amine, C. Abdeselem and A. Ben Abdelkader, "Modelling and Control a DC-Microgrid Based on PV and HESS Hybrid Energy Storage System," in First International Conference on Smart Grids CIREI', Oran, Algeria, 28-29 April 2019, Available online: https://www.researchgate.net/publication/333774379_Modeling_and_Control_a_DC-Microgrid_Based_on_PV_and_HESS_Hybrid_Energy_Storage_System

[62] J. Li, B. Cornelusse, P. Vanderbemden and D. Ernst, "A SC/Battery Hybrid Energy Storage System in the Microgrid," in 9th Intenational Conference on Applied Energy,

Energy Procedia, Cardiff, UK, 21-24 August 2017, pp. 3697-3702, Available online: https://doi.org/10.1016/j.egypro.2017.12.264

[63] W. Jing, C. H. Lai, W. S. Wong and M. D. Wong, "Dynamic Power Allocation of Battery-Supercapacitor Hybrid Energy Storage for Standalone PV Microgrid Applications," Sustainable Energy Technology and Assessments, August 2017, vol. 22, pp. 55-64, Available online: https://doi.org/10.1016/j.seta.2017.07.001

[64] J. Li, R. Xiong, H. Mu, B. Cornélusse, P. Vanderbemden, D. Ernst, W. Yuan, “Design and real-time test of a hybrid energy storage system in the microgrid with the benefit of improving the battery lifetime”, Applied Energy, 15 May 2018, vol. 218, pp. 470-478, Available Online: https://doi.org/10.1016/j.apenergy.2018.01.096

[65] A. M. Gee and R. W. Dunn, "Novel battery / supercapacitor hybrid energy storage control strategy for battery life extension in isolated wind energy conversion systems," 45th International Universities Power Engineering Conference UPEC2010, Cardiff, UK, 31 August - 03 September 2010, pp. 1-6, Available Online: https://ieeexplore.ieee.org/document/5649908

[66] M. Bahloul and S. K. Khadem, "Impact of Power Sharing Method on Battery Life Extension in HESS for Grid Ancillary Services," in IEEE Transactions on Energy Conversion, September 2019, vol. 34, issue no. 3, pp. 1317-1327, Available Online: https://doi.org/10.1109/TEC.2018.2886609

[67] M. Mahzarnia, A. Sheikholislami and J. Adabi, "A Voltage Stabilizer for a Microgrid System with Two Types of Distributed Generation Resources," IIUm Engineering Journal, November 2013, vol. 14, issue no. 2, pp. 191-205, Available Online: https://doi.org/10.31436/iiumej.v14i2.450

[68] A. EL-Shahat and S. Sumaiya, "DC-Micro grid System Design, Control, and Analysis," Electronics, 2019, vol. 8, issue no. 2, pp. 124 Available Online: https://doi.org/10.3390/electronics8020124

[69] B. K. Myla, “Modelling and Control of PV/Wind Microgrid”, Dissertation Halmstad University, 2017, Available online: urn:nbn:se:hh:diva-34788

[70] S. Ganesan, V. Ramesh and S. Umashankar, "Performance Improvement of Micro Grid Energy Management System using Interleaved Boost Converter and P&O MPPT Technique," International Journal of Renewable Energy Research, 2016, vol.

6, issue no. 2, pp. 663-671, Available online: https://www.researchgate.net/publication/305417756_Performance_improvement_of_micro_grid_energy_management_system_using_interleaved_boost_converter_and_PO_MPPT_technique

[71] Q. Xu, H. Cai, G. Tang, K. Yukita and K. Ichiyanagi "Charge evaluation of EDLC for autonomous microgrid energy storage," Electrical Engineering, March 2011, vol. 93, issue no. 1, pp. 1-8, Available online: 10.1007/s00202-010-0185-z

[72] M. Danko, J. Adamec, M. Taraba and P. Drgona, "Overview of Batteries State of Charge Estimation Methods", Transportation Research Procedia, 29-31 May 2019, vol. 40, pp. 186-192, Available Online: https://doi.org/10.1016/j.trpro.2019.07.029

[73] E. Lee, W. Shi, R. Gadh and W. Kim, "Design and Implementation of a Microgrid Energy Management System," Sustainability, 7 November 2016, vol. 8, issue no.11, pp. 1143, Available Online: https://doi.org/10.3390/su8111143

[74] I. D. Serna-Suárez, G. Ordóñez-Plata and G. Carrillo-Caicedo, "Microgrid's Energy Management Systems: A survey", 12th International Conference on the European Energy Market (EEM), Lisbon, Portugal, 19-22 May 2015, pp. 1-6, Available Online: 10.1109/EEM.2015.7216662

[75] S. Gaurav, C. Birla, A. Lamba, S. Umashankar and S. Ganesan, "Energy Management of PV-Battery based Microgrid System", SMART GRID technologies, Procedia Technology, August 2015, vol. 21, pp. 103-111, Available online: https://doi.org/10.1016/j.protcy.2015.10.016

[76] C.T. Tshiani, P. Umenne," The Characterization of the Electric Double-Layer Capacitor (EDLC) Using Python/MATLAB/Simulink (PMS)-Hybrid Model, Energies, vol. 15, issue no. 14, Article number 5193, Available online: https://doi.org/10.3390/en15145193

[77] J. O'Grady, "State of Charge Estimation with a Kalman Filter", Battery Management System, Technology for the Planet, 13 May 2019, Online site, Available Online: https://www.jackogrady.me/battery-management-system/state-of-charge

[78] C. T. Tshiani, P. Umenne," An investigation into the impact of the Electric Double Layer Capacitor (EDLC) in reducing battery stress and improving battery lifespan in a hybrid Energy Storage System (HESS) system" **SUBMITTED**

APPENDIX A: code in Matlab representing equations that automatically calculates EDLC parameters using values from charge/discharge profile

```
%Voltage and time vales taking from P1 and P2 from the experimental charge/dishcrage
%profile
v1 = 7.2
t1 = 43.2
v2 = 13.8
t2 = 87.4
ic = 10
tc = 50
v2f = 16.2
Vr0 = 0.48

%function to calculate value of C0
function C0=cap(t1,v1,t2,v2,ic)

A = t1/v1;
B = (v1*t2) - (t1*v2);
C = v1^2 - v1*v2;
```

```
C0 = (A -B/C)*ic;

end

% function to calculate value of KV
function Kv=value(t1,v1,t2,v2,ic)

D = (v1*t2) - (t1*v2);
E = v1*v2^2 - v1^2*v2;

Kv = 2*(D/E)*ic

end

%function to calculate value of C2
function C2=param(Tc,ic,C0,Kv,V2f)

F = ic*Tc;
G = (C0 + (Kv/2)*V2f)*V2f;

C2 = (F - G)/V2f;
```

```
end


%function to calculate value of R0

function R0=paramR0(v1,v2,ic)


A = v2-v1;

R0 = A/ic;


End
```

APPENDIX B: Python code that takes in EDLC parameter values, solve the EDLC differential equations and returns the simulated EDLC charge/discharge profile

```
#Code starts here

import math
import numpy as np
import matplotlib.pyplot as plt
from scipy.integrate import odeint
import xlsxwriter

def pythonEdlc(Isc,R1,C0,Kv,R2,C2,Np,Ns):
    #return math.sqrt(C0)
    #Constants
    Isc = Isc
    R1 = R1
    C0 = C0
    Kv = Kv
    R2 = R2
    C2 = C2
    Np = Np
    Ns = Ns
#EDLC charge section
    #Differential function to calcualte Q1 and Q2
    def dSdt(t,S):
        Q1,Q2 = S
        #Calculate V1
        V1 = (-C0+math.sqrt((C0**2) + (2*Kv*Q1)))/(Kv)
        # To calculate V2
```

```
        V2 = Q2/C2
        """ Check if EDLC voltage has reached maximum 2.7V """
        V_EDLC = V1 + ((Isc/Np)*R1)
        if V_EDLC < 16.2:
            dQ1dt = (Isc/Np) - (V1-V2)/R2
            dQ2dt =  (V1-V2)/R2
            # return differential equation
            return [dQ1dt,dQ2dt]
        return [0,0]
    #Initial values of Q1 and Q2
    Q1 = 0
    Q2= 0
    S_0 = [Q1,Q2]
    # integrate the equations
    t = np.linspace(0,350,350) # times to report solution 428 for 300F.548 for 400 F
    y = odeint(dSdt,y0=S_0,t=t,tfirst=True) # integrate
    #get Q1 and Q2 from solution
    Q1_sol = y[:,0]
    Q2_sol = y[:,1]
    # Calculate V1 using the list values of Q1
    Q1_list = list(Q1_sol)
    Q2_list = list(Q2_sol)
    V1= [i*2*Kv for i in Q1_list]
    V1= [i+ (C0**2) for i in V1]
    d= np.sqrt(V1)
    V1_final = [i - C0 for i in d]
    quotients = []
    for i in V1_final:
        quotients.append(i/Kv)
      SC_voltage = [i+ ((Isc/Np)*R1) for i in quotients]        #SC_voltage = (V1 +
(2/1)*0.01)*1  #V1 + (Isc/Np)*R0)*Ns
```

```
return SC_voltage

Q2quotients =[]
for i in Q2_list:
    Q2quotients.append(i/C2)
#Plot in excel sheet
""" Create excel work sheet"""
workbook = xlsxwriter.Workbook('400F_3_March_PY.xlsx')
worksheet = workbook.add_worksheet()
""" Insert final EDLC voltage values in excel """
row = 0
col = 0
for i in (SC_voltage):
    worksheet.write_number(row,col,i)
    row +=1
""" Insert Q1 values in excel """
row = 0
col = 0
for i in (Q1_list):
    worksheet.write_number(row,col+1,i)
    row +=1
""" Insert V1 values in excel """
row = 0
col = 0
for i in (quotients):
    worksheet.write_number(row,col+2,i)
    row +=1
""" Insert Q2 values in excel """
row = 0
col = 0
for i in (Q2_list):
```

```
    worksheet.write_number(row,col+3,i)
    row +=1
""" Insert V2 values in excel """
row = 0
col = 0
for i in (Q2quotients):
    worksheet.write_number(row,col+4,i)
    row +=1
workbook.close()

#Plot date on a gragh
plt.figure(1)
plt.plot(t,SC_voltage,'b-')
plt.xlabel('Time (S)')
plt.ylabel('Voltage (V)')
plt.legend(['EDLC Charging 400 F,2 A'])
plt.show()

#EDLC Discharge section
def dSdt1(t,S):
    Q1,Q2 = S
    #Calculate V1
    V1 = (-C0+math.sqrt((C0**2) + (2*Kv*Q1)))/(Kv)
    # To calculate V2
    V2 = Q2/C2
    """ Check if EDLC voltage has reached maximum 2.7V """
    V_EDLC = V1 + ((Isc/Np)*R1)
    if V_EDLC > 0:
        dQ1dt = -((Isc/Np) - (V1-V2)/R2)
        dQ2dt =  -((V1-V2)/R2)
        # return differential equation
```

```
            return [dQ1dt,dQ2dt]
        return [0,0] #blah blah blah
    #Initial values of Q1 and Q2
    Q1 = 1049  #833.26,1049
    Q2= 47     #29.69,47
    S_0 = [Q1,Q2]
    # integrate the equations
    t = np.linspace(0,700,700) # times to report solution 428 for 300F.548 for 400 F
    y = odeint(dSdt1,y0=S_0,t=t,tfirst=True) # integrate
    #get Q1 and Q2 from solution
    Q1_sol = y[:,0]
    Q2_sol = y[:,1]
    # Calculate V1 using the list values of Q1
    Q1_list = list(Q1_sol)
    Q2_list = list(Q2_sol)
    V1= [i*2*Kv for i in Q1_list]
    V1= [i+ (C0**2) for i in V1]
    d= np.sqrt(V1)
    V1_final = [i - C0 for i in d]
    quotients = []
    for i in V1_final:
        quotients.append(i/Kv)
      SC_voltage = [i+ ((Isc/Np)*R1) for i in quotients]        #SC_voltage = (V1 +
(2/1)*0.01)*1  #V1 + (Isc/Np)*R0)*Ns
##    #return SC_voltage
##
##    Q2quotients =[]
##    for i in Q2_list:
##        Q2quotients.append(i/C2)

##    #Plot in excel sheet
```

```
##    """ Create excel work sheet"""
##    workbook = xlsxwriter.Workbook('EDLC_Voltage.xlsx')
##    worksheet = workbook.add_worksheet()
##    row = 900
##    col = 0
    for i in (SC_voltage):
        worksheet.write_number(row,col,i)
        row +=1
####    """ Insert Q1 values in excel """
####    row = 900
####    col = 0
####    for i in (Q1_list):
####        worksheet.write_number(row,col+1,i)
####        row +=1
####    """ Insert V1 values in excel """
####    row = 900
####    col = 0
####    for i in (quotients):
####        worksheet.write_number(row,col+2,i)
####        row +=1
####    """ Insert Q2 values in excel """
####    row = 900
####    col = 0
####    for i in (Q2_list):
####        worksheet.write_number(row,col+3,i)
####        row +=1
####    """ Insert V2 values in excel """
####    row = 900
####    col = 0
####    for i in (Q2quotients):
####        worksheet.write_number(row,col+4,i)
```

```
####        row +=1
    workbook.close()

    #Plot date on a gragh
    plt.figure(2)
    plt.plot(t,SC_voltage,'b-')
    plt.xlabel('Time (S)')
    plt.ylabel('Voltage (V)')
    plt.legend(['EDLC Discharging 300 F,2 A'])
    plt.show()

#code end here.
```

APPENDIX C: Sub-sectional Codes representing the EDLC in python, that is encapsulated in MATLAB

PYTHON

```
import math

import numpy as np

import matplotlib.pyplot as plt

from scipy.integrate import odeint


def EdlcLinear(current,Np,R0,Ns):

    Isc = current

    Ns = Ns

    Np = Np

    R0 = R0

    output1 = Isc/Np

    output2 = output1 * R0


  return output1,output2
```

MATLAB (Encapsulate the python part, does more calculations then returns a value)

```
function [V1,I1,EDLC_Voltage] = func(Isc,Np,R0,Ns,Q1,C0,Kv)

    I1 = 0
```

```
    EDLC_Voltage = 0
    V1= 0
    coder.extrinsic('py.edlcLinear.EdlcLinear')
    out = cell(py.edlcLinear.EdlcLinear(Isc,Np,R0,Ns));
    coder.extrinsic('py.V1func.cal')
    V1 = py.V1func.cal(Q1,C0,Kv)
    I1 = Isc/Np
    out_ = (I1*R0) + V1
    EDLC_Voltage = out_*Ns
    if EDLC_Voltage > 16.2
        EDLC_Voltage = 16.2
End
```

PYTHON

```
import math
import numpy as np
import matplotlib.pyplot as plt
from scipy.integrate import odeint


def cal(Q1,CO,KV):
    C0 = CO
    Kv = KV
    V1 = (-C0+math.sqrt((C0**2) + (2*Kv*Q1)))/(Kv)
```

```
    return V1
```

MATLAB (Encapsulate the python part, does more calculations then returns a value)

```
function I2  = V2_Cal(Q2,C2,V1,R2)
    V2 = 0
    coder.extrinsic('py.edlcLinear.EdlcLinear')
    out = cell(py.edlcLinear.EdlcLinear(Isc,Np,R0,Ns));
    V2 = Q2/C2
    I2 = (V1 - V2)/R2
End
```

Appendix D: EDLC code

Python MATLAB Simulink (PMS) – Hybrid model of the EDLC

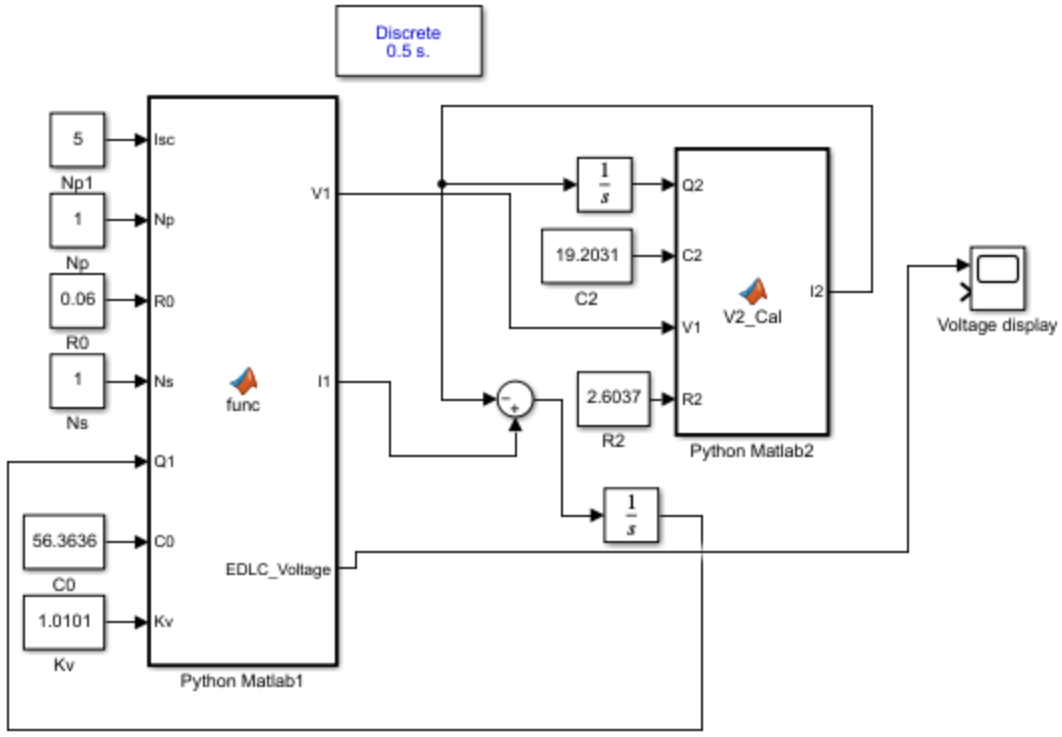

EDLC.C

```
* Code generation for model "edlc1".

*

* Model version              : 1.21

* Simulink Coder version : 9.7 (R2022a) 13-Nov-2021

* C source code generated on : Wed Aug 10 13:37:14 2022

*

* Target selection: rsim.tlc

* Note: GRT includes extra infrastructure and instrumentation for prototyping
```

```
 * Embedded hardware selection: Intel->x86-64 (Windows64)
 * Code generation objectives: Unspecified
 * Validation result: Not run
 */

#include "edlc1.h"
#include "rtwtypes.h"
#include "edlc1_private.h"
#include "edlc1_dt.h"

/* user code (top of parameter file) */
const int_T gblNumToFiles = 0;
const int_T gblNumFrFiles = 0;
const int_T gblNumFrWksBlocks = 0;
const char *gblSlvrJacPatternFileName = "edlc1_rsim_rtw\\edlc1_Jpattern.mat";

/* Root inports information  */
const int_T gblNumRootInportBlks = 0;
const int_T gblNumModelInputs = 0;
```

```
extern rtInportTUtable *gblInportTUtables;

extern const char *gblInportFileName;

const int_T gblInportDataTypeIdx[] = { -1 };


const int_T gblInportDims[] = { -1 } ;


const int_T gblInportComplex[] = { -1 };


const int_T gblInportInterpoFlag[] = { -1 };


const int_T gblInportContinuous[] = { -1 };


#include "simstruc.h"

#include "fixedpoint.h"


const real_T edlc1_RGND = 0.0;        /* real_T ground */


/* Block signals (default storage) */

B rtB;
```

```
/* Continuous states */
X rtX;

/* Block states (default storage) */
DW rtDW;

/* Parent Simstruct */
static SimStruct model_S;
SimStruct *const rtS = &model_S;

/* System initialize for root system: '<Root>' */
void MdlInitialize(void)
{
  /* InitializeConditions for Integrator: '<Root>/Integrator1' */
  rtX.Integrator1_CSTATE = rtP.Integrator1_IC;

  /* InitializeConditions for Integrator: '<Root>/Integrator' */
  rtX.Integrator_CSTATE = rtP.Integrator_IC;
```

```
}

/* Start for root system: '<Root>' */
void MdlStart(void)
{
  /* SetupRuntimeResources for Scope: '<Root>/Voltage display' */
  {
    RTWLogSignalInfo rt_ScopeSignalInfo;
    static int_T rt_ScopeSignalWidths[] = { 1, 1 };

    static int_T rt_ScopeSignalNumDimensions[] = { 1, 1 };

    static int_T rt_ScopeSignalDimensions[] = { 1, 1 };

    static void *rt_ScopeCurrSigDims[] = { (NULL), (NULL) };

    static int_T rt_ScopeCurrSigDimsSize[] = { 4, 4 };

    static const char_T *rt_ScopeSignalLabels[] = { "",
```

```
  "" };

static char_T rt_ScopeSignalTitles[] = "";

static int_T rt_ScopeSignalTitleLengths[] = { 0, 0 };

static boolean_T rt_ScopeSignalIsVarDims[] = { 0, 0 };

static int_T rt_ScopeSignalPlotStyles[] = { 0, 1 };

BuiltInDTypeId dTypes[2] = { SS_DOUBLE, SS_DOUBLE };

static char_T rt_ScopeBlockName[] = "edlc1/Voltage display";

static int_T rt_ScopeFrameData[] = { 0, 0 };

static RTWPreprocessingFcnPtr rt_ScopeSignalLoggingPreprocessingFcnPtrs[] =

 {

  (NULL), (NULL)

};
```

```
rt_ScopeSignalInfo.numSignals = 2;

rt_ScopeSignalInfo.numCols = rt_ScopeSignalWidths;

rt_ScopeSignalInfo.numDims = rt_ScopeSignalNumDimensions;

rt_ScopeSignalInfo.dims = rt_ScopeSignalDimensions;

rt_ScopeSignalInfo.isVarDims = rt_ScopeSignalIsVarDims;

rt_ScopeSignalInfo.currSigDims = rt_ScopeCurrSigDims;

rt_ScopeSignalInfo.currSigDimsSize = rt_ScopeCurrSigDimsSize;

rt_ScopeSignalInfo.dataTypes = dTypes;

rt_ScopeSignalInfo.complexSignals = (NULL);

rt_ScopeSignalInfo.frameData = rt_ScopeFrameData;

rt_ScopeSignalInfo.preprocessingPtrs =

  rt_ScopeSignalLoggingPreprocessingFcnPtrs;

rt_ScopeSignalInfo.labels.cptr = rt_ScopeSignalLabels;

rt_ScopeSignalInfo.titles = rt_ScopeSignalTitles;

rt_ScopeSignalInfo.titleLengths = rt_ScopeSignalTitleLengths;

rt_ScopeSignalInfo.plotStyles = rt_ScopeSignalPlotStyles;

rt_ScopeSignalInfo.blockNames.cptr = (NULL);

rt_ScopeSignalInfo.stateNames.cptr = (NULL);

rt_ScopeSignalInfo.crossMdlRef = (NULL);
```

```
  rt_ScopeSignalInfo.dataTypeConvert = (NULL);

  rtDW.Voltagedisplay_PWORK.LoggedData[0] = rt_CreateStructLogVar(
    ssGetRTWLogInfo(rtS),
    ssGetTStart(rtS),
    ssGetTFinal(rtS),
    0.0,
    (&ssGetErrorStatus(rtS)),
    "ScopeData",
    1,
    0,
    1,
    0.0,
    &rt_ScopeSignalInfo,
    rt_ScopeBlockName);
  if (rtDW.Voltagedisplay_PWORK.LoggedData[0] == (NULL))
    return;
}


/* Start for Constant: '<Root>/Np1' */
```

```
rtB.Np1 = rtP.Np1_Value;

/* Start for Constant: '<Root>/Np' */
rtB.Np = rtP.Np_Value;

/* Start for Constant: '<Root>/R0' */
rtB.R0 = rtP.R0_Value;

/* Start for Constant: '<Root>/Ns' */
rtB.Ns = rtP.Ns_Value;

/* Start for Constant: '<Root>/C0' */
rtB.C0 = rtP.C0_Value;

/* Start for Constant: '<Root>/Kv' */
rtB.Kv = rtP.Kv_Value;

/* Start for Constant: '<Root>/C2' */
rtB.C2 = rtP.C2_Value;
```

```
  /* Start for Constant: '<Root>/R2' */
  rtB.R2 = rtP.R2_Value;
  MdlInitialize();
}

/* Outputs for root system: '<Root>' */
void MdlOutputs(int_T tid)
{
  real_T rtb_EDLC_Voltage;
  if (ssIsSampleHit(rtS, 1, 0)) {
    /* Constant: '<Root>/Np1' */
    rtB.Np1 = rtP.Np1_Value;

    /* Constant: '<Root>/Np' */
    rtB.Np = rtP.Np_Value;

    /* Constant: '<Root>/R0' */
    rtB.R0 = rtP.R0_Value;
```

```
  /* Constant: '<Root>/Ns' */
  rtB.Ns = rtP.Ns_Value;

  /* Constant: '<Root>/C0' */
  rtB.C0 = rtP.C0_Value;

  /* Constant: '<Root>/Kv' */
  rtB.Kv = rtP.Kv_Value;
}

/* Integrator: '<Root>/Integrator1' */
rtB.Integrator1 = rtX.Integrator1_CSTATE;

/* MATLAB Function: '<Root>/Python Matlab1' */
rtb_EDLC_Voltage = 0.0;

/* Scope: '<Root>/Voltage display' */
if (ssGetLogOutput(rtS)) {
```

```
StructLogVar *svar = (StructLogVar *)rtDW.Voltagedisplay_PWORK.LoggedData[0];
LogVar *var = svar->signals.values;

/* time */
{
  double locTime = ssGetTaskTime(rtS,0)
    ;
  rt_UpdateLogVar((LogVar *)svar->time, &locTime, 0);
}

/* signals */
{
  real_T up0[1];
  up0[0] = rtb_EDLC_Voltage;
  rt_UpdateLogVar((LogVar *)var, up0, 0);
  var = var->next;
}

{
```

```
    real_T up1[1];
    up1[0] = 0.0;
    rt_UpdateLogVar((LogVar *)var, up1, 0);
  }
}

if (ssIsSampleHit(rtS, 1, 0)) {
  /* Constant: '<Root>/C2' */
  rtB.C2 = rtP.C2_Value;

  /* Constant: '<Root>/R2' */
  rtB.R2 = rtP.R2_Value;
}

/* Integrator: '<Root>/Integrator' */
rtB.Integrator = rtX.Integrator_CSTATE;

/* MATLAB Function: '<Root>/Python Matlab2' incorporates:
 *  MATLAB Function: '<Root>/Python Matlab1'
```

```
   */
  rtB.I2 = (0.0 - rtB.Integrator / rtB.C2) / rtB.R2;

  /* Sum: '<Root>/Sum2' incorporates:
   *  MATLAB Function: '<Root>/Python Matlab1'
   */
  rtB.Sum2 = 0.0 - rtB.I2;
  UNUSED_PARAMETER(tid);
}

/* Update for root system: '<Root>' */
void MdlUpdate(int_T tid)
{
  UNUSED_PARAMETER(tid);
}
```

EDLC.h

```
/*
 * edlc1.h
 * Code generation for model "edlc1".
 *
```

```
 * Model version              : 1.21
 * Simulink Coder version : 9.7 (R2022a) 13-Nov-2021
 * C source code generated on : Wed Aug 10 13:37:14 2022
 *
 * Target selection: rsim.tlc
 * Note: GRT includes extra infrastructure and instrumentation for prototyping
 * Embedded hardware selection: Intel->x86-64 (Windows64)
 * Code generation objectives: Unspecified
 * Validation result: Not run
 */

#ifndef RTW_HEADER_edlc1_h_
#define RTW_HEADER_edlc1_h_
#ifndef edlc1_COMMON_INCLUDES_
#define edlc1_COMMON_INCLUDES_
#include <stdlib.h>
#include "rtwtypes.h"
#include "simstruc.h"
#include "fixedpoint.h"
```

```
#include "rsim.h"

#include "rt_logging.h"

#include "dt_info.h"

#endif                         /* edlc1_COMMON_INCLUDES_ */


#include "edlc1_types.h"

#include <stddef.h>

#include "rt_defines.h"

#include <string.h>

#include "rtGetInf.h"

#include "rt_nonfinite.h"

#define MODEL_NAME              edlc1

#define NSAMPLE_TIMES           (2)             /* Number of sample times */

#define NINPUTS                 (0)             /* Number of model inputs */

#define NOUTPUTS                (0)             /* Number of model outputs */

#define NBLOCKIO                (12)            /* Number of data output port
signals */

#define NUM_ZC_EVENTS           (0)             /* Number of zero-crossing
events */

#ifndef NCSTATES

#define NCSTATES                (2)             /* Number of continuous states */
```

```
#elif NCSTATES != 2

# error Invalid specification of NCSTATES defined in compiler command

#endif


#ifndef rtmGetDataMapInfo

#define rtmGetDataMapInfo(rtm)        (NULL)

#endif


#ifndef rtmSetDataMapInfo

#define rtmSetDataMapInfo(rtm, val)

#endif


/* Block signals (default storage) */

typedef struct {

  real_T Np1;                      /* '<Root>/Np1' */

  real_T Np;                       /* '<Root>/Np' */

  real_T R0;                       /* '<Root>/R0' */

  real_T Ns;                       /* '<Root>/Ns' */

  real_T Integrator1;                /* '<Root>/Integrator1' */
```

```
  real_T C0;                           /* '<Root>/C0' */
  real_T Kv;                           /* '<Root>/Kv' */
  real_T C2;                           /* '<Root>/C2' */
  real_T Integrator;                   /* '<Root>/Integrator' */
  real_T R2;                           /* '<Root>/R2' */
  real_T Sum2;                         /* '<Root>/Sum2' */
  real_T I2;                           /* '<Root>/Python Matlab2' */
} B;


/* Block states (default storage) for system '<Root>' */
typedef struct {
  struct {
    void *LoggedData[2];
  } Voltagedisplay_PWORK;              /* '<Root>/Voltage display' */
} DW;


/* Continuous states (default storage) */
typedef struct {
  real_T Integrator1_CSTATE;           /* '<Root>/Integrator1' */
```

```
  real_T Integrator_CSTATE;            /* '<Root>/Integrator' */
} X;

/* State derivatives (default storage) */
typedef struct {
  real_T Integrator1_CSTATE;           /* '<Root>/Integrator1' */
  real_T Integrator_CSTATE;            /* '<Root>/Integrator' */
} XDot;

/* State disabled  */
typedef struct {
  boolean_T Integrator1_CSTATE;        /* '<Root>/Integrator1' */
  boolean_T Integrator_CSTATE;         /* '<Root>/Integrator' */
} XDis;

/* Continuous State Absolute Tolerance  */
typedef struct {
  real_T Integrator1_CSTATE;           /* '<Root>/Integrator1' */
  real_T Integrator_CSTATE;            /* '<Root>/Integrator' */
```

```
} CStateAbsTol;

/* Continuous State Perturb Min  */
typedef struct {
  real_T Integrator1_CSTATE;           /* '<Root>/Integrator1' */
  real_T Integrator_CSTATE;            /* '<Root>/Integrator' */
} CXPtMin;

/* Continuous State Perturb Max  */
typedef struct {
  real_T Integrator1_CSTATE;           /* '<Root>/Integrator1' */
  real_T Integrator_CSTATE;            /* '<Root>/Integrator' */
} CXPtMax;

/* Parameters (default storage) */
struct P_ {
  real_T Np1_Value;                    /* Expression: 5
                                        * Referenced by: '<Root>/Np1'
                                        */
```

```
real_T Np_Value;                /* Expression: 1
                                 * Referenced by: '<Root>/Np'
                                 */
real_T R0_Value;                /* Expression: 0.06
                                 * Referenced by: '<Root>/R0'
                                 */
real_T Ns_Value;                /* Expression: 1
                                 * Referenced by: '<Root>/Ns'
                                 */
real_T Integrator1_IC;           /* Expression: 0
                                 * Referenced by: '<Root>/Integrator1'
                                 */
real_T C0_Value;                /* Expression: 56.3636
                                 * Referenced by: '<Root>/C0'
                                 */
real_T Kv_Value;                /* Expression: 1.0101
                                 * Referenced by: '<Root>/Kv'
                                 */
real_T C2_Value;                /* Expression: 19.2031
```

```
                                * Referenced by: '<Root>/C2'
                                */
  real_T Integrator_IC;                 /* Expression: 0
                                * Referenced by: '<Root>/Integrator'
                                */
  real_T R2_Value;                      /* Expression: 2.6037
                                * Referenced by: '<Root>/R2'
                                */
};

/* External data declarations for dependent source files */
extern const real_T edlc1_RGND;       /* real_T ground */
extern const char *RT_MEMORY_ALLOCATION_ERROR;
extern B rtB;                         /* block i/o */
extern X rtX;                         /* states (continuous) */
extern DW rtDW;                       /* states (dwork) */
extern P rtP;                         /* parameters */

/* Simulation Structure */
```

```
extern SimStruct *const rtS;


/*-
 * The generated code includes comments that allow you to trace directly
 * back to the appropriate location in the model.  The basic format
 * is <system>/block_name, where system is the system number (uniquely
 * assigned by Simulink) and block_name is the name of the block.
 *
 * Use the MATLAB hilite_system command to trace the generated code back
 * to the model.  For example,
 *
 * hilite_system('<S3>')    - opens system 3
 * hilite_system('<S3>/Kp') - opens and selects block Kp which resides in S3
 *
 * Here is the system hierarchy for this model
 *
 * '<Root>' : 'edlc1'
 * '<S1>'   : 'edlc1/Python Matlab1'
 * '<S2>'   : 'edlc1/Python Matlab2'
```

```
 * '<S3>'   : 'edlc1/powergui'
 */

/* user code (bottom of header file) */
extern const int_T gblNumToFiles;
extern const int_T gblNumFrFiles;
extern const int_T gblNumFrWksBlocks;
extern rtInportTUtable *gblInportTUtables;
extern const char *gblInportFileName;
extern const int_T gblNumRootInportBlks;
extern const int_T gblNumModelInputs;
extern const int_T gblInportDataTypeIdx[];
extern const int_T gblInportDims[];
extern const int_T gblInportComplex[];
extern const int_T gblInportInterpoFlag[];
extern const int_T gblInportContinuous[];

#endif                         /* RTW_HEADER_edlc1_h_ */
```

Appendix E: EDLC with the Voltage Controlled Current Source (VCCS) code

EDLC with VCCS

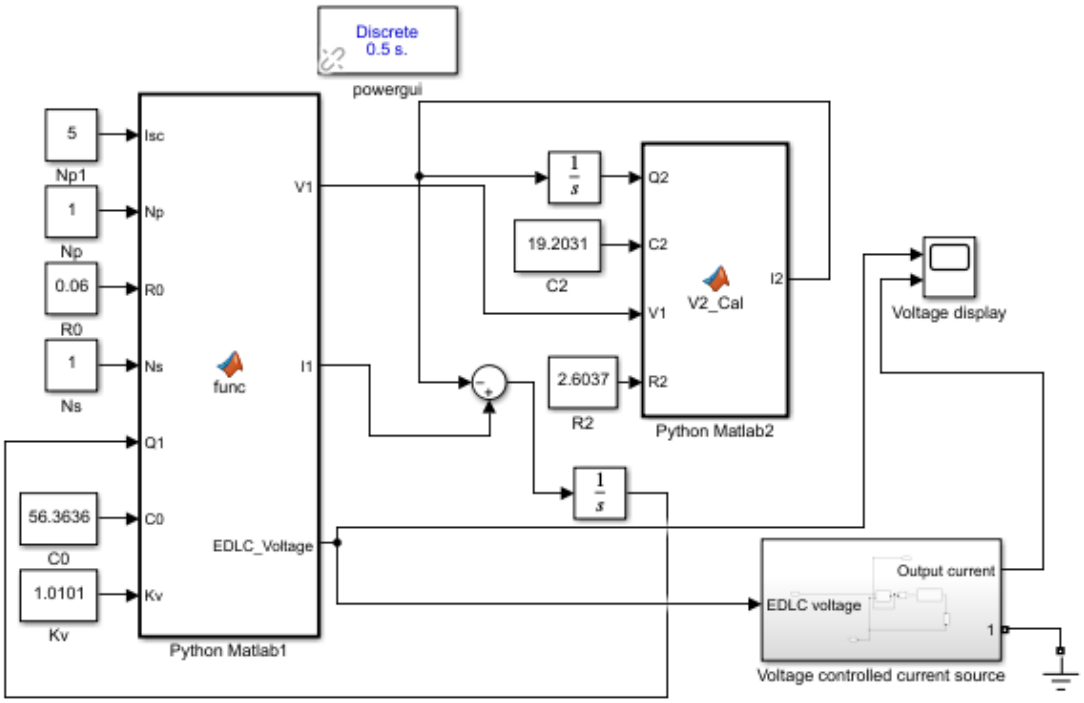

EDLC1.C

```
* Code generation for model "edlc1".

*

* Model version              : 1.20

* Simulink Coder version : 9.7 (R2022a) 13-Nov-2021

* C source code generated on : Wed Aug 10 12:54:14 2022

*

* Target selection: rsim.tlc
```

```
 * Note: GRT includes extra infrastructure and instrumentation for prototyping
 * Embedded hardware selection: Intel->x86-64 (Windows64)
 * Code generation objectives: Unspecified
 * Validation result: Not run
 */

#include "edlc1.h"
#include "edlc1_private.h"
#include "edlc1_dt.h"

/* user code (top of parameter file) */
const int_T gblNumToFiles = 0;
const int_T gblNumFrFiles = 0;
const int_T gblNumFrWksBlocks = 0;
const char *gblSlvrJacPatternFileName = "edlc1_rsim_rtw\\edlc1_Jpattern.mat";

/* Root inports information  */
const int_T gblNumRootInportBlks = 0;
const int_T gblNumModelInputs = 0;
```

```
extern rtInportTUtable *gblInportTUtables;

extern const char *gblInportFileName;

const int_T gblInportDataTypeIdx[] = { -1 };


const int_T gblInportDims[] = { -1 } ;


const int_T gblInportComplex[] = { -1 };


const int_T gblInportInterpoFlag[] = { -1 };


const int_T gblInportContinuous[] = { -1 };


#include "simstruc.h"

#include "fixedpoint.h"


/* Block signals (default storage) */

B rtB;


/* Continuous states */
```

```
X rtX;


/* Block states (default storage) */

DW rtDW;


/* Parent Simstruct */

static SimStruct model_S;

SimStruct *const rtS = &model_S;


/* System initialize for root system: '<Root>' */

void MdlInitialize(void)

{

  /* InitializeConditions for Integrator: '<Root>/Integrator1' */

  rtX.Integrator1_CSTATE = rtP.Integrator1_IC;


  /* InitializeConditions for S-Function (sfun_spssw_discc): '<S10>/State-Space'
incorporates:

   *  Constant: '<S9>/DC'

   */

  {
```

```
    int32_T i, j;
    real_T *Ds = (real_T*)rtDW.StateSpace_PWORK.DS;

    /* Copy and transpose D */
    for (i=0; i<1; i++) {
      for (j=0; j<2; j++)
        Ds[i*2 + j] = (rtP.StateSpace_DS_param[i + j*1]);
    }
  }

  /* InitializeConditions for Integrator: '<Root>/Integrator' */
  rtX.Integrator_CSTATE = rtP.Integrator_IC;
}

/* Start for root system: '<Root>' */
void MdlStart(void)
{
  /* SetupRuntimeResources for Scope: '<Root>/Voltage display' */
  {
```

```
RTWLogSignalInfo rt_ScopeSignalInfo;

static int_T rt_ScopeSignalWidths[] = { 1, 1 };


static int_T rt_ScopeSignalNumDimensions[] = { 1, 1 };


static int_T rt_ScopeSignalDimensions[] = { 1, 1 };


static void *rt_ScopeCurrSigDims[] = { (NULL), (NULL) };


static int_T rt_ScopeCurrSigDimsSize[] = { 4, 4 };


static const char_T *rt_ScopeSignalLabels[] = { "",

  "" };


static char_T rt_ScopeSignalTitles[] = "";

static int_T rt_ScopeSignalTitleLengths[] = { 0, 0 };


static boolean_T rt_ScopeSignalIsVarDims[] = { 0, 0 };
```

```
static int_T rt_ScopeSignalPlotStyles[] = { 0, 1 };

BuiltInDTypeId dTypes[2] = { SS_DOUBLE, SS_DOUBLE };

static char_T rt_ScopeBlockName[] = "edlc1/Voltage display";
static int_T rt_ScopeFrameData[] = { 0, 0 };

static RTWPreprocessingFcnPtr rt_ScopeSignalLoggingPreprocessingFcnPtrs[] =
 {
  (NULL), (NULL)
};

rt_ScopeSignalInfo.numSignals = 2;
rt_ScopeSignalInfo.numCols = rt_ScopeSignalWidths;
rt_ScopeSignalInfo.numDims = rt_ScopeSignalNumDimensions;
rt_ScopeSignalInfo.dims = rt_ScopeSignalDimensions;
rt_ScopeSignalInfo.isVarDims = rt_ScopeSignalIsVarDims;
rt_ScopeSignalInfo.currSigDims = rt_ScopeCurrSigDims;
rt_ScopeSignalInfo.currSigDimsSize = rt_ScopeCurrSigDimsSize;
```

```
rt_ScopeSignalInfo.dataTypes = dTypes;

rt_ScopeSignalInfo.complexSignals = (NULL);

rt_ScopeSignalInfo.frameData = rt_ScopeFrameData;

rt_ScopeSignalInfo.preprocessingPtrs =

  rt_ScopeSignalLoggingPreprocessingFcnPtrs;

rt_ScopeSignalInfo.labels.cptr = rt_ScopeSignalLabels;

rt_ScopeSignalInfo.titles = rt_ScopeSignalTitles;

rt_ScopeSignalInfo.titleLengths = rt_ScopeSignalTitleLengths;

rt_ScopeSignalInfo.plotStyles = rt_ScopeSignalPlotStyles;

rt_ScopeSignalInfo.blockNames.cptr = (NULL);

rt_ScopeSignalInfo.stateNames.cptr = (NULL);

rt_ScopeSignalInfo.crossMdlRef = (NULL);

rt_ScopeSignalInfo.dataTypeConvert = (NULL);

rtDW.Voltagedisplay_PWORK.LoggedData[0] = rt_CreateStructLogVar(

  ssGetRTWLogInfo(rtS),

  ssGetTStart(rtS),

  ssGetTFinal(rtS),

  0.0,

  (&ssGetErrorStatus(rtS)),
```

```
    "ScopeData",
    1,
    0,
    1,
    0.0,
    &rt_ScopeSignalInfo,
    rt_ScopeBlockName);
  if (rtDW.Voltagedisplay_PWORK.LoggedData[0] == (NULL))
    return;
}

/* Start for Constant: '<Root>/Np1' */
rtB.Np1 = rtP.Np1_Value;

/* Start for Constant: '<Root>/Np' */
rtB.Np = rtP.Np_Value;

/* Start for Constant: '<Root>/R0' */
rtB.R0 = rtP.R0_Value;
```

```
/* Start for Constant: '<Root>/Ns' */
rtB.Ns = rtP.Ns_Value;

/* Start for Constant: '<Root>/C0' */
rtB.C0 = rtP.C0_Value;

/* Start for Constant: '<Root>/Kv' */
rtB.Kv = rtP.Kv_Value;

/* Start for S-Function (sfun_spssw_discc): '<S10>/State-Space' incorporates:
 *  Constant: '<S9>/DC'
 */

/* S-Function block: <S10>/State-Space */
{
  rtDW.StateSpace_PWORK.DS = (real_T*)calloc(1 * 2, sizeof(real_T));
  rtDW.StateSpace_PWORK.DX_COL = (real_T*)calloc(1, sizeof(real_T));
  rtDW.StateSpace_PWORK.TMP2 = (real_T*)calloc(2, sizeof(real_T));
```

```
  }

  /* Start for Constant: '<Root>/C2' */
  rtB.C2 = rtP.C2_Value;

  /* Start for Constant: '<Root>/R2' */
  rtB.R2 = rtP.R2_Value;
  MdlInitialize();
}

/* Outputs for root system: '<Root>' */
void MdlOutputs(int_T tid)
{
  if (ssIsSampleHit(rtS, 1, 0)) {
    /* Constant: '<Root>/Np1' */
    rtB.Np1 = rtP.Np1_Value;

    /* Constant: '<Root>/Np' */
    rtB.Np = rtP.Np_Value;
```

```
  /* Constant: '<Root>/R0' */
  rtB.R0 = rtP.R0_Value;

  /* Constant: '<Root>/Ns' */
  rtB.Ns = rtP.Ns_Value;

  /* Constant: '<Root>/C0' */
  rtB.C0 = rtP.C0_Value;

  /* Constant: '<Root>/Kv' */
  rtB.Kv = rtP.Kv_Value;
}

/* Integrator: '<Root>/Integrator1' */
rtB.Integrator1 = rtX.Integrator1_CSTATE;

/* MATLAB Function: '<Root>/Python Matlab1' */
rtB.EDLC_Voltage = 0.0;
```

```
if (ssIsSampleHit(rtS, 2, 0)) {
  /* S-Function (sfun_spssw_discc): '<S10>/State-Space' incorporates:
   *  Constant: '<S9>/DC'
   */

  /* S-Function block: <S10>/State-Space */
  {
    real_T accum;

    /*
     * Compute outputs:
     * ---------------
     */
    real_T *Ds = (real_T*)rtDW.StateSpace_PWORK.DS;
    accum = 0.0;
    accum += *(Ds++) * rtP.DCvoltagesource_Amplitude;
    accum += *(Ds++) * rtB.EDLC_Voltage;
    rtB.StateSpace = accum;
  }
```

```
  /* Gain: '<S6>/do not delete this gain' */
  rtB.donotdeletethisgain = rtP.donotdeletethisgain_Gain * rtB.StateSpace;
}

/* Scope: '<Root>/Voltage display' */
if (ssGetLogOutput(rtS)) {
  StructLogVar *svar = (StructLogVar *)rtDW.Voltagedisplay_PWORK.LoggedData[0];
  LogVar *var = svar->signals.values;

  /* time */
  {
    double locTime = ssGetTaskTime(rtS,0)
      ;
    rt_UpdateLogVar((LogVar *)svar->time, &locTime, 0);
  }
```

EDLC1.h

```
/*
```

```
* edlc1.h

* Code generation for model "edlc1".

*

* Model version              : 1.20

* Simulink Coder version : 9.7 (R2022a) 13-Nov-2021

* C source code generated on : Wed Aug 10 12:54:14 2022

*

* Target selection: rsim.tlc

* Note: GRT includes extra infrastructure and instrumentation for prototyping

* Embedded hardware selection: Intel->x86-64 (Windows64)

* Code generation objectives: Unspecified

* Validation result: Not run

*/


#ifndef RTW_HEADER_edlc1_h_

#define RTW_HEADER_edlc1_h_

#ifndef edlc1_COMMON_INCLUDES_

#define edlc1_COMMON_INCLUDES_

#include <stdlib.h>
```

```
#include "rtwtypes.h"

#include "simstruc.h"

#include "fixedpoint.h"

#include "rsim.h"

#include "rt_logging.h"

#include "dt_info.h"

#endif                         /* edlc1_COMMON_INCLUDES_ */


#include "edlc1_types.h"

#include <stddef.h>

#include "rt_defines.h"

#include <string.h>

#include "rtGetInf.h"

#include "rt_nonfinite.h"

#define MODEL_NAME              edlc1

#define NSAMPLE_TIMES           (3)             /* Number of sample times */

#define NINPUTS                 (0)             /* Number of model inputs */

#define NOUTPUTS                (0)             /* Number of model outputs */

#define NBLOCKIO                (15)            /* Number of data output port
signals */
```

```
#define NUM_ZC_EVENTS                (0)                    /* Number of zero-crossing
events */

#ifndef NCSTATES

#define NCSTATES                     (2)                    /* Number of continuous states */

#elif NCSTATES != 2

# error Invalid specification of NCSTATES defined in compiler command

#endif


#ifndef rtmGetDataMapInfo

#define rtmGetDataMapInfo(rtm)       (NULL)

#endif


#ifndef rtmSetDataMapInfo

#define rtmSetDataMapInfo(rtm, val)

#endif


/* Block signals (default storage) */

typedef struct {

  real_T Np1;                        /* '<Root>/Np1' */

  real_T Np;                         /* '<Root>/Np' */
```

```
  real_T R0;                       /* '<Root>/R0' */
  real_T Ns;                       /* '<Root>/Ns' */
  real_T Integrator1;                 /* '<Root>/Integrator1' */
  real_T C0;                       /* '<Root>/C0' */
  real_T Kv;                       /* '<Root>/Kv' */
  real_T StateSpace;                  /* '<S10>/State-Space' */
  real_T donotdeletethisgain;         /* '<S6>/do not delete this gain' */
  real_T C2;                       /* '<Root>/C2' */
  real_T Integrator;                  /* '<Root>/Integrator' */
  real_T R2;                       /* '<Root>/R2' */
  real_T Sum2;                        /* '<Root>/Sum2' */
  real_T I2;                       /* '<Root>/Python Matlab2' */
  real_T EDLC_Voltage;                /* '<Root>/Python Matlab1' */
} B;


/* Block states (default storage) for system '<Root>' */
typedef struct {
  struct {
    void *AS;
```

```
void *BS;

void *CS;

void *DS;

void *DX_COL;
```

Appendix F: HESS Model Code

EDLC in a HESS SYSTEM

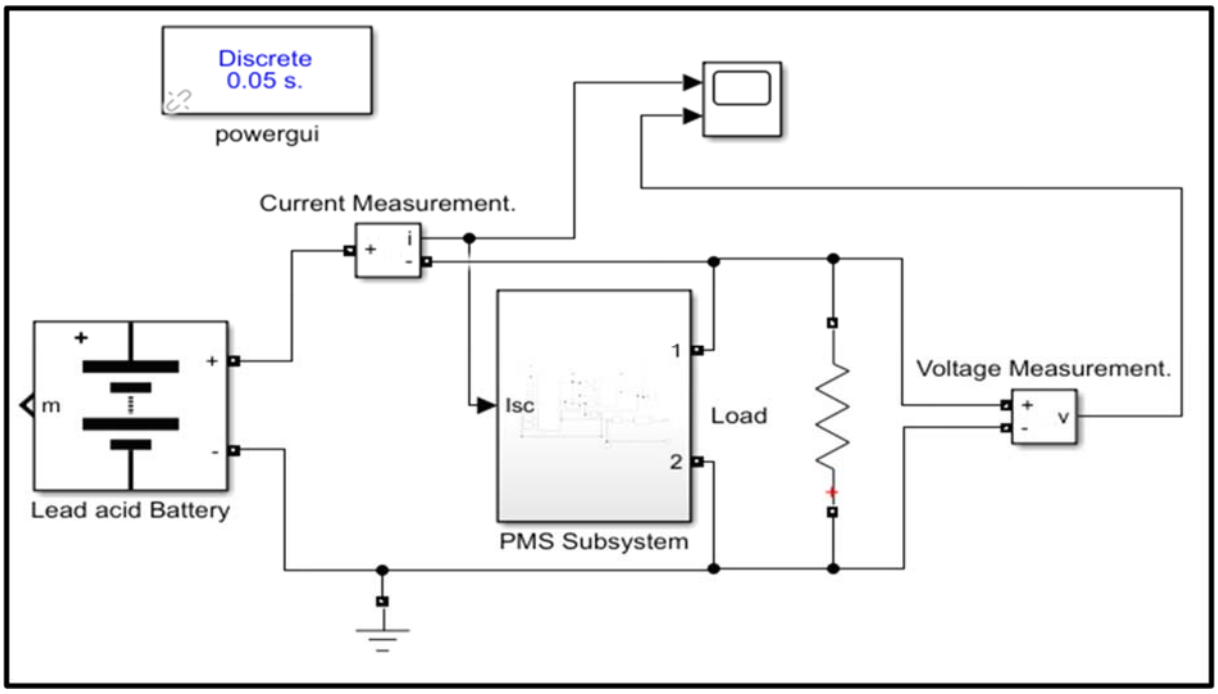

HESS.C

```
* Code generation for model "HESS_New".

*

* Model version              : 1.18

* Simulink Coder version : 9.7 (R2022a) 13-Nov-2021

* C source code generated on : Wed Aug 10 13:29:26 2022

*

* Target selection: rsim.tlc

* Note: GRT includes extra infrastructure and instrumentation for prototyping

* Embedded hardware selection: Intel->x86-64 (Windows64)
```

```
 * Code generation objectives: Unspecified
 * Validation result: Not run
 */

#include "HESS_New.h"
#include "rtwtypes.h"
#include <math.h>
#include "HESS_New_private.h"
#include "HESS_New_dt.h"

/* user code (top of parameter file) */
const int_T gblNumToFiles = 0;
const int_T gblNumFrFiles = 0;
const int_T gblNumFrWksBlocks = 0;
const char *gblSlvrJacPatternFileName =
  "HESS_New_rsim_rtw\\HESS_New_Jpattern.mat";

/* Root inports information  */
const int_T gblNumRootInportBlks = 0;
```

```
const int_T gblNumModelInputs = 0;

extern rtInportTUtable *gblInportTUtables;

extern const char *gblInportFileName;

const int_T gblInportDataTypeIdx[] = { -1 };


const int_T gblInportDims[] = { -1 } ;


const int_T gblInportComplex[] = { -1 };


const int_T gblInportInterpoFlag[] = { -1 };


const int_T gblInportContinuous[] = { -1 };


#include "simstruc.h"

#include "fixedpoint.h"


/* Block signals (default storage) */

B rtB;
```

```
/* Continuous states */
X rtX;

/* Block states (default storage) */
DW rtDW;

/* Parent Simstruct */
static SimStruct model_S;
SimStruct *const rtS = &model_S;

/* System initialize for root system: '<Root>' */
void MdlInitialize(void)
{
  real_T itinit_PreviousInput_tmp;

  /* InitializeConditions for Memory: '<S9>/it init1' */
  rtDW.itinit1_PreviousInput = rtP.itinit1_InitialCondition;

  /* InitializeConditions for DiscreteTransferFcn: '<S9>/Current filter' */
```

```
rtDW.Currentfilter_states = rtP.Currentfilter_InitialStates;

/* InitializeConditions for Memory: '<S9>/it init' incorporates:
 *  DiscreteIntegrator: '<S14>/Discrete-Time Integrator'
 */
itinit_PreviousInput_tmp = 1.0 - rtP.LeadacidBattery_SOC / 100.0;
rtDW.itinit_PreviousInput = itinit_PreviousInput_tmp * 9.24999999999991 *
  0.9009009009009098 * 3600.0;

/* InitializeConditions for DiscreteIntegrator: '<S9>/int(i)' */
rtDW.inti_PrevResetState = 2;
rtDW.inti_IC_LOADING = 1U;

/* InitializeConditions for DiscreteIntegrator: '<S14>/Discrete-Time Integrator' */
rtDW.DiscreteTimeIntegrator_DSTATE = exp(itinit_PreviousInput_tmp *
  -112.50000000000001 * 9.24999999999991) * 0.81645428384289542;

/* InitializeConditions for Memory: '<S9>/Memory2' */
rtDW.Memory2_PreviousInput = rtP.Memory2_InitialCondition;
```

```
  /* InitializeConditions for Integrator: '<S3>/Integrator1' */
  rtX.Integrator1_CSTATE = rtP.Integrator1_IC;

  /* InitializeConditions for S-Function (sfun_spssw_discc): '<S23>/State-Space' */
  {
    int32_T i, j;
    real_T *Ds = (real_T*)rtDW.StateSpace_PWORK.DS;

    /* Copy and transpose D */
    for (i=0; i<3; i++) {
      for (j=0; j<2; j++)
        Ds[i*2 + j] = (rtP.StateSpace_DS_param[i + j*3]);
    }
  }

  /* InitializeConditions for Integrator: '<S3>/Integrator' */
  rtX.Integrator_CSTATE = rtP.Integrator_IC;
}
```

```
/* Start for root system: '<Root>' */
void MdlStart(void)
{
  /* SetupRuntimeResources for Scope: '<Root>/Scope' */
  {
    RTWLogSignalInfo rt_ScopeSignalInfo;
    static int_T rt_ScopeSignalWidths[] = { 1, 1 };

    static int_T rt_ScopeSignalNumDimensions[] = { 1, 1 };

    static int_T rt_ScopeSignalDimensions[] = { 1, 1 };

    static void *rt_ScopeCurrSigDims[] = { (NULL), (NULL) };

    static int_T rt_ScopeCurrSigDimsSize[] = { 4, 4 };

    static const char_T *rt_ScopeSignalLabels[] = { "",
      "" };
```

```
    static char_T rt_ScopeSignalTitles[] = "";

    static int_T rt_ScopeSignalTitleLengths[] = { 0, 0 };


    static boolean_T rt_ScopeSignalIsVarDims[] = { 0, 0 };


    static int_T rt_ScopeSignalPlotStyles[] = { 1, 1 };
```

HESS.h

```
/*
 * HESS_New.h
* Code generation for model "HESS_New".
 *
 * Model version              : 1.18
 * Simulink Coder version : 9.7 (R2022a) 13-Nov-2021
 * C source code generated on : Wed Aug 10 13:29:26 2022
 *
 * Target selection: rsim.tlc
 * Note: GRT includes extra infrastructure and instrumentation for prototyping
 * Embedded hardware selection: Intel->x86-64 (Windows64)
```

```
 * Code generation objectives: Unspecified
 * Validation result: Not run
 */

#ifndef RTW_HEADER_HESS_New_h_
#define RTW_HEADER_HESS_New_h_
#ifndef HESS_New_COMMON_INCLUDES_
#define HESS_New_COMMON_INCLUDES_
#include <stdlib.h>
#include "rtwtypes.h"
#include "simstruc.h"
#include "fixedpoint.h"
#include "rsim.h"
#include "rt_logging.h"
#include "dt_info.h"
#endif                         /* HESS_New_COMMON_INCLUDES_ */

#include "HESS_New_types.h"
#include <stddef.h>
```

```
#include "rtGetInf.h"

#include "rt_defines.h"

#include <string.h>

#include "rt_nonfinite.h"

#define MODEL_NAME                HESS_New

#define NSAMPLE_TIMES             (3)                 /* Number of sample times */

#define NINPUTS                   (0)                 /* Number of model inputs */

#define NOUTPUTS                  (0)                 /* Number of model outputs */

#define NBLOCKIO                  (28)                /* Number of data output port
signals */

#define NUM_ZC_EVENTS             (0)                 /* Number of zero-crossing
events */

#ifndef NCSTATES

#define NCSTATES                  (2)                 /* Number of continuous states */

#elif NCSTATES != 2

# error Invalid specification of NCSTATES defined in compiler command

#endif


#ifndef rtmGetDataMapInfo

#define rtmGetDataMapInfo(rtm)        (NULL)

#endif
```

```
#ifndef rtmSetDataMapInfo
#define rtmSetDataMapInfo(rtm, val)
#endif


/* Block signals (default storage) */
typedef struct {
  real_T Currentfilter;                /* '<S9>/Current filter' */
  real_T DataTypeConversion2;          /* '<S9>/Data Type Conversion2' */
  real_T itinit;                       /* '<S9>/it init' */
  real_T Gain;                         /* '<S9>/Gain' */
  real_T Switch;                       /* '<S16>/Switch' */
  real_T DataTypeConversion1;          /* '<S9>/Data Type Conversion1' */
  real_T DiscreteTimeIntegrator;       /* '<S14>/Discrete-Time Integrator' */
  real_T Memory2;                      /* '<S9>/Memory2' */
  real_T Switch2;                      /* '<S15>/Switch2' */
  real_T Np1;                          /* '<S3>/Np1' */
  real_T Np;                           /* '<S3>/Np' */
  real_T R0;                           /* '<S3>/R0' */
```

```
real_T Ns;                     /* '<S3>/Ns' */

real_T Integrator1;               /* '<S3>/Integrator1' */

real_T C0;                     /* '<S3>/C0' */
```

This is the End, I thank you !!